DAHLGREN DIVISION
NAVAL SURFACE WARFARE CENTER
Dahlgren, Virginia 22448-5100

NSWCDD/TR-00/46

ON GLOBAL THREAT PRIORITIZATION

BY GORDON W. GROVES

COMBAT SYSTEMS DEPARTMENT

JOHN E. GRAY

SYSTEMS RESEARCH AND TECHNOLOGY DEPARTMENT

MAY 2003

REPORT DOCUMENTATION PAGE

Form Approved
OMB No. 0704-0188

1. AGENCY USE ONLY (Leave blank)	2. REPORT DATE	3. REPORT TYPE AND DATES COVERED
	May 2003	Final

4. TITLE AND SUBTITLE

ON GLOBAL THREAT PRIORITIZATION

5. FUNDING NUMBERS

---

6. AUTHOR(s)

Gordon W. Groves (Combat Systems Department)
John E. Gray (Systems Research and Technology Department)

7. PERFORMING ORGANIZATION NAME(S) AND ADDRESS(ES)

Commander
Naval Surface Warfare Center
Dahlgren Division (Codes N92 and B32)
17320 Dahlgren Road
Dahlgren, VA 22448-5100

8. PERFORMING ORGANIZATION REPORT NUMBER

NSWCDD/TR-00/46

9. SPONSORING/MONITORING AGENCY NAME(S) AND ADDRESS(ES)

10. SPONSORING/MONITORING AGENCY REPORT NUMBER

---

11. SUPPLEMENTARY NOTES

12a. DISTRIBUTION/AVAILABILITY STATEMENT

Approved for public release; distribution is unlimited.

12b. DISTRIBUTION CODE

---

13. ABSTRACT (Maximum 200 words)

In this report, we consider two classes of threats: Anti-Ship Cruise Missiles (ASCMs) and Tactical Ballistic Missiles (TBMs). ASCMs are treated as being capable of maneuver, while the trajectory of a TBM is determined solely by its initial state.

A threat is evaluated according to two basic criteria: the amount of damage it can potentially cause, and the time remaining during which it can be engaged. Both criteria depend on the types and positions of the threat's potential target. These targets fall into two classes: defended points (*e.g.*, ships) and defended areas (*e.g.*, cities). The defended targets are assigned values. The threat-evaluation process is repeated each time a threat's estimated state is updated and for every appreciable position change of a target.

From the initial estimation of the state of an ASCM, simplified trajectories to each defended target reachable by the threat are calculated. Thus, the targets in jeopardy are identified, and the earliest arrival times and energy requirements are determined.

TBMs are treated differently. From the initial estimation of the state of a TBM, its footprint on the earth's surface is determined. Uncertainties in the impact point are related to uncertainties in the initial state estimation and in the physical characteristics of the threat vehicle.

An algorithm is proposed that calculates the probability of each defended asset becoming the target of a given threat. The result is a matrix of "Objective Probabilities" that is used to calculate the parameters used for the evaluation of the threats. One of these is the "Maximum Expected Value Loss" that quantifies at any time the loss that any given threat might cause. It is a monotonic function of time that summarizes the importance of the threats to aid the subsequent decision process.

14. SUBJECT TERMS	15. NUMBER OF PAGES
Threat Prioritization, Anti-Ship Cruise Missile, ASCM, Tactical Ballistic Missile, TBM, objective probabilities, targeting, algorithm	150
	16. PRICE CODE

17. SECURITY CLASSIFICATION OF REPORT	18. SECURITY CLASSIFICATION OF THIS PAGE	19. SECURITY CLASSIFICATION OF ABSTRACT	20. LIMITATION OF ABSTRACT
UNCLASSIFIED	UNCLASSIFIED	UNCLASSIFIED	UL

NSN 7540-01-280-5500
Standard Form 298 (Rev 2-89)
Prescribed by ANSI std. Z39-18
298-102

FOREWORD

This work reflects ongoing research that has been sponsored within the Combat Systems Department, Naval Surface Warfare Center, Dahlgren Division, that responds to the need for improved techniques in dealing with the situation where many threats are attacking a battle group. In such a situation, each threat has a large number of potential targets from which to choose. Prioritization of the threats within a raid that involves a large number of Anti-Ship Cruise Missiles (ASCMs) presents a problem to a global scheduler in terms of both selection of shooting platforms and determining the queue for engagement scheduling. This problem becomes particularly challenging when placed in the context of the network centric paradigm envisioned for the future of the surface navy, and represents a significant potential problem that needs to be addressed.

This work not only addresses the problem by discussing its formulation and occurrence, it also proposes a solution. Threats targeting high valued assets such as a carrier would be ranked above those targeting a destroyer. Similarly, a threat arriving earlier would be ranked above one arriving later. But what makes this problem not straightforward is such concerns as: How does one rank a threat arriving at a destroyer earlier than one arriving later at a carrier? The ranking scheme proposed here is based on the "Loss Threshold Time" (LTT), which is defined as the time at which the expected destructive potential of a threat exceeds a specified value. Then, threats with earlier LTTs are ranked higher. An algorithm is proposed that estimates the probability of each defended ship becoming the target of a given threat. The result is a matrix of "Objective Probabilities", which is used to calculate the "Expected Loss" (EL) function of each threat. The objective probabilities are higher for ships that can be reached earlier and more easily. The combination of these two concepts represents a conceptual shift in how warfare planning is considered in algorithm design and implementation. This work represents a significant conceptual breakthrough that may have practical consequences in future combat systems.

This work was supported by the Office of Naval Research (Code 311).

Approved by:

KENNETH C. BAILE, Head
Combat Systems Department

CONTENTS

Contents (Continued)

ILLUSTRATIONS

CHAPTER 1

INTRODUCTION

The purpose of this study is to determine for each individual threat in an AAW or TBM engagement the likelihood that the combat system will engage a defended area or a particular ship in a task force. The threats include both Anti-Ship Cruise Missiles (ASCM) and Tactical Ballistic Missiles (TBM). Their intended targets may include ships at sea and/or extended shore areas and/or specified shore positions. Any of these potential targets are to be defended.

Matters of engageability or fire control are not considered. Each threat is to be assigned a value indicating both the potential harm it is capable of inflicting and the urgency by which the defenders should deal with it. These two metrics, of "Potential Harm" and "Urgency" are quantized so that they are available to the decision-maker that prioritizes and engages the threats. Or, these two measures may be combined into a single value. This approach does not consider the decision procedure invoked after the threat evaluation.

In view of the limited scope of the present study as outlined, the inputs required in this study are threat state information and the positions of the defended points and areas. The shooting capacity of a particular defensive platform or defense strategy is not needed. The positions of the ships may change during the engagement. An assignment of value is given each defended point and area. We do not consider complications related to situational variation in value (*e.g.*, the increased value of a surviving carrier after loss of the others).

The threat information ideally consists of the time histories of all threats. The past track history of a threat undoubtedly contains information of use in its identification as well as prediction of its potential future behavior. However, for simplicity, the only threat information used is the latest threat-state estimate and error covariance for each threat, plus any estimate of its physical parameters that may be available. Usage of past flight history in the estimation of physical parameters is assumed to have been carried out previously.

The metrics Potential Harm and Urgency each require knowledge or a hypothesis regarding the threat goal. Since the state of a threat cannot be known with certainty, an "Objective Probability" is estimated for each of its possible targets.

Chapter 2 gives an overview of how the threats are evaluated. Chapters 3, 4, and 5 discuss the treatment of ASCM threats. Chapters 6, 7, and 8 discuss the TBM threat. Chapter 9 discusses the method by which the Objective Probabilities and other evaluation parameters are estimated. Chapter 10 discusses the organization of the computations. Chapter 11 gives a summary and conclusions.

Of crucial importance is the estimation of the Earliest Time of Arrival (ETA) of a given threat to a given asset (for all threat-asset pairings). Without knowledge of the intention or capability of the threat, the assumed future time history of the threat position is hypothetical. The assumptions on which the ETA is based are designed to result in a simple algorithm that can be implemented without great expenditure of computing resources and still provide a usable value to represent a rough *lower bound* of the possible ETA. Thus, the objective is to represent the most pessimistic (*i.e.*, conservative) situation. The ASCM threat is assumed to be unpowered and flying with constant speed. Not only is this a questionable assumption, but selection of the speed value introduces further error.

For an ASCM this value is set equal to the expected speed from the latest state estimate. For a small to moderate threat range these assumptions may not be too bad. But when the latest observed threat altitude is high, this estimate may grossly underestimate the average speed and correspondingly overestimate the ETA. This suggests a future upgrade in which a "constant energy" rather than a "constant speed" trajectory is used in some cases for the estimation of ETA.

CHAPTER 2

OVERVIEW OF THREAT EVALUATION

We make provision for treating two kinds of threats,

ASCM

TBM

and two kinds of defended positions,

Defended Points (*e.g.*, ships)

Defended Shore Areas (*e.g.*, cities)

Treatment of ASCMs differs from treatment of TBMs in the following respects. Each ASCM is considered potentially able to target any of the Defended Points. These are given "Objective Probabilities" to indicate which are more likely to be targeted. These Objective Probabilities therefore depend on each Threat-Objective pairing.

For simplicity, the Objective Probabilities are based on the *expected* state of the threat, regardless of the errors in the state estimation. Maneuver is required for the threat to reach any of the Defended Points. The Objective Probability is high for points that can be reached quickly (early time of arrival) and easily (low drag loss). The Objective Probability is zero for those points impossible for the threat to reach under reasonable assumptions regarding its flight capabilities.

In contrast, the trajectory of a TBM is considered determined by its characteristics (*e.g.*, mass, drag coefficient, etc.) and initial state. Maneuver is not considered. A trajectory calculated by simple prediction from the initial expected state may not reach any of the defended assets. But these are possible targets because the initial threat state and aerodynamic characteristics are not precisely known. Accordingly, both the expected initial threat state and the covariance matrix of the threat-state estimation errors, as well as the aerodynamic uncertainties, are calculated. These determine a "footprint," which is the Probability Density Function (PDF) of the threat's impact point. (The reader is cautioned that the term "footprint" has been given other meanings.) Defended Points lying within this footprint are assigned Objective Probabilities related to the footprint PDF.

Extended shore areas may be targets of TBMs, but not of ASCMs unless there are Defended Points within the area. The Defended Points are represented by their positions, which may move during the engagement, and by an "Actual Value" (V_a), and a "Perceived Value" (V_p). The Perceived Value is used to calculate the Objective Probability, while the Actual Value determines how much effort is to be expended in its defense.

A Defended Area can be represented geometrically by a stationary circle, ellipse, or a polygon. The programs and examples presented here use ellipses. A TBM generates an Objective Probability determined by the intersection of its footprint onto the Defended Area. There is no structure. A real defended area such as a city might have variation in value throughout its area. This feature can be simulated by placing defended points within the area.

The Objective Probabilities form a two-dimensional matrix whose dimensions equal the number of threats (active at a given time) in one dimension, and the number of Defended Points and Defended Areas in the other. These values, along with the V_a and V_p values, constitute an important input into the evaluation of the threats.

Engageability of the threat is not considered. The number and positions of the shooting platforms is not included among the data used. No PIPs are generated. The Objective Probabilities are estimated without regard to whether or not the threat can be engaged, or the most favorable launch times, etc.

2.1 Simplified Trajectories

For each (ASCM - Defended Point) pair a trajectory producing the soonest arrival time is determined. The initial threat-state error covariance is ignored, and the trajectory is based entirely on the initial *expected* state. The initial speed is maintained constant throughout the flight. The trajectory producing the earliest arrival time is determined. This will usually lie on the plane determined by the initial threat velocity and the Defended Point. Initially there is a maximum-g turn followed by a CV segment to the Defended Point. Cases where this pattern would require the threat to fly below the sea surface are adjusted.

The initial state estimate of a TBM including the covariance matrix generates a suite of trajectories, one for each possible initial state. The flight maintains constant speed with no maneuver, following a Keplerian orbit modified for liftless drag in an exponential atmosphere.

2.2 Determination of the Objective Probabilities

At any given time, all the threats that are active at that time are considered one by one.

The ASCMs are treated separately from the TBMs.

For an ASCM, all the Defended Points are considered one by one. For each Defended Point the drag loss along the simplified trajectory is approximated based upon available threat information. Incomplete threat information is assumed to satisfy the hypotheses that it minimizes both flight time and drag loss. The Objective Probability for each Defended Point is based on these two values. After all Objective Probabilities have been approximated in this way, they are normalized so that their sum over all Defended Points is unity.

For a TBM, the first step is to estimate its footprint in order to determine where it will land on the Earth's surface. The expected initial threat state is used to determine a single Keplerian trajectory to the Earth surface, to find an impact position and arrival time. Next, the atmospheric effect is approximated by using a simplified dynamic model of a mass point falling in a planar orbit, without lift, from the expected initial state to the Earth's surface. The resulting flight time and distance provide a correction to the previously-determined Keplerian orbit to give a more accurate impact position and flight time.

The initial state covariance is assumed to be Gaussian. Even with this idealization, the complicated nonlinear flight path makes it difficult to get a closed-form footprint PDF. Instead, the impact position covariance is determined by assuming small errors and a parabolic planar trajectory through an airless medium. This impact covariance is centered on the expected impact point and is used to generate a two-dimensional Gaussian PDF to represent the impact footprint.

Defended Points lying within the impact footprint are assigned Objective Probabilities related to the Perceived Value and the PDF density at that position. Defended Areas intersecting the footprint are assigned Objective Probabilities related to their Perceived Values and the integrated footprint probability of impact in the intersection.

2.3 Coordinate Transformations

Basically, all positions are referred to (rotating) geographic coordinates (ϕ, L, r). Velocities, on the other hand, are represented as dimensional components (u, v, w) in [L/T] in the directions (ϕ, L, r) at each point. (This means that the vector represented by certain components at one point is not parallel to the vector represented by the same components at another point.) It is useful to find the transformation between velocity components at two different points. To do this, it is convenient to define a Cartesian coordinate system (x_1, y_1, z_1) tangent to the Earth at the geographic position (ϕ_1, L_1, a), with x_1 increasing Eastward, y_1 Northward, and z_1 up. This will be referred to as a "Local Cartesian System".

The velocity in this system is represented by the components (u_1, v_1, w_1) in the directions (x_1, y_1, z_1).

A velocity vector at a given geographic point (ϕ, L, r) is represented by components (u, v, w), assumed to be given in the Local Cartesian System referred to the point (ϕ, L, a) (directly below). It is required to relate the coordinates of points and the components of vectors in one Local Cartesian System to those in another.

Define two intermediate coordinate systems. One is the rotating Earth-Centered Cartesian System (ECCS) $(\tilde{x}_1, \tilde{y}_1, \tilde{z}_1)$, where $\tilde{y}_1$ is along the rotation axis pointing toward the North Pole, $\tilde{z}_1$ is in the direction of the meridian ϕ_1, and $\tilde{x}_1$ ninety degrees East of this meridian. The transformation between (ϕ, L, r) to $(\tilde{x}_1, \tilde{y}_1, \tilde{z}_1)$ is

$$\begin{aligned} \tilde{x}_1 &= r\cos L \sin(\phi - \phi_1) \\ \tilde{y}_1 &= r \sin L \\ \tilde{z}_1 &= r\cos L \cos(\phi - \phi_1) \end{aligned} \tag{2.1}$$

The second is a rotating Cartesian Coordinate system $(\hat{x}_1, \hat{y}_1, \hat{z}_1)$, with axes parallel to the ECCS but centered on the position (ϕ_1, L_1, a). The transformation between these systems is

$$\begin{aligned} \hat{x}_1 &= \tilde{x}_1 \\ \hat{y}_1 &= \tilde{y}_1 - a \sin L_1 \\ \hat{z}_1 &= \tilde{z}_1 - a \cos L_1 \end{aligned} \tag{2.2}$$

Then the system (x_1, y_1, z_1) is obtained from $(\hat{x}_1, \hat{y}_1, \hat{z}_1)$ by a rotation about the $\hat{x}_1$ axis, according to

$$\begin{aligned} x_1 &= \hat{x}_1 & \hat{x}_1 &= x_1 \\ y_1 &= \hat{y}_1 \cos L_1 - \hat{z}_1 \sin L_1 & \hat{y}_1 &= y_1 \cos L_1 + z_1 \sin L_1 \\ z_1 &= \hat{y}_1 \sin L_1 + \hat{z}_1 \cos L_1 & \hat{z}_1 &= -y_1 \sin L_1 + z_1 \cos L_1 \end{aligned} \tag{2.3}$$

All these systems are non-inertial, being attached to the rotating Earth.

Consider now a second Local Cartesian System, and corresponding intermediate systems defined in the same way as the above, with all the subscripts "1" replaced by "2". Then transformation of the components of velocity referred to system "1" to components in system "2" is done by

$$\begin{pmatrix} u_2 \\ v_2 \\ w_2 \end{pmatrix} = \frac{\partial(x_2, y_2, z_2)}{\partial(x_1, y_1, z_1)} \begin{pmatrix} u_1 \\ v_1 \\ w_1 \end{pmatrix} \tag{2.4}$$

where

$$\frac{\partial(x_2, y_2, z_2)}{\partial(x_1, y_1, z_1)} = \begin{pmatrix} \frac{\partial x_2}{\partial x_1} & \frac{\partial x_2}{\partial y_1} & \frac{\partial x_2}{\partial z_1} \\ \frac{\partial y_2}{\partial x_1} & \frac{\partial y_2}{\partial y_1} & \frac{\partial y_2}{\partial z_1} \\ \frac{\partial z_2}{\partial x_1} & \frac{\partial z_2}{\partial y_1} & \frac{\partial z_2}{\partial z_1} \end{pmatrix} \tag{2.5}$$

is a Jacobian (matrix), and will be denoted by J_{21}. This matrix can be found by

$$J_{21} = J_{2\hat{2}} J_{\hat{2}\tilde{2}} J_{\tilde{2}g} J_{g\tilde{1}} J_{\tilde{1}\hat{1}} J_{\hat{1}1} \tag{2.6}$$

where the suffix "g" stands for the geographic coordinates (ϕ, L, r). Reversing the subscripts is equivalent to taking the inverse since the transformation matrices are orthogonal. It is noted that $J_{\hat{2}\tilde{2}}$ and $J_{\tilde{1}\hat{1}}$ are just the identity matrices. Since J_{21} transforms between two Cartesian systems, its value is independent of position. This can be seen by calculating the product of the inner four factors of (2.6) obtaining

$$J_p = J_{\hat{2}\tilde{2}} J_{\tilde{2}g} J_{g\tilde{1}} J_{\tilde{1}\hat{1}} = \begin{pmatrix} \cos(\phi_1 - \phi_2) & 0 & \sin(\phi_1 - \phi_2) \\ 0 & 1 & 0 \\ \sin(\phi_2 - \phi_1) & 0 & \cos(\phi_1 - \phi_2) \end{pmatrix} \tag{2.7}$$

The transformation (2.6) is then

$$J_{21} = \begin{pmatrix} \cos(\phi_1 - \phi_2) & -\sin L_1 \sin(\phi_1 - \phi_2) & \cos L_1 \sin(\phi_1 - \phi_2) \\ \sin L_2 \sin(\phi_1 - \phi_2) & \cos L_1 \cos L_2 + \sin L_1 \sin L_2 \cos(\phi_1 - \phi_2) & \sin L_1 \cos L_2 - \cos L_1 \sin L_2 \cos(\phi_1 - \phi_2) \\ -\cos L_2 \sin(\phi_1 - \phi_2) & \cos L_1 \sin L_2 - \sin L_1 \cos L_2 \cos(\phi_1 - \phi_2) & \sin L_1 \sin L_2 + \cos L_1 \cos L_2 \cos(\phi_1 - \phi_2) \end{pmatrix} \tag{2.8}$$

As an example of the importance of this transformation, consider a missile at 30 degrees N travelling due E at 1000 m/s. Relative to a Local Cartesian System based on a point one degree further East, this missile has a Southward velocity of 8 m/s and an upward velocity of 15 m/s.

2.4 Representation of Defended Areas

Defended areas are represented by ellipses with specified semimajor axes a, semiminor axes b, centers (x_0, y_0), and directions ϕ_a of their lines of apsides (with $\phi_a \in (-\pi/2, \pi/2]$). These quantities determine the eccentricities

$$e = \sqrt{1 - \frac{b^2}{a^2}} \tag{2.9}$$

and the positions of their foci,

$$\begin{aligned} x_{f1} &= x_0 - ae\cos\phi_a, & x_{f2} &= x_0 + ae\cos\phi_a \\ y_{f1} &= y_0 - ae\sin\phi_a, & y_{f2} &= y_0 + ae\sin\phi_a \end{aligned} \tag{2.10}$$

The equation for the ellipse in polar form is

$$r = \frac{a(1 - e^2)}{1 - e\cos(\theta - \phi_a)} \tag{2.11}$$

where (r, θ) are polar coordinates relative to the point (x_{f1}, y_{f1}). Either focus could have been used. For (r, θ) to represent polar coordinates relative to the point (x_{f2}, y_{f2}), the first minus sign in the denominator of (2.11) is replaced by a plus. The area within the ellipse is

$$\text{area} = \pi ab \tag{2.12}$$

Each defended area j is assigned a "perceived value" per unit area, $W_j^{(p)}$ and an "actual value" per unit area, $W_j^{(a)}$.

CHAPTER 3

SIMPLIFIED ASCM TRAJECTORIES

It is necessary to prioritize engagements against threats in scenarios with a large number n of threats, and also a large number m of possible targeted assets. The amount of computation for an engagement schedule needs to be kept within reasonable bounds. The objective of each threat is not known, but the number of threat-objective pairs is of the order of nm. Even if the objective were known, the threat trajectory is not. If all possible trajectories are considered the amount of computing can easily grow unacceptably large for only a few engagements. For this reason, the "Simplified Trajectories" approach presented in this section is needed.

The information needed to prioritize the threats includes arrival times to all defended assets. The arrival time to a given asset for a given threat is determined by a single simplified hypothetical "Earliest Arrival Time" (ETA) trajectory. This trajectory is based on the following assumptions:

- A maximum allowed lateral-acceleration magnitude, a_m, is specified. This value can be determined by intelligence data or classification based on imaging or past threat behavior. A generic value is used if there is complete ignorance of the threat type. The value a_m can be altered at any time additional information becomes available.
- A maximum allowed heading error (HE), ϕ_m, is specified. The HE is the angle between the threat velocity and the asset direction. The value ϕ_m attempts to represent the limitation on the threat's seeker geometry. Ideally, we would be concerned with the look angle, *i.e.*, the angle between the threat body axis and the asset direction. However, the simple analysis proposed here treats the threat as a moving point, and consequently there is no body axis to which to refer the look angle. The velocity vector serves as a reasonable substitute, and thus the limitation ϕ_m is placed on the HE. As in the case of a_m, the value ϕ_m can be determined by intelligence data or classification based on any available information, and can be altered during the course of the battle.
- Constant speed is assumed. This speed is determined by the latest threat-state estimate.

It is evident that these assumptions require that the ETA trajectory lie on a single flight

plane and consist of two segments, "primary" and "secondary". The primary segment is CTR with the maximum-allowed lateral acceleration a_m, terminating when the velocity is directed toward the targeted asset. The secondary segment is CV to reach the asset. It will be shown below that if the HE constraint is initially satisfied it will remain so.

There is also a "Latest Time of Arrival" (LTA) trajectory, defined as a single CTR arc. It may be possible to artificially reduce the threat speed by applying a "maneuver factor", f_m. As a guide for selecting f_m, note that a planar weaving track consisting of alternate CTR turns is longer than the corresponding CV track by the factor $1/f_m = \phi/\sin\phi$, where ϕ is the maximum heading error. Even though the LTA trajectory is not used at this time for threat evaluation, it is included in our discussion both for general interest as well as for providing the most natural limiting case for delayed arrivals.

The previous paragraphs define the two limiting trajectories including the exceptional case when blind application of the trajectory rule drives the threat trajectory beneath the sea surface, as may happen in some cases with a diving threat. This case is taken up in Section 3.3 and in Chapter 4.

Let $\vec{r}_0$, $\vec{r}_s$, and $\dot{\vec{r}}_0$ be the given initial threat and objective positions and threat velocity. The vectors $\vec{r}_s - \vec{r}_0$ and $\dot{\vec{r}}_0$ determine the plane upon which the trajectory is assumed to lie. On this flight plane, two very idealized trajectories are constructed. One is used to find an approximate ETA, the other to find an approximate LTA. The former (ETA) is an important quantity used in the threat prioritization. The latter (LTA) is of lesser interest.

3.1 The ETA Trajectory

It is self-evident that the trajectory allowing the soonest arrival will execute a maximum acceleration magnitude arc until headed toward the objective and then fly CV (constant velocity). While it is impossible to guess the threat's intention, it can at least be said that the arrival time determined by this ETA trajectory provides a lower bound for the arrival time.

Consider first the maximum g arc. Let the center of curvature lie at the point

$$\vec{r}_c = \vec{r}_0 + A\dot{\vec{r}}_0 + B(\vec{r}_0 - \vec{r}_s) \tag{3.1}$$

where A and B are constants to be determined. The conditions determining these constants are

$$\begin{aligned} |\vec{r}_0 - \vec{r}_c|^2 &= b_m^2 \\ \dot{\vec{r}}_0 \cdot (\vec{r}_0 - \vec{r}_c) &= 0 \end{aligned} \tag{3.2}$$

These conditions determine the constants in (3.1) to be

$$B = \frac{\pm b_m V_t}{\sqrt{V_t^2 |\vec{r}_0 - \vec{r}_s|^2 - [\dot{\vec{r}}_0 \cdot (\vec{r}_s - \vec{r}_0)]^2}}, \qquad A = \frac{\dot{\vec{r}}_0 \cdot (\vec{r}_s - \vec{r}_0)}{V_t^2} B \tag{3.3}$$

If the radical in (3.3) is too small for practical computation, the direction of $\dot{\vec{r}}_0$ is close to the direction of $\vec{r}_s - \vec{r}_0$, (or in the opposite direction) and the entire trajectory can be taken as CV. (A test should be performed to exclude the case where the directions are opposite to each other, which normally is excluded by the HE constraint.) The two signs in (3.3) determine points on the flight plane right and left of the threat's directional motion. The point lying closer to the objective is the appropriate arc center, and is determined by the condition

$$(\vec{r}_c - \vec{r}_0) \cdot (\vec{r}_s - \vec{r}_0) > 0 \tag{3.4}$$

This condition selects the negative sign in (3.3).

Consider the point $\vec{r}_t$ where flight transitions from the arc to the CV segment. Movement in the CTR segment can be represented by the formula

$$\vec{r}(t) = \vec{r}_0 + \omega^{-1} \dot{\vec{r}}_0 \sin \omega t + \omega^{-2} \ddot{\vec{r}}_0 (1 - \cos \omega t) \tag{3.5}$$

(see Groves et al, 1992 or 1994), where the subscripts "0" refer to the initial state, and

$$\omega = \frac{|\ddot{\vec{r}}_0|}{|\dot{\vec{r}}_0|} = \frac{V_t}{b} \tag{3.6}$$

being the turning rate and b the turn radius. With a maximum "g" turn, the initial acceleration is

$$\ddot{\vec{r}}_0 = \frac{V_t^2 (\vec{r}_c - \vec{r}_0)}{b_m^2} \tag{3.7}$$

with $b_m = V_t^2 / a_m$ being the minimum allowed turn radius. If t_t is the time when the threat reaches the transition point, we have

$$\vec{r}_t = \vec{r}_0 + V_t^{-1} b_m \dot{\vec{r}}_0 \sin \omega t_t + (1 - \cos \omega t_t)(\vec{r}_c - \vec{r}_0) \tag{3.8}$$

The condition

$$(\vec{r}_t - \vec{r}_c) \cdot (\vec{r}_t - \vec{r}_s) = 0 \tag{3.9}$$

requires that

$$C \cos \omega t_t + D \sin \omega t_t = b_m^2 \tag{3.10}$$

where

$$C = b_m^2 - (\vec{r}_c - \vec{r}_0) \cdot (\vec{r}_s - \vec{r}_0), \qquad D = V_t^{-1} b_m \dot{\vec{r}}_0 \cdot (\vec{r}_s - \vec{r}_0) \tag{3.11}$$

If

$$C^2 + D^2 < b_m^4 \tag{3.12}$$

there is no solution. Otherwise, the argument of the trig functions in (3.10) is given by either of

$$\begin{aligned} \alpha_1 = \omega t_t &= \arccos\left(b_m^2/\sqrt{C^2+D^2}\right) - \text{atan2}(-D, C) \\ \alpha_2 = \omega t_t &= 2\pi - \arccos\left(b_m^2/\sqrt{C^2+D^2}\right) - \text{atan2}(-D, C) \end{aligned} \tag{3.13}$$

These values are placed into the interval $[0, 2\pi)$ by adding or subtracting 2π if necessary. The smaller value is then used to determine $\vec{r}_t$ from (3.8). At this point, $\vec{r}_t$ is tested to insure that it lie above the sea surface ($z_t \geq 0$). Otherwise the threat is unable to reach its objective by the simplified trajectory under discussion here, and the possibility of a different suitable trajectory is considered in Section 3.3 and Chapter 4.

It can be demonstrated that if the HE constraint is satisfied initially, it remains satisfied. Consider

$$\cos\phi = \frac{\dot{\vec{r}} \cdot (\vec{r}_s - \vec{r})}{V_t |\vec{r}_s - \vec{r}|} \tag{3.14}$$

In a special coordinate system in which $\vec{r}_0$ is translated to the origin, rotated so that $\vec{r}_c = (-b_m, 0)$ and the linear dimensions scaled by defining

$$\begin{aligned} x_s &= \xi / b_m \\ y_s &= \eta / b_m \end{aligned} \tag{3.15}$$

and representing the (x, y) coordinates of a point on the CTR arc in terms of the polar angle,

$$\begin{aligned} x &= \cos\theta \\ y &= \sin\theta \end{aligned} \tag{3.16}$$

(3.14) becomes

$$\cos\phi = \frac{-\xi \sin\theta + \eta \cos\theta}{\sqrt{\xi^2 + \eta^2 + 1 - 2\xi\cos\theta + \eta\sin\theta}} \tag{3.17}$$

The initial rate of change of (3.17) with respect to θ is

$$\frac{d}{d\theta}[\cos\phi]_{\theta=0} = \frac{-\xi(\xi^2+\eta^2) - \xi^2}{\sqrt{[(\xi-1)^2+\eta^2]^3}} \tag{3.18}$$

Since for a valid trajectory the point (x_s, y_s) must lie outside the circle

$$(x_s + b_m)^2 + y_s^2 = b_m^2$$

the relation

$$\eta^2 > 1 - (\xi + 1)^2 \tag{3.19}$$

must hold. Then the expression (3.17) is always positive for negative ξ showing that ϕ is always increasing. The situation at positive ξ is irrelevant because in that case the CTR arc would turn in the opposite sense.

3.2 The LTA Trajectory

It is difficult to find an objective way to estimate how late the threat could delay its arrival. A reasonable assumption is that he will not want to delay more than required to execute a few evasive maneuvers. In any case, estimation of LTA is not as important as the ETA, since it is not used for threat evaluation.

Define a rough LTA trajectory as consisting of a single circular arc on the same flight plane as was used for ETA. This will provide an arrival time somewhat later than the ETA, but perhaps not late enough. Further massaging may be done by subsequently applying a "Maneuver Factor".

Again representing $\vec{r}_c$ by (3.1), determination of the center of curvature is somewhat different than for ETA because the radius of curvature b is not known a priori. The conditions to determine $\vec{r}_c$ are

$$\begin{aligned} |\vec{r}_s - \vec{r}_c|^2 = |\vec{r}_0 - \vec{r}_c|^2 = b^2 \\ \dot{\vec{r}}_0 \cdot (\vec{r}_0 - \vec{r}_c) = 0 \end{aligned} \tag{3.20}$$

requiring that the arc radius b be the same at the initial and final threat positions. These conditions lead to the following linear equations in A and B.

$$\begin{aligned} V_t^2 A + \dot{\vec{r}}_0 \cdot (\vec{r}_0 - \vec{r}_s) B = 0 \\ 2\dot{\vec{r}}_0 \cdot (\vec{r}_0 - \vec{r}_s) A + 2|\vec{r}_0 - \vec{r}_s|^2 B = -|\vec{r}_0 - \vec{r}_s|^2 \end{aligned} \tag{3.21}$$

After B and A are determined by (3.21), the arc radius b is given by (3.14), and the arc length θ_s is given by

$$\cos\theta_s = (\vec{r}_0 - \vec{r}_c) \cdot (\vec{r}_s - \vec{r}_c)/b^2 \tag{3.22}$$

A test is now made to insure that the LTA trajectory thus obtained lie entirely above the sea surface. The direction of the derivative (3.13) with θ_s and $\vec{r}_s$ replacing θ_t and $\vec{r}_t$ will be downward in a "dry" trajectory. If this is not the case the LTA trajectory can be modified to keep it out of the water (see Section 3.3). Examples of the ETA and the LTA trajectories are shown in Figure 3.1

3.3 Keeping the ASCM Above the Sea Surface

If the ETA trajectory as described above indicates flight below the sea surface, an alternative "dry" trajectory is sometimes available (see Chapter 4). If the ETA trajectory is entirely above the sea surface but the LTA trajectory is not, an alternative "dry" LTA trajectory is possible. Whether or not the original LTA trajectory crosses the sea surface is determined by examining the sign of the vertical velocity component upon arrival at the target. If $\dot{z}_s < 0$, the final velocity is downward and the original LTA trajectory is ok. Otherwise, a "dry" LTA trajectory is found as described below.

The modified trajectory will consist of an initial CTR segment followed by a terminal sea-skimming CV segment. The point of transition between these segments is denoted by $\vec{r}_t$. Both segments, and the transition point, lie on a flight plane containing the points $\vec{r}_0$ and $\vec{r}_s$, and oriented so that it contain the initial velocity vector $\dot{\vec{r}}_0$. First, determine the hypothetical "splash" point $\vec{r}_i$, where the threat would hit the water if it continued in CV flight from its initial state. This splash point is given by

$$\vec{r}_i = \vec{r}_0 - \frac{z_0 \dot{\vec{r}}_0}{\dot{z}_0} \tag{3.23}$$

(see Figure 3.2). It is evident that this splash point also lies on the flight plane. From symmetry, it is seen that the distance from the splash point to the transition point is equal to the distance from the splash point to the initial position. Call this distance a. Then the transition point is determined by

$$\vec{r}_t = \frac{a(\vec{r}_s - \vec{r}_i)}{|\vec{r}_s - \vec{r}_i|}, \quad \text{where} \quad a = \frac{V_t z_0}{|\dot{z}_0|} \tag{3.24}$$

The Pythagoras relation in the triangle OTS is

$$a^2 + b^2 = |\vec{r}_i - \vec{r}_t|^2 \tag{3.25}$$

determining the radius of curvature b. This value should be no smaller than the allowed b_m in view of the fact that the ETA trajectory did not cross the sea surface. The arc length of the CTR segment is then given by

$$\theta = 2 \arctan(a/b) \tag{3.26}$$

and the length of the CV segment is

$$s = |\vec{r}_s - \vec{r}_t| \tag{3.27}$$

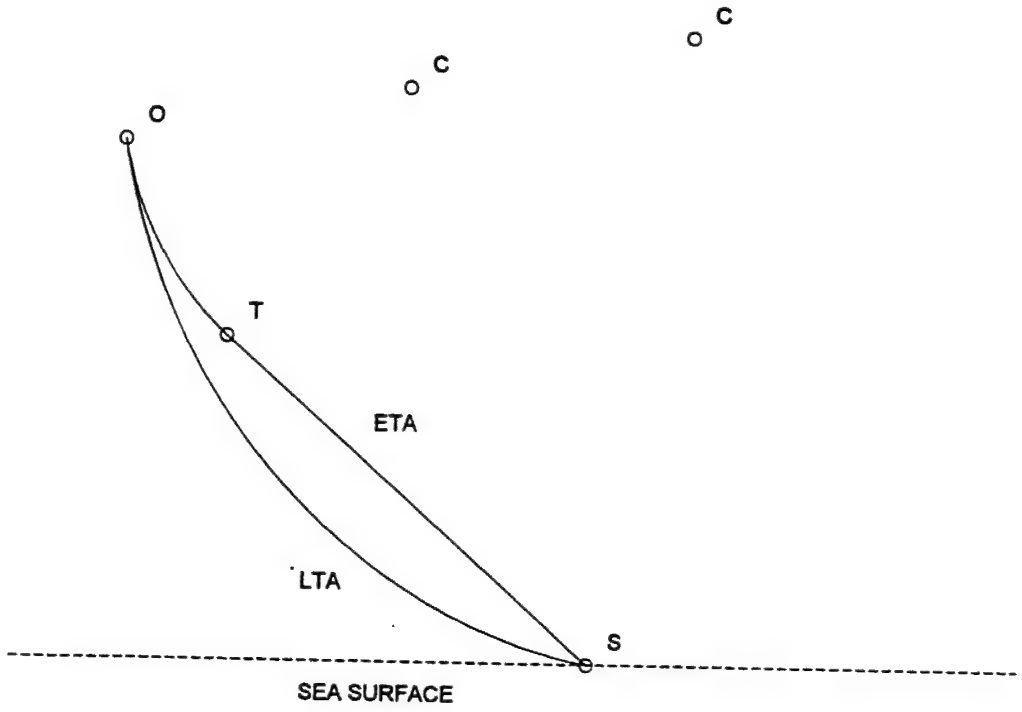

Figure 3.1. Geometry of the ETA and LTA Trajectories. The flight plane contains the initial threat position "O" and velocity "V", and defended point position "S". The two centers of curvature are indicated by "C".

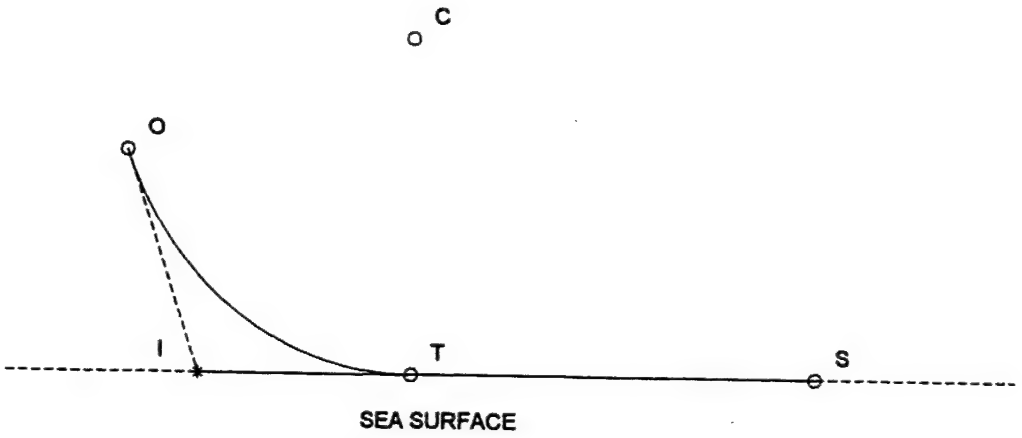

Figure 3.2. Geometry of the "Dry" LTA Trajectory. The impact point "I" is where the threat would hit the sea surface if it flew an initial CV track.

CHAPTER 4

SEASKIMMING TRAJECTORIES

4.1 The "Dual-Arc" Conjecture

This conjecture is related to finding an alternative simplified ASCM trajectory when the ETA trajectory determined according to the process described in Chapter 3 is partially under water. There are not many cases where this will occur in practice. But when it does, as in some cases of diving threats, there will be a few instances where a valid trajectory can be kept out of the water. Although this situation may occur rarely, it is safer to account for this possibility than to ignore cases where an asset could be in jeopardy.

First, a definition:

A *Valid Trajectory* for a given expected initial state, targeted point, maximum allowed heading error and lateral-acceleration magnitude ($\vec{r}_0$, $\dot{\vec{r}}_0$, $\vec{r}_s$, ϕ_m, and a_m) is one consisting of a number of CV and CTR segments terminating at the targeted point, with continuity of position and velocity at the transition points between segments, where the speed is constant, and $z \geq 0$ everywhere.

The Conjecture: If a valid trajectory exists, there will also exist a valid trajectory consisting of two CTR arcs, the final arc lying along the sea surface. (Here it is understood that CV is a special case of CTR.) We have been unable to prove this and invite any interested reader to communicate his results to us if he is able to find a proof or a counter example.

Consider a flight plane of a primary arc, which contains the initial velocity vector $\dot{\vec{r}}_0$ but otherwise is unconstrained, allowing a one-parameter family of such planes. A Cartesian coordinate system (ξ, η, ζ) is attached to this flight plane with its origin at the initial threat position $\vec{r}_0$. Orthogonal unit vectors $(\dot{\vec{r}}_0 V_t^{-1}, \vec{u}, \vec{v})$ form a right-handed system and point in the direction of increasing (ξ, η, ζ). The flight plane contains the vectors $\dot{\vec{r}}_0$ and $\vec{v}$, is perpendicular to $\vec{u}$, and is characterized by the equation $\eta = 0$.

One parameter, λ, determines the orientation of the flight plane according to the relation

$$\begin{aligned} \vec{u} &= \vec{\alpha}\cos\lambda - \vec{\beta}\sin\lambda \\ \vec{v} &= \vec{\alpha}\sin\lambda + \vec{\beta}\cos\lambda \end{aligned} \tag{4.1}$$

where $(\dot{\vec{r}}_0 V^{-1}, \vec{\alpha}, \vec{\beta})$ is another right-handed set of orthogonal unit vectors that obey the

conditions

$$\vec{\alpha}\cdot\dot{\vec{r}}_0 = 0, \quad \vec{\beta}\cdot\dot{\vec{r}}_0 = 0, \quad \vec{\alpha}\cdot\vec{\beta} = 0, \quad \vec{\beta}\cdot\vec{k} = 0, \quad \vec{\alpha}\cdot\vec{k} \geq 0 \tag{4.2}$$

According to these definitions, the unit vectors $\vec{\alpha}$ and $\vec{\beta}$ are related to the Cartesian unit vectors $(\vec{i},\vec{j},\vec{k})$ by

$$\vec{\alpha} = \frac{-(\dot{x}_0\vec{i}+\dot{y}_0\vec{j})\dot{z}_0 + V_{h0}^2\vec{k}}{V_t V_{h0}}, \quad \vec{\beta} = \frac{\dot{y}_0\vec{i}-\dot{x}_0\vec{j}}{V_{h0}} \tag{4.3}$$

where

$$V_{h0} = \sqrt{\dot{x}_0^2+\dot{y}_0^2} \tag{4.4}$$

A point on the flight plane having coordinates (ξ,ζ) is located at

$$\vec{r} = \vec{r}_0 + \dot{\vec{r}}_0 V_t^{-1}\xi + \zeta\vec{v} \tag{4.5}$$

In other words,

$$\begin{aligned} \xi &= (\vec{r}-\vec{r}_0)\cdot\dot{\vec{r}}_0 V_t^{-1} \\ \zeta &= (\vec{r}-\vec{r}_0)\cdot\vec{v} \end{aligned} \tag{4.6}$$

The Cartesian components of (4.5) are

$$\begin{aligned} x &= x_0 + \dot{x}_0 V_t^{-1}\xi + [-\dot{x}_0\dot{z}_0\sin(\lambda) + \dot{y}_0 V_t\cos(\lambda)]V_t^{-1}V_{h0}^{-1}\zeta \\ y &= y_0 + \dot{y}_0 V_t^{-1}\xi + [-\dot{y}_0\dot{z}_0\sin(\lambda) - \dot{x}_0 V_t\cos(\lambda)]V_t^{-1}V_{h0}^{-1}\zeta \\ z &= z_0 + \dot{z}_0 V_t^{-1}\xi + V_{h0}\sin(\lambda)V_t^{-1}\zeta \end{aligned} \tag{4.7}$$

Constant-speed flight in a circular arc can be expressed in the form

$$\vec{r}(t) = \vec{r}_0 + \dot{\vec{r}}_0\omega^{-1}\sin(\omega t) + \ddot{\vec{r}}_0\omega^{-2}[1-\cos(\omega t)] \tag{4.8}$$

(see Groves et al, 1992 or 1994) where

$$\omega = |\ddot{\vec{r}}|/|\dot{\vec{r}}| \tag{4.9}$$

is constant. If the arc (4.8) is tangent at the sea surface, both z and $\dot{z}$ vanish there, and we have

$$\begin{aligned} z(t_t) &= z_0 + \dot{z}_0\omega^{-1}\sin(\omega t_t) + \ddot{z}_0\omega^{-2}[1-\cos(\omega t_t)] = 0 \\ \dot{z}(t_t) &= \dot{z}_0\cos(\omega t_t) + \ddot{z}_0\omega^{-1}\sin(\omega t_t) = 0 \end{aligned} \tag{4.10}$$

at the instant $t = t_t$ the threat arrives at the transition point $\vec{r}_t$ on the sea surface. Taking linear combinations of (4.10), it is seen that

$$\cos(\omega t_t) = \frac{\ddot{z}_0}{\ddot{z}_0 + z_0\omega^2}, \quad \sin(\omega t_t) = \frac{-\dot{z}_0\omega}{\ddot{z}_0 + z_0\omega^2} \tag{4.11}$$

Summing the squares of (4.11) it is seen that

$$z_0^2\omega^2 = \dot{z}_0^2 - 2z_0\ddot{z}_0 \tag{4.12}$$

is a condition that an arc on the flight plane meet the sea surface at a point of tangency.

Consider the problem of determining $\ddot{\vec{r}}_0$ from a given $\vec{r}_0$, $\dot{\vec{r}}_0$, and λ. The conditions (4.9), (4.12), and the relation $\ddot{\vec{r}}_0 \cdot \vec{u} = 0$ give the equations

$$\begin{aligned} \dot{x}_0\ddot{x}_0 + \dot{y}_0\ddot{y}_0 + \dot{z}_0\ddot{z}_0 &= 0 \\ u_x\ddot{x}_0 + u_y\ddot{y}_0 + u_z\ddot{z}_0 &= 0 \\ z_0^2(\ddot{x}_0^2 + \ddot{y}_0^2 + \ddot{z}_0^2) + 2V_t^2 z_0\ddot{z}_0 &= \dot{z}_0^2 V_t^2 \end{aligned} \tag{4.13}$$

Eliminating $\ddot{x}_0$ and $\ddot{y}_0$ from (4.13) gives a quadratic equation in $\ddot{z}_0$ that may or may not have real solutions.

If the initial lateral acceleration magnitude $|\ddot{\vec{r}}_0|$ (and hence the radius of curvature $b = V_t^2/|\ddot{\vec{r}}_0|$) is given instead of λ, then $\vec{u}$ is unknown and instead of (4.13) the initial acceleration is determined by solving the equations

$$\begin{aligned} \dot{x}_0\ddot{x}_0 + \dot{y}_0\ddot{y}_0 + \dot{z}_0\ddot{z}_0 &= 0 \\ 2V_t^2 z_0\ddot{z}_0 &= \dot{z}_0^2 V_t^2 - z_0^2|\ddot{\vec{r}}_0|^2 \\ \ddot{x}_0^2 + \ddot{y}_0^2 + \ddot{z}_0^2 &= |\ddot{\vec{r}}_0|^2 \end{aligned} \tag{4.14}$$

Consider (4.14) in the space of the acceleration components. The three equations represent, respectively, a plane through the origin, a plane parallel to the $(\ddot{x}_0, \ddot{y}_0)$ plane, and a sphere. The intersection of the plane through the origin with the sphere occurs at values of $\ddot{z}_0$ contained in the interval

$$|\ddot{z}_0| \leq \frac{V_{h0}|\ddot{\vec{r}}_0|}{V_t} \tag{4.15}$$

If the value $\ddot{z}_0$ determined by the second equation of (4.14) lies in this interval, then a real solution exists. This condition requires that

$$\frac{V_t - V_{h0}}{z_0} \leq \omega \leq \frac{V_t + V_{h0}}{z_0} \tag{4.16}$$

The equation in $\ddot{x}_0$ obtained by eliminating $\ddot{y}_0$ from (4.14) is

$$V_{h0}^2\ddot{x}_0^2 + 2\dot{x}\dot{z}\ddot{z}_0\ddot{x}_0 + \ddot{z}_0^2(\dot{y}^2 + \dot{z}^2) - |\ddot{\vec{r}}_0|^2\dot{y}^2 = 0 \tag{4.17}$$

This equation has real roots (for $\ddot{x}_0$) if (4.16) is satisfied. Then the flight plane (λ) is obtained by getting

$$\begin{aligned} \vec{v} &= \ddot{\vec{r}}_0/|\ddot{\vec{r}}_0| \\ \cos\lambda &= \vec{\beta} \cdot \vec{v} \\ \sin\lambda &= \vec{\alpha} \cdot \vec{v} \end{aligned} \tag{4.18}$$

Consider all the possible flight paths that could serve as the primary arc without consideration, for the moment, of the position of the targeted point. Figure 4.1 is a three-dimensional plot on an arbitrary scale of such an example in which a one-dimensional family of candidate trajectories is shown leaving the initial threat position. The trajectories displayed correspond to values of ω at equal increments between the limits (4.16). Each arc is tangent to the sea surface at a point indicated by a dot. These points of tangency lie on a circle, as will now be demonstrated.

Let us introduce a "Special Coordinate System" (SCS) on the sea surface, with coordinates (ξ, η), so that the SCS origin is under the initial threat position, with the ξ axis in the direction of the initial horizontal velocity. With respect to the heretofore used "Basic Coordinate System" (BCS) on the sea surface with coordinates (x, y), the two systems are related by

$$\begin{aligned} \xi &= (x - x_0)\cos\lambda + (y - y_0)\sin\lambda, \qquad & x - x_0 &= \xi\cos\lambda - \eta\sin\lambda \\ \eta &= -(x - x_0)\sin\lambda + (y - y_0)\cos\lambda, \qquad & y - y_0 &= \xi\sin\lambda + \eta\cos\lambda \end{aligned} \tag{4.19}$$

where λ is the azimuth of the initial horizontal threat velocity in the BCS,

$$\lambda = \text{atan2}(v_0, u_0) \tag{4.20}$$

Equations (4.10), (4.11), and (4.12) determine the coordinates of the point of tangency in the SCS, giving

$$\xi_t = \frac{-\dot{\xi}_0\dot{z}_0 + \ddot{\xi}_0 z_0}{\ddot{z}_0 + z_0\omega^2}, \qquad \eta_t = \frac{\ddot{\eta}_0 z_0}{\ddot{z}_0 + z_0\omega^2} \tag{4.21}$$

It is convenient to use ω as the parameter that selects one out of the family of arcs. The initial acceleration is determined by (4.9), (4.12), and the orthogonality of the acceleration and velocity vectors. The result is

$$\begin{aligned} \ddot{\xi}_0 &= -\dot{z}_0(\dot{z}_0^2 - z_0^2\omega^2)/2z_0\dot{\xi}_0 \\ \ddot{\eta}_0 &= \pm V_t\sqrt{\omega^2 - (\dot{z}_0^2 - z_0^2\omega^2)^2/4z_0^2\dot{\xi}_0^2} \\ \ddot{z}_0 &= (\dot{z}_0^2 - z_0^2\omega^2)/2z_0 \end{aligned} \tag{4.22}$$

Substituting these values into (4.21) we obtain the equation of the curve passing thru the points of tangency on the sea surface in terms of the parameter ω. Eliminating ω by first expressing it in terms of ξ_t,

$$\omega^2 = \frac{\dot{z}_0(2z_0\dot{\xi}_0^2 + z_0\dot{z}_0^2 + \dot{\xi}_0\dot{z}_0\xi_t)}{z_0^2(z_0\dot{z}_0 - \dot{\xi}_0\xi_t)} \tag{4.23}$$

after some rearrangement gives

$$\eta_t^2 + \left(\xi_t + \frac{z_0\dot{\xi}_0}{\dot{z}_0}\right)^2 = \frac{z_0^2 V_t^2}{\dot{z}_0^2} \tag{4.24}$$

demonstrating the circular nature of the locus of tangency points, and determining the center and radius. Note that the center of this tangency circle, according to (4.24), is just the point on the sea surface where the threat would impact if it continued in a CV trajectory from its initial condition.

Just as amusing is the fact that the velocity at the points of tangency is directed outward from the center of this "tangency" circle. This velocity is

$$\dot{\vec{r}}_t = \dot{\vec{r}}_0 \cos\omega t_t + \ddot{\vec{r}}_0 \omega^{-1} \sin\omega t_t \tag{4.25}$$

according to (4.8). Combining this with the conditions (4.11) gives

$$\dot{\xi}_t = \frac{\ddot{z}_0\dot{\xi}_0 - \dot{z}_0\ddot{\xi}_0}{\ddot{z}_0 + z_0\omega^2}, \qquad \dot{\eta}_t = -\frac{\dot{z}_0\ddot{\eta}_0}{\ddot{z}_0 + z_0\omega^2} \tag{4.26}$$

Using the relations (4.22) and (4.23), it can be shown that

$$\dot{\vec{r}}_t = -\frac{\dot{z}_0}{z_0}\vec{\rho} \tag{4.27}$$

where $\vec{\rho}$ is the vector from the center of the tangency circle to the point of tangency, given by

$$\vec{\rho} = \vec{r}_t + \frac{z_0\dot{\vec{r}}_0}{\dot{z}_0} \tag{4.28}$$

These vectors are shown on an arbitrary scale on the plane of the sea surface in Figure 4.2 for the arcs of Figure 4.1, where the initial threat position projected down onto the sea surface is indicated. The points of tangency are indicated by the dots.

Returning to the BCS, a targeted point $\vec{r}_s$ is added to the example of Figure 4.1. To find the secondary segment of the dual-arc trajectory, use the sea surface as the complex plane, since the segment sought lies on this plane. To find the arc center for the segment continuing from any transition point $\vec{r}_t$, note that its complex value is

$$W_c = W_t + b\,e^{i(\phi+\pi/2)} \tag{4.29}$$

where b is the (signed) radius of curvature and W_t is the position of the transition point, and ϕ is the argument (direction) of the final velocity of the primary segment. The radius b is to be determined by the condition

$$|W_c - W_t|^2 = |W_c - W_s|^2 \tag{4.30}$$

This equation gives the value

$$b = \frac{W_s W_s^* + W_t W_t^* - W_t W_s^* - W_s W_t^*}{(W_s^* - W_t^*)e^{i(\phi+\pi/2)} + (W_s - W_t)e^{-i(\phi+\pi/2)}}$$
$$= \frac{V_t|\vec{r}_s - \vec{r}_t|^2}{2|\dot{\vec{r}}_t \times (\vec{r}_s - \vec{r}_t)|} \tag{4.31}$$

Since both factors in the cross product of (4.31) lie in the (x, y) plane, the product is in the $\pm\vec{k}$ direction, where $\vec{k}$ is in the upward direction. If the product is in the $+\vec{k}$ direction the turn is toward the left, and vice versa. The length of the arc is given by

$$\theta_c = \arccos[b^{-2}(\vec{r}_t - \vec{r}_c) \cdot (\vec{r}_s - \vec{r}_c)] \tag{4.32}$$

Points along this secondary arc are conveniently computed using equation (4.8).

Consider the limiting simplified trajectory, either ETA or LTA, of Chapter 3, whose transition point is on the sea surface. This trajectory will lie on a *single* flight plane, while the dual-arc trajectories generally lie on two flight planes. To determine the single-plane limiting trajectory, find the "impact point" $\vec{r}_i$ on the sea surface if the threat were to fly CV from its initial position. This point is given by

$$\vec{r}_i = \vec{r}_0 - \left(\frac{z_0}{\dot{z}_0}\right)\dot{\vec{r}}_0 \tag{4.33}$$

Referring to Figure 3.2, it is evident from symmetry that the transition point $\vec{r}_t$ is given by

$$\vec{r}_t = \vec{r}_i + \frac{|\vec{r}_0 - \vec{r}_i|}{|\vec{r}_s - \vec{r}_i|}(\vec{r}_s - \vec{r}_i) \tag{4.34}$$

Figure 4.3 shows a plan view of the single family of dual-arc trajectories as solid curves on an arbitrary scale, plus the limiting simplified trajectory shown by the dashed curve. The trajectories have been projected vertically onto the sea surface. The dots indicate the points on the dual-arc trajectories where the primary segment is tangent at the sea surface. The portions of all the trajectories lying outside these tangent points are on the sea surface, while the portions inside these points are above the sea surface. The secondary arc is shown only if the heading error at the transition point does not exceed $\pi/2$.

If a dual-arc trajectory is needed, the dashed limiting trajectory must require a lateral acceleration in excess of the allowed maximum value. It is apparent in Figure 4.3 and similar cases, that there is a dual-arc trajectory (one of the solid curves) in which the maximum lateral acceleration is less than that in the single-segment (dashed) curve. Thus, there exist valid dual-arc trajectories in some cases for which the usual simplified ASCM trajectory would require the threat to fly under water.

Figure 4.4 shows in perspective on an arbitrary scale a family of possible primary arcs for an initial threat velocity that is somewhat downward. The dots at the ends of these arcs lie on the tangency circle on the sea surface.

Examples of other possible dual arc trajectories are shown on an arbitrary scale in Figures 4.5, 4.6, 4.7, and 4.8.

4.2 Dry Trajectories

Consider the "Tangency Circle Coordinate System" (TCCS) in which the origin of the coordinates (X, Y) is at the center of the circle, and the targeted ship is at $(X, Y) = (|\vec{r}_s - \vec{r}_c|, 0)$. The Y axis of the TCCS intersects the ξ axis of the SCS at an angle σ given by

$$\sigma = \text{atan2}[(\xi_s - \xi_c), -\eta_s] \tag{4.35}$$

where $\vec{r}_c$ is the center of the tangency circle and $\vec{r}_s$ is the position of the targeted asset. The transformation between the SCS and the TCCS is

$$\begin{aligned} \xi - \xi_c &= Y\cos\sigma + X\sin\sigma, \qquad & X &= -\eta\cos\sigma + (\xi - \xi_c)\sin\sigma \\ \eta &= Y\sin\sigma - X\cos\sigma, \qquad & Y &= \quad \eta\sin\sigma + (\xi - \xi_c)\cos\sigma \end{aligned} \tag{4.36}$$

The relations between the three coordinate systems are shown in Figure 4.9. Starting with the original BCS represented by the (x, y) axes, the SCS is determined by the position of the threat at point T with horizontal velocity in the direction of C. The ξ axis is along the line TC, which makes the angle λ with the x axis, with the point C being determined by the offset of the center of the tangency circle indicated in (4.24). The SCS origin is at the point T. The TCCS then has its origin at the tangency circle center, C, with the X axis toward the targeted asset position S. The Y axis intersects the ξ axis at an angle σ. The locus of the secondary arc centers is the line parallel to the Y axis, as will be shown below, intersecting the X axis at the point P. The location of P is given by (4.42).

We can assume that the targeted asset lies outside this tangency circle. Otherwise, either a valid simplified trajectory would reach the asset, or no valid dual-arc trajectory would reach it. In either case, there is no need for a dual-arc trajectory.

Position on the tangency circle, $\vec{r}_a$, is specified by the angle β measured counterclockwise from the direction of the targeted asset, according to the relation

$$\vec{r}_a(\beta) = \vec{r}_c + b_c(\vec{i}\cos\beta + \vec{j}\sin\beta) \tag{4.37}$$

where here $\vec{i}$ and $\vec{j}$ are unit vectors in the X and Y directions, and b_c is the radius of the tangency circle. Recall that the threat velocity at a point on the tangency circle is perpendicular to the circle.

The secondary arc begins at $\vec{r}_a(\beta)$ and ends at $\vec{r}_s$ in a circular arc. Let $\vec{r}_{ac}(\beta)$ be the center of this arc. The relations

$$\begin{aligned} |\vec{r}_s - \vec{r}_{ac}(\beta)| &= |\vec{r}_a(\beta) - \vec{r}_{ac}(\beta)| = b_2(\beta) \\ [\vec{r}_a(\beta) - \vec{r}_{ac}(\beta)] \cdot [\vec{r}_a(\beta) - \vec{r}_c] &= 0 \end{aligned} \tag{4.38}$$

determine $\vec{r}_{ac}(\beta)$, where b_2 is the (unspecified) arc radius. Let

$$\vec{r}_{ac} = \vec{r}_c + A\vec{r}_a + B\vec{r}_s \tag{4.39}$$

where A and B are to be determined by (4.38).

In terms of the TCCS coordinates X and Y, (4.38) becomes

$$\begin{aligned} 2b_c(b_c - X_s\cos\beta)A + 2X_s(b_c\cos\beta - X_s)B &= b_c^2 - X_s^2 \\ Ab_c + BX_s\cos\beta &= b_c \end{aligned} \tag{4.40}$$

giving

$$A = \frac{2b_cX_s - (b_c^2 + X_s^2)\cos\beta}{2b_cX_s\sin^2\beta}, \qquad B = \frac{b_c^2 - 2b_cX_s\cos\beta + X_s^2}{2X_s^2\sin^2\beta} \tag{4.41}$$

The locus of the secondary arc centers is then

$$X_{ac} = \frac{b_c^2 + X_s^2}{2X_s}, \qquad Y_{ac} = \frac{2b_cX_s - (b_c^2 + X_s^2)\cos\beta}{2X_s\sin\beta} \tag{4.42}$$

according to (4.39). It is seen that this locus is a line because X_{ac} is independent of β.

The geometry of this secondary-arc construction is shown in Figure 4.10 as a family of possible arcs. The dashed circle is the tangency circle. The threat position is generally not at the center of this circle. The dashed line is the locus of arc centers.

Consider the region of the tangency circle permitted by "g" constraint. For the moment we shall ignore the constraint on Heading Error and consider only how the limitation on the maximum allowed lateral acceleration magnitude limits the possibilities. Representing (4.16) in terms of the radius of curvature, b_1, of the primary arc, there is the relation

$$b_a \le b_1 \le b_b \tag{4.43}$$

where

$$b_a = \frac{z_0V_t}{V_t + V_{h0}}, \qquad b_b = \frac{z_0V_t}{V_t - V_{h0}} \tag{4.44}$$

If $b_m < b_a$ the simple trajectory will generate a transition point $\vec{r}_t$ above the sea surface, and there is no need to consider the dual-arc trajectories. If $b_b < b_m$ the threat cannot turn

sharp enough to avoid the sea surface regardless of how he orients his flight plane, and thus no dual-arc trajectory is possible. The remaining case is where

$$b_a \leq b_m \leq b_b \tag{4.45}$$

There always exist valid trajectories for the secondary arc, because the arc from the point on the tangency circle nearest to $\vec{r}_s$ is a straight line. Moving along the tangency circle in either direction the associated arcs reach a minimum radius of curvature, then again get larger without limit. The arcs with minimum radius of curvature have their center on the line between $\vec{r}_c$ and $\vec{r}_s$. The radii of these arcs is given by

$$b_{2m} = \frac{X_s^2 - b_c^2}{2X_s} = \frac{|\vec{r}_s - \vec{r}_c|^2 - b_c^2}{2|\vec{r}_s - \vec{r}_c|} \tag{4.46}$$

This is the minimum radius of all the possible secondary arcs. If $b_m < b_{2m}$ the secondary arcs departing from any point on the tangency circle are valid. If $b_{2m} < b_m$ some are not valid. To find the points (X_{2m}, Y_{2m}) on the tangency circle corresponding to the arc of minimal radius, the conditions

$$\begin{aligned} (X_{2m} - X_{ac})^2 + Y_{2m}^2 &= b_{2m}^2 \\ X_{2m}^2 + Y_{2m}^2 &= b_c^2 \end{aligned} \tag{4.47}$$

determine two points on the tangency circle.

The situation is described by Figure 4.11, which again depicts the plane of the sea surface. The point "T" is the projection of the threat position, "S" is the targeted ship, and "C" is the center of the tangency circle. If condition (4.43) holds, there is a segment of the tangency circle associated with valid trajectories in the primary arc. The points "β_1" and "β_2" denote the points of tangency of primary arcs having the limiting radius of curvature b_m, and are determined by (4.21) and (4.22). If the maximum allowed turning rate, $\omega_m = V_t/b_m$, satisfies (4.16), then the two final primary-arc positions on the tangency circle are determined. The corresponding values β_1 and β_2 divide the tangency circle into a permitted and a prohibited arc. The permitted arc is identified by the fact that it must include the angle $\beta_p = \pi/2 - \sigma$ (see Figure 4.9).

The dashed line perpendicular to CS is the locus of arc centers for possible trajectories in the secondary arc. The points "P1" and "P2" are where the secondary arc of minimum radius intersects the tangency circle, and has coordinates (X_{2m}, Y_{2m}) as determined by (4.47). There are two solutions, which determine the two points. The center of this arc is the point "P". if $b_{2m} \geq b_m$, then all the secondary arcs satisfy the "g" constraint. If $b_{2m} < b_m$ the secondary arcs arriving at the tangency circle in the vicinity of the points "P1" or "P2"

require a turn sharper than allowed. In this case, to find the secondary arc having the radius of curvature b_m, consider the conditions

$$\begin{aligned}(X_m - X_{ac})^2 + (Y_m - Y_{c1})^2 &= b_m^2 \\ X_m^2 + Y_m^2 &= b_c^2\end{aligned} \tag{4.48}$$

where Y_{c1} is the (positive) coordinate of the point C1 in Figure 4.11, given by the relation

$$Y_{c1}^2 + (X_s - X_{ac})^2 = b_m^2 \tag{4.49}$$

If there is no real solution for Y_{c1}, then all the possible secondary arcs satisfy the 'g' constraint. Otherwise, there are two solutions to (4.48), (X_{m1}, Y_{m1}) and (X_{m2}, Y_{m2}), with Y_{m1} and Y_{m2} having opposite signs. Define Y_{m1} as the negative solution. Then the azimuth angles on the tangency circle where these secondary arcs impinge are given by

$$\begin{aligned}\gamma_1 &= -\text{atan2}(Y_{m1}, X_{m1}) \\ \gamma_2 &= \quad \text{atan2}(Y_{m2}, X_{m2})\end{aligned} \tag{4.50}$$

with both values being positive. Secondary arcs arriving at the tangency circle within the arc "$-\gamma_2$ to $-\gamma_1$" or within "γ_1 to γ_2" have radii less than allowed, and accordingly are not valid. The remaining points along the tangency circle have secondary arcs that satisfy the 'g'constraint.

Consider the region of the tangency circle permitted by HE constraint. Figure 4.12 shows the tangency circle and the plane of the sea surface including the targeted ship "S", the projection of the threat position "T", the center of the tangency circle "C", and the line (dashed) locus of the secondary-arc centers. Consider a secondary arc whose center is denoted by "C_m". It is evident that the HE along this arc is greatest where this trajectory departs from the tangency circle. If this angle is equal to ϕ_m, the maximum allowed HE, denote the azimuth angle β on the tangency circle where these limiting secondary arcs intersect the circle by $-\beta_m$ and β_m.

Denote the TCCS coordinates of the lowest of the pair of critical points by (X_m, Y_m), given by

$$X_m = b_c \cos\beta_m, \qquad Y_m = -b_c \sin\beta_m \tag{4.51}$$

where b_c is the radius of the tangency circle. Note that the angle at S subtended by the points C and $-\beta_m$ is equal to $\phi_m - \beta_m$. Accordingly, there is the relation

$$\tan(\phi_m - \beta_m) = \frac{b_c \sin\beta_m}{X_s - b_c \cos\beta_m} \tag{4.52}$$

or

$$\phi_m = \beta_m + \text{atan2}\left(b_c \sin\beta_m, X_s - b_c \cos\beta_m\right) \tag{4.53}$$

Taking the tangent of both sides and rearranging gives a quadratic equation in $\sin\beta_m$,

$$X_s^2\sec^2\phi_m\sin^2\beta_m + 2X_s b_c\tan\phi_m\sin\beta_m + (b_c^2 - X_s^2)\tan^2\phi_m = 0 \tag{4.54}$$

The discriminant of this equation is

$$\sqrt{4X_s^2\tan^2\phi_m[(X_s^2 - b_c^2)\tan^2\phi_m + X_s^2]} \tag{4.55}$$

and is always real for a targeted ship outside the tangency circle (*i.e.*, $X_s > b_c$). It is also seen that the largest root is always non-negative. After obtaining $\sin\beta_m$ from (4.54) the appropriate quadrant of β_m is found using (4.53), giving β_m on $[0, \pi)$.

The arc from the point labeled β_m to S is obtained by symmetry. The permitted region of the tangency circle under the HE constraint is the arc between $-\beta_m$ and β_m.

Consider now the HE constraint on the primary arc. The geometry is complicated in the general case, and therefore the following simplifying assumption is made. This assumption can be phrased in the form of a conjecture:

> If both the initial and final HE of the primary arc satisfy the HE constraint, the HE at all points of the arc satisfy the constraint.

It may be possible to show that this conjecture is true, although we have been unable to do so. However, if there are some unlikely cases where the HE constraint is violated somewhere along the primary arc even though the constraint is satisfied at the end points, the HE there will only slightly exceed the allowed limiting value. The HE at the end of the primary arc is the same as at the beginning of the secondary arc. Therefore, the permitted region of the tangency circle is the arc $\beta \in [\beta_1, \beta_2]$.

Figure 4.13 shows how the geometry of Figure 4.11 determines the regions of validity. A point on the tangency circle determines both the primary and the secondary arc. Regions of this tangency circle are mapped into the angle β, measured counterclockwise around the circle from the point nearest to "S". In Figure 4.12, β along the tangency circle has the values indicated by the point labels. Figure 4.13 depicts a situation with the most complicated region of valid trajectories, namely, three disjoint intervals. Other situations will correspond to two intervals or a single interval.

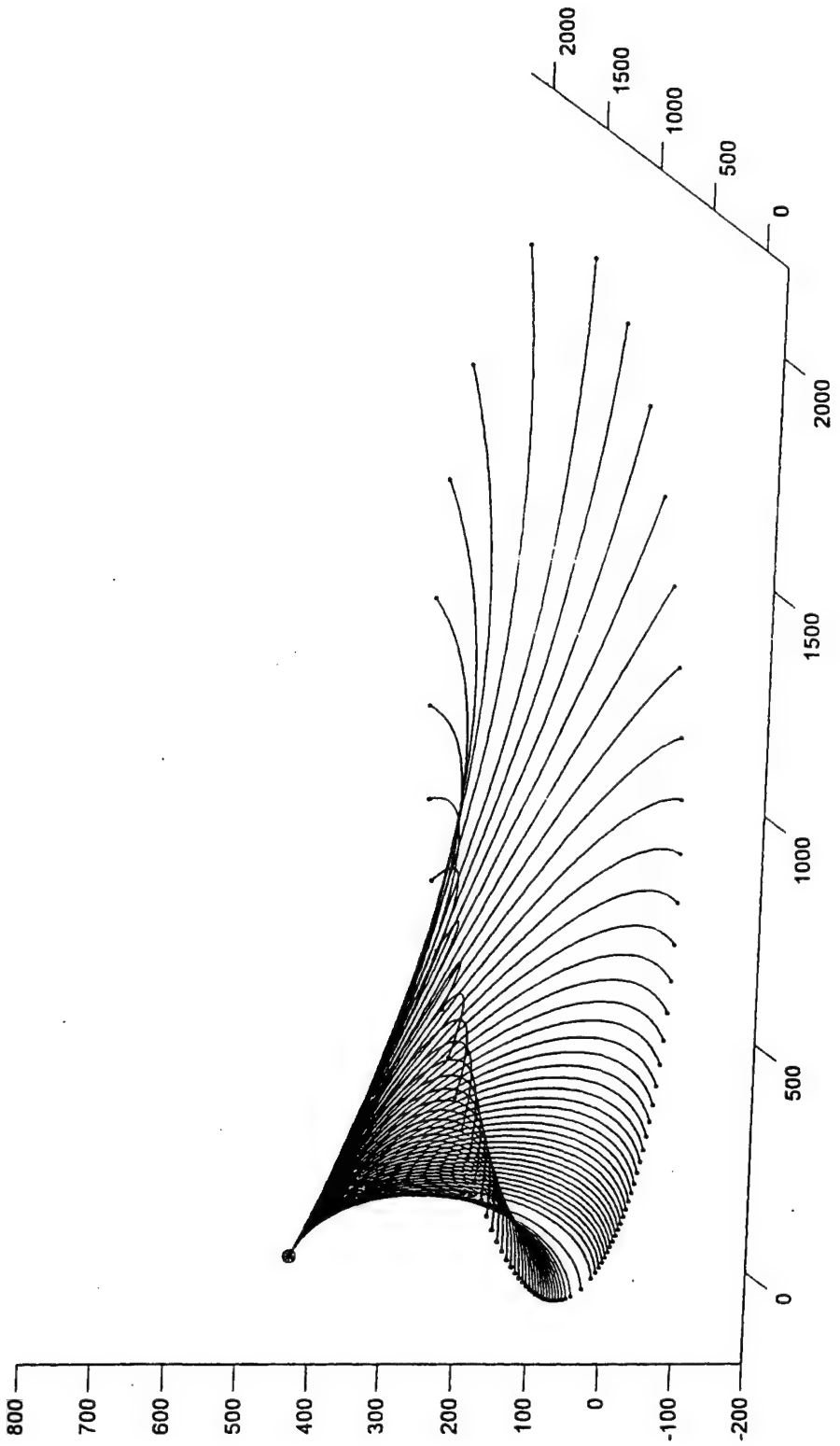

Figure 4.1. CTR arcs from initial threat position to points of tangency on the sea surface.

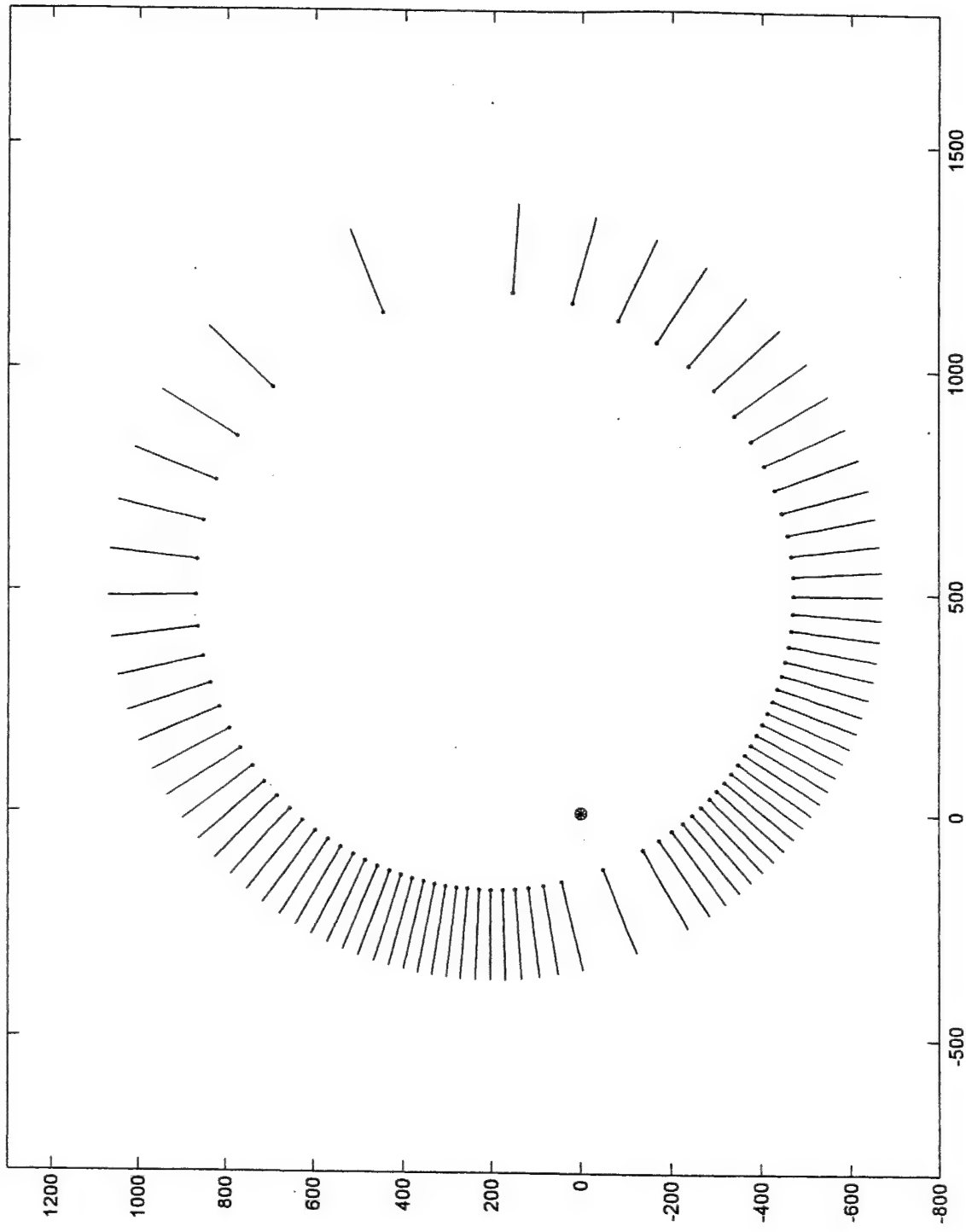

Figure 4.2. Points of tangency on the sea surface of the arcs shown in Figure 4.1, indicated by the dots. The line segments indicate the velocity direction at these points.

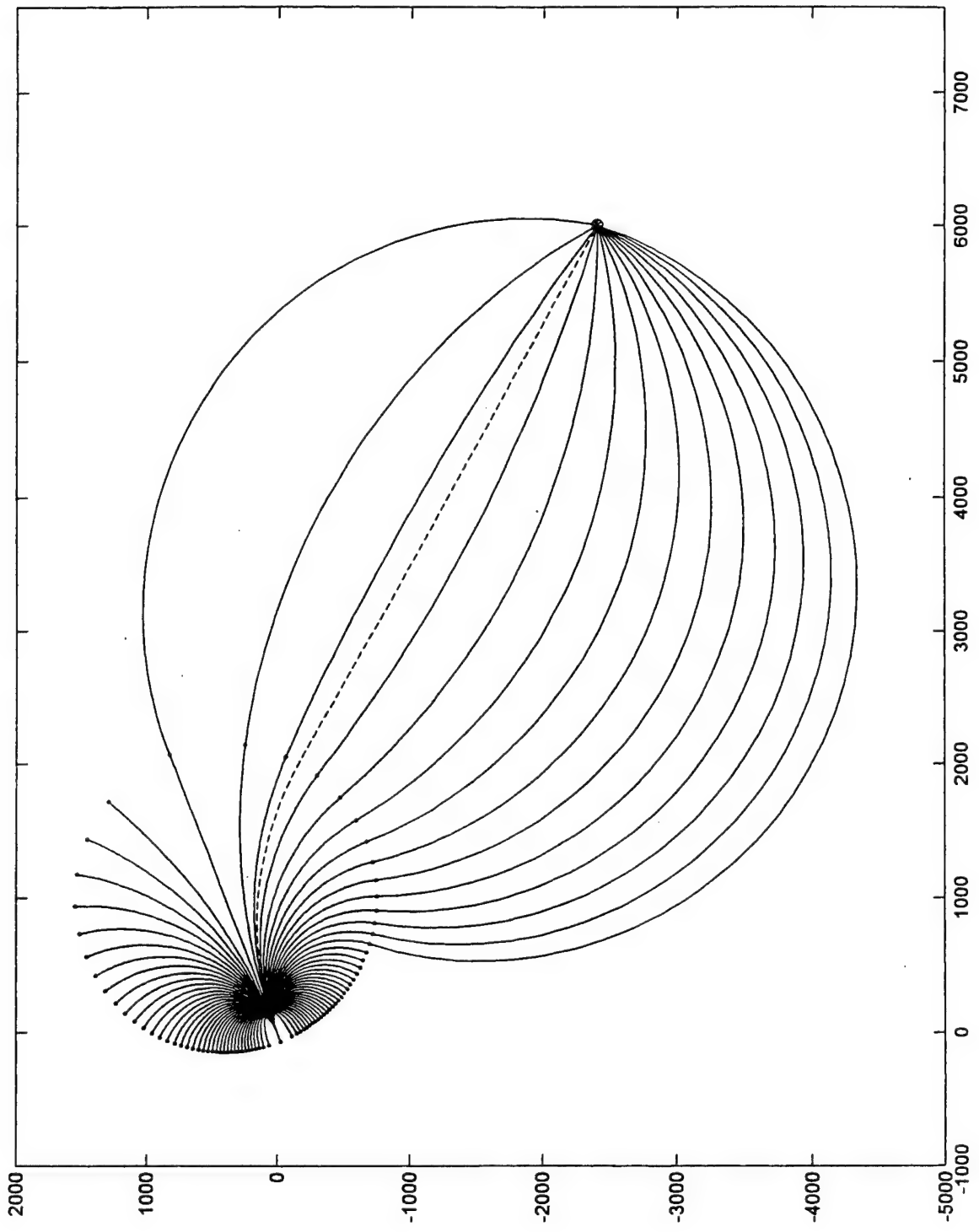

Figure 4.3. Projection onto the sea surface of two-arc trajectories reaching the indicated targeted point (solid curves). The initial arcs are those of Figure 4.1 departing from threat located above the origin. The dashed curve is the trajectory lying on a single flight plane, terminating in CV segment.

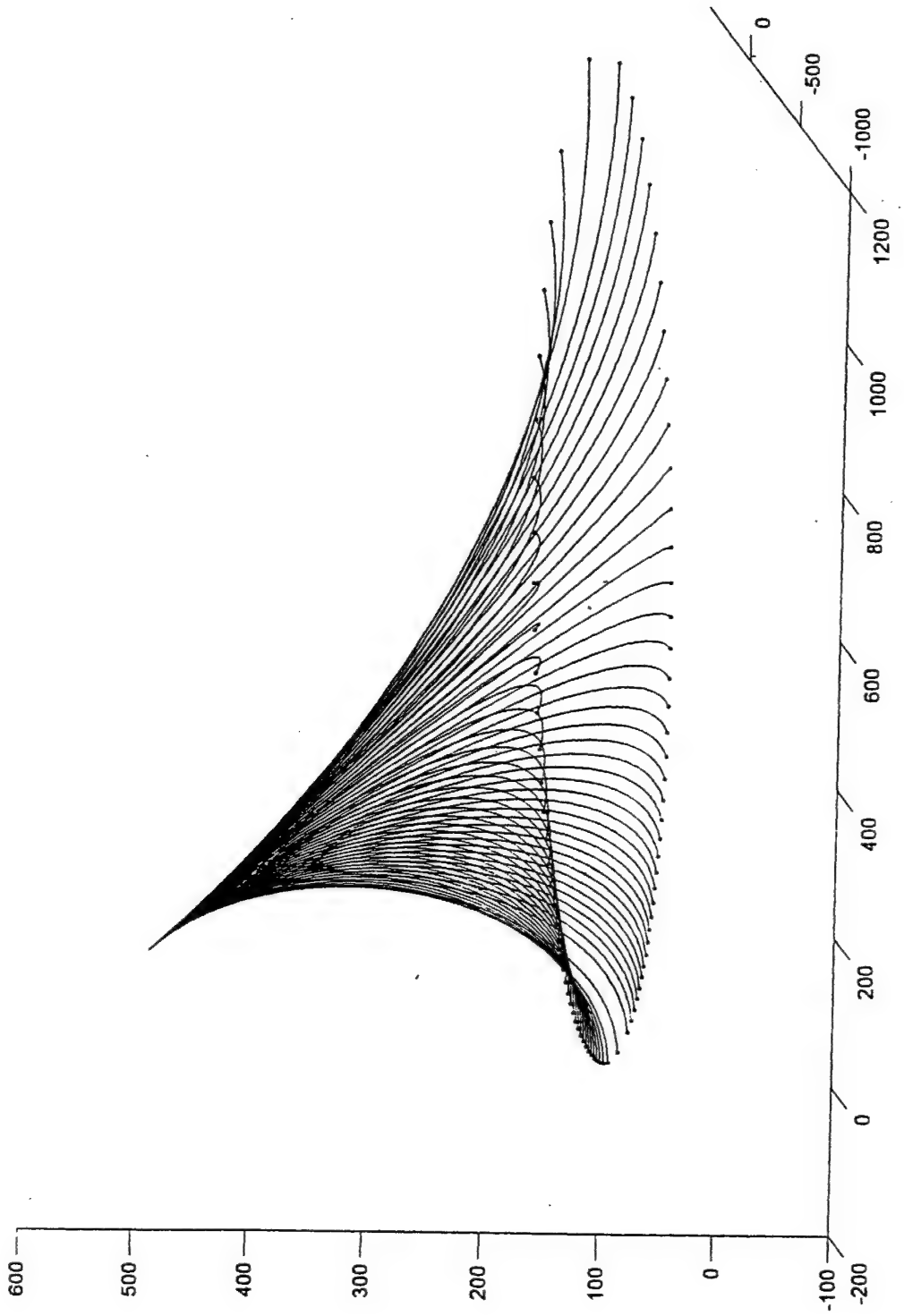

Figure 4.4. CTR arcs from initial threat position to points of tangency on the sea surface.

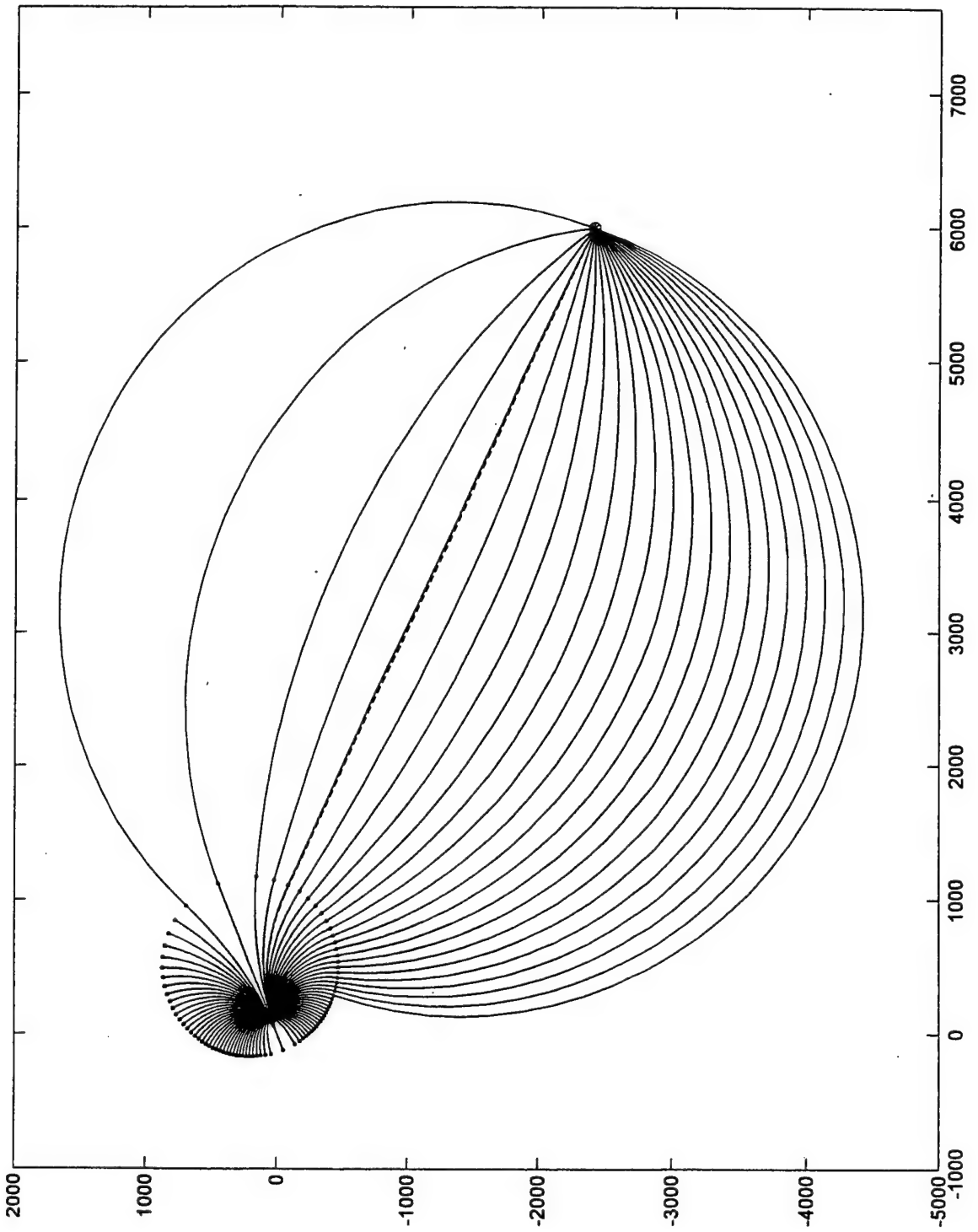

Figure 4.5. Projection onto the sea surface of two-arc trajectories reaching the indicated targeted point (solid curves). The initial arcs are those of Figure 4.4 departing from threat located above the origin. The dashed curve is the trajectory lying on a single flight plane, terminating in CV segment.

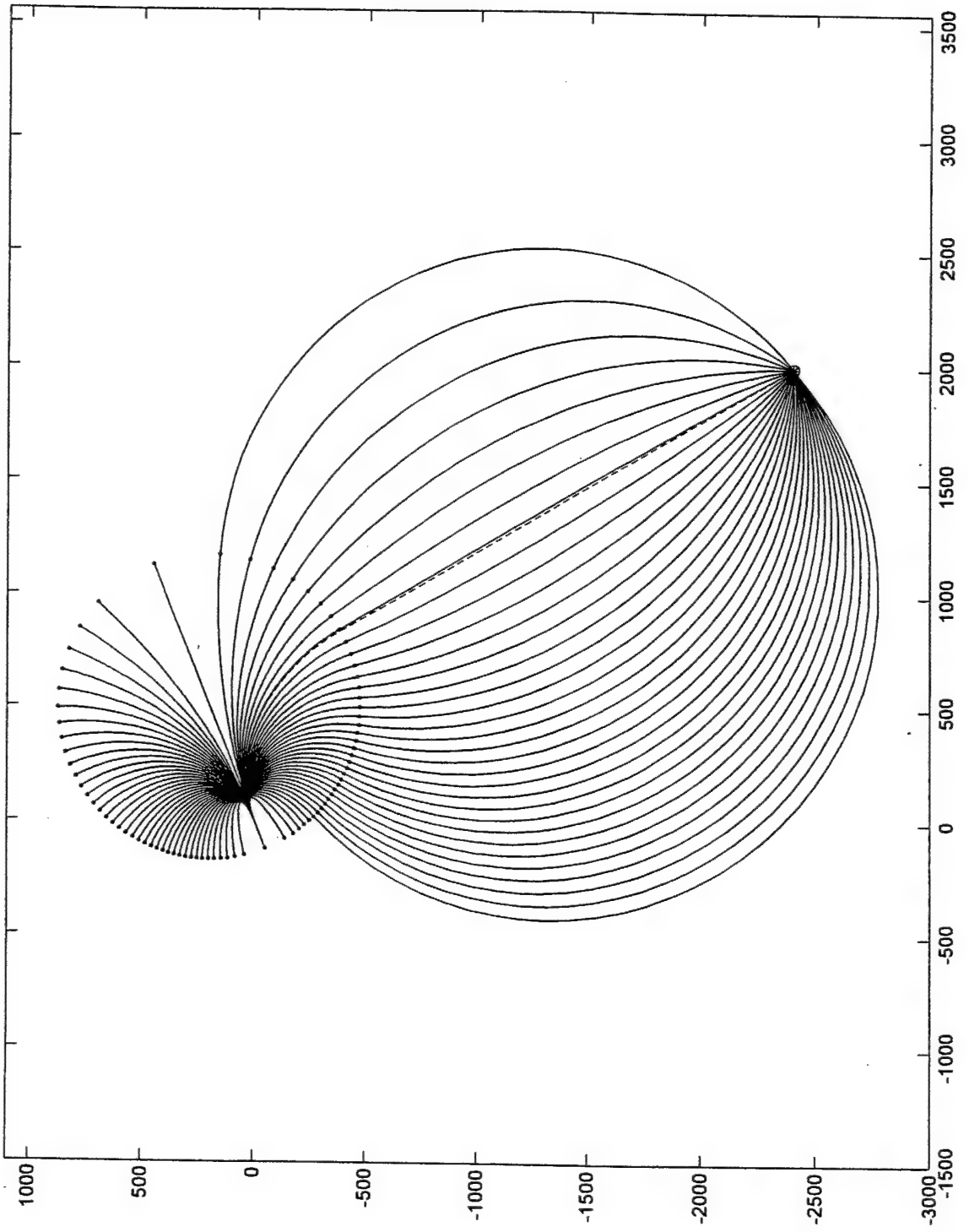

Figure 4.6. Projection onto the sea surface of two-arc trajectories reaching the indicated targeted point (solid curves). The initial arcs are those of Figure 4.4 departing from threat located above the origin. The dashed curve is the trajectory lying on a single flight plane, terminating in CV segment.

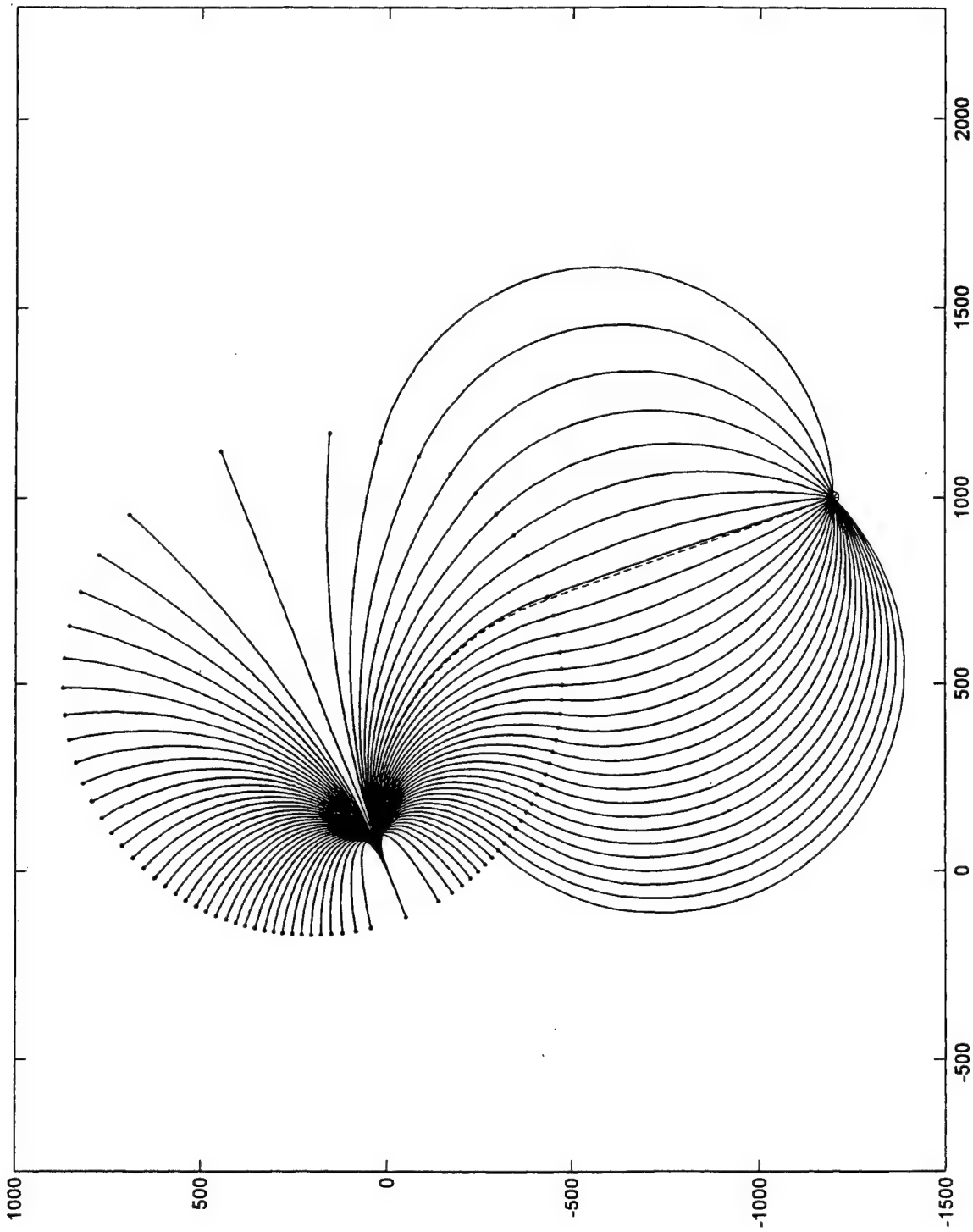

Figure 4.7. Projection onto the sea surface of two-arc trajectories reaching the indicated targeted point (solid curves). The initial arcs are those of Figure 4.4 departing from threat located above the origin. The dashed curve is the trajectory lying on a single flight plane, terminating in CV segment.

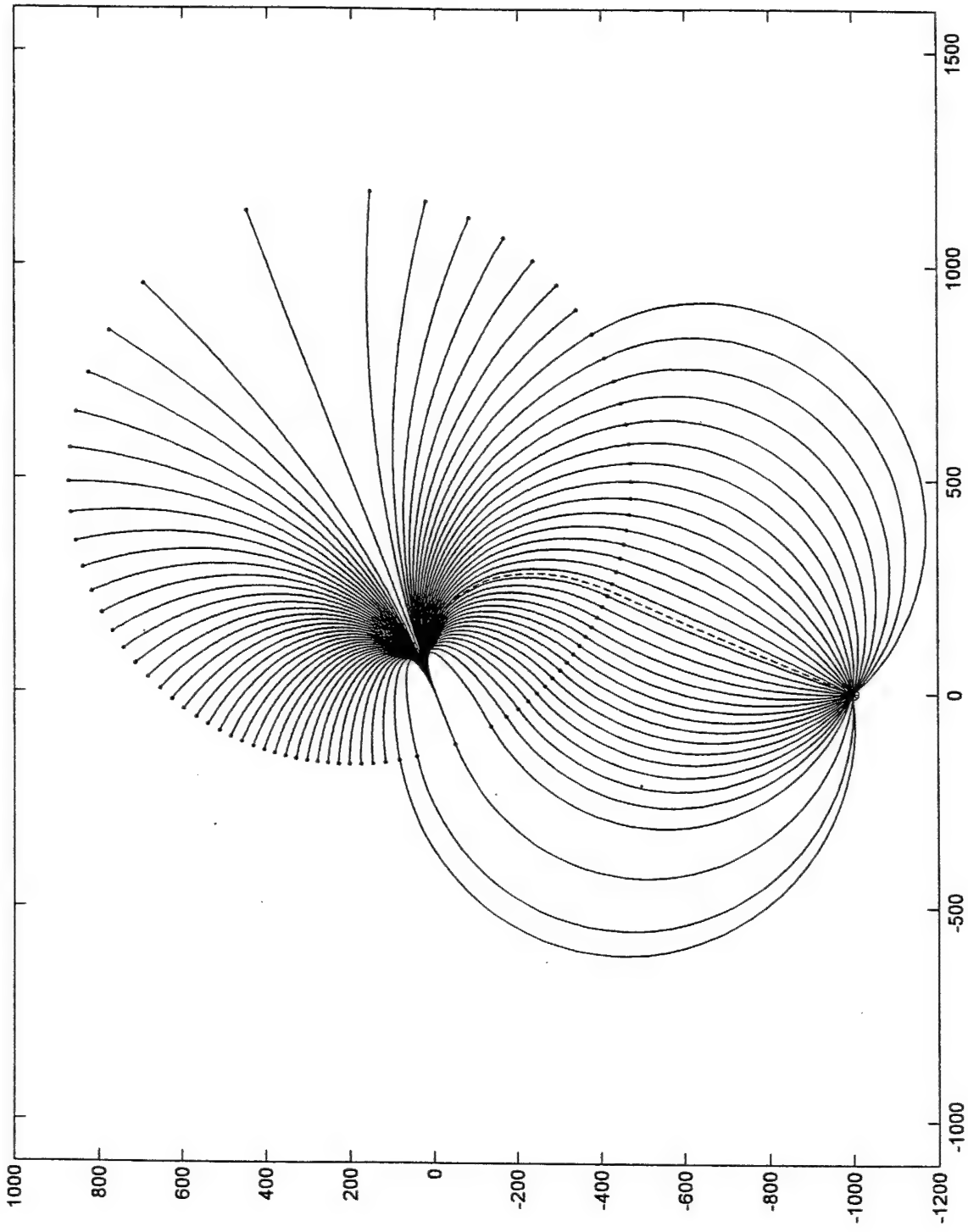

Figure 4.8. Projection onto the sea surface of two-arc trajectories reaching the indicated targeted point (solid curves). The initial arcs are those of Figure 4.4 departing from threat located above the origin. The dashed curve is the trajectory lying on a single flight plane, terminating in CV segment.

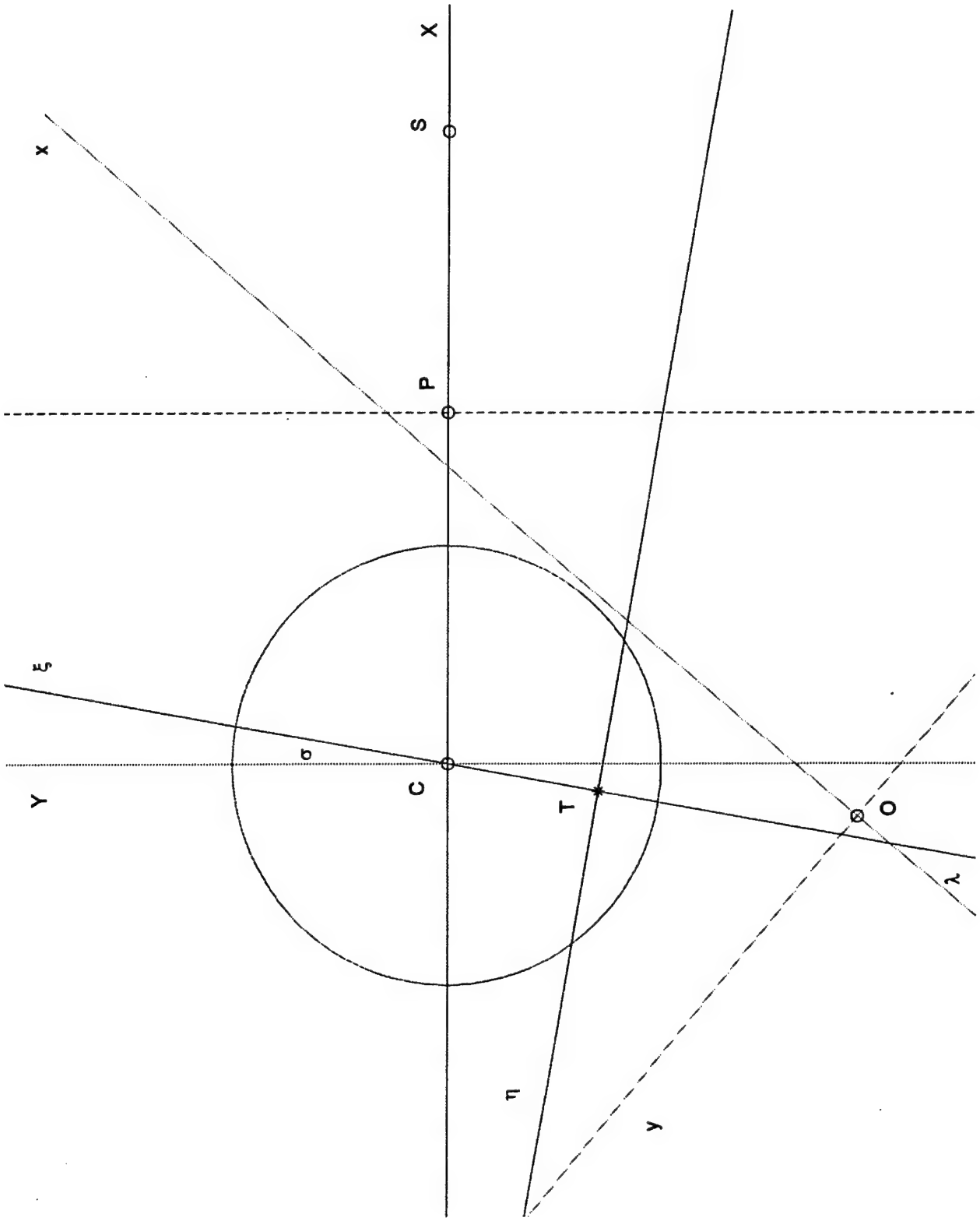

Figure 4.9. Relation between the BC (x, y), SC (ξ, η), and TSC (X, Y) Systems.

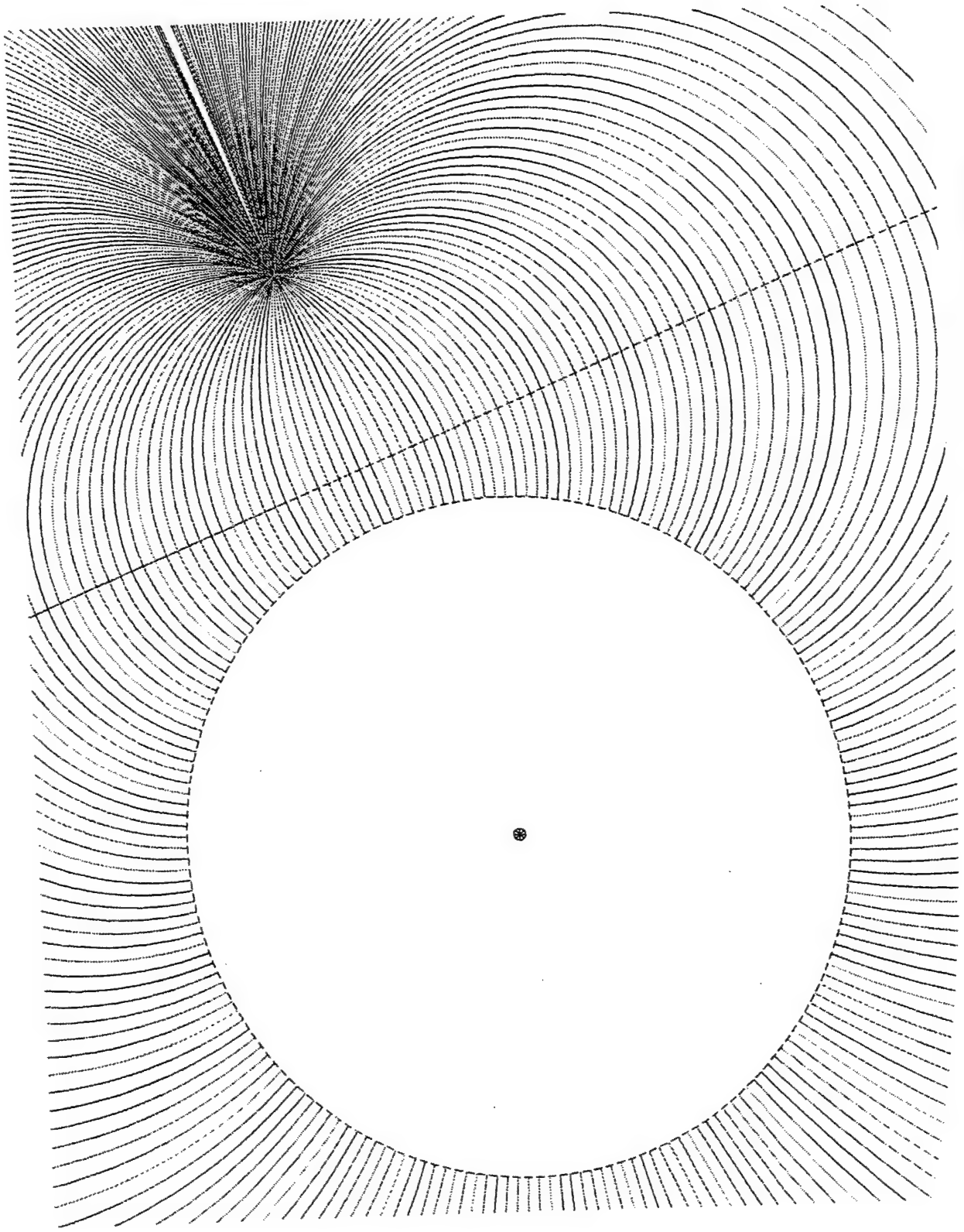

Figure 4.10. Family of possible secondary arcs, meeting at the targeted point. The tangency circle and line of arc centers are indicated.

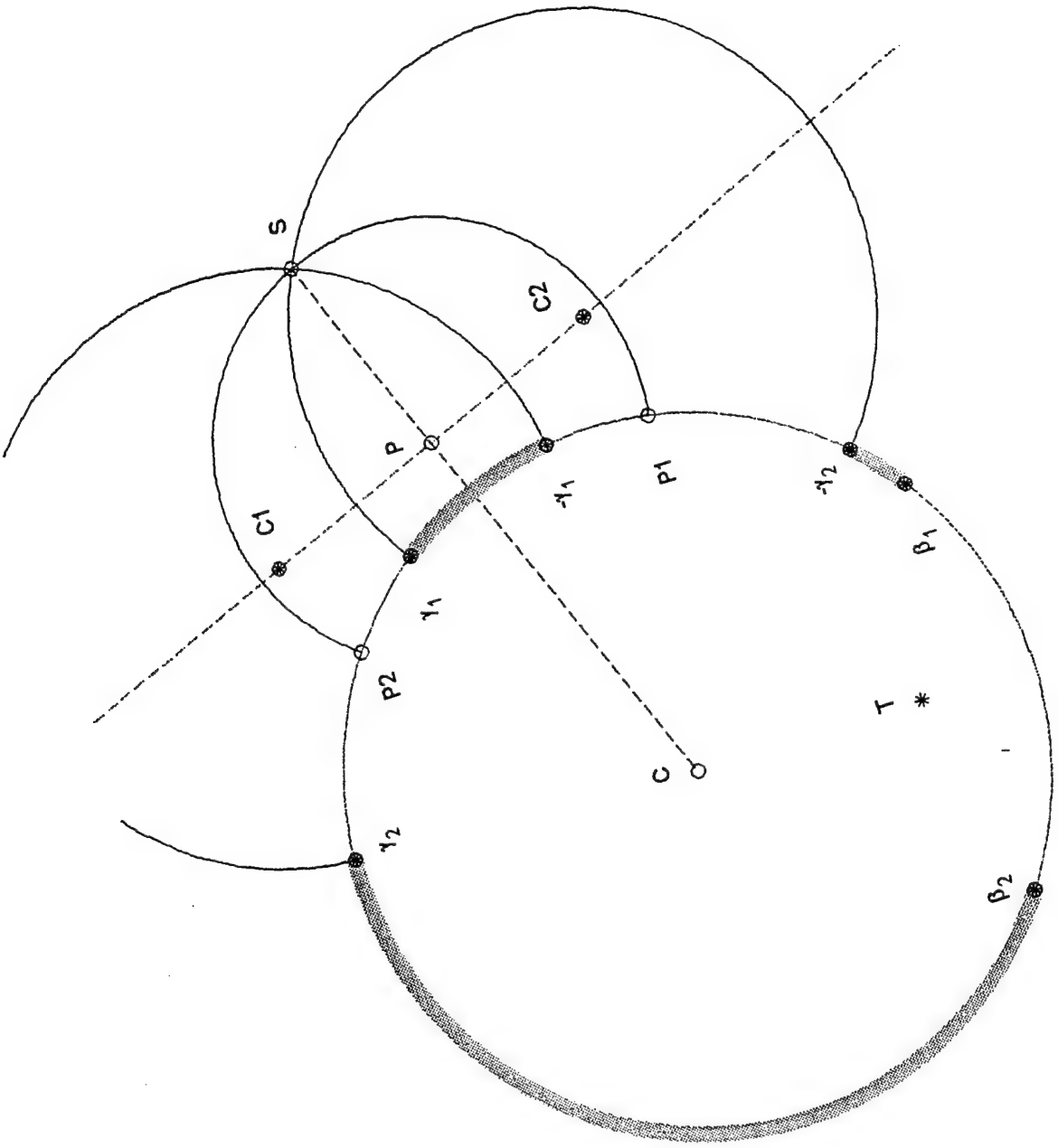

Figure 4.11. The tangency circle and limiting secondary arcs determined by the 'g' constraint.

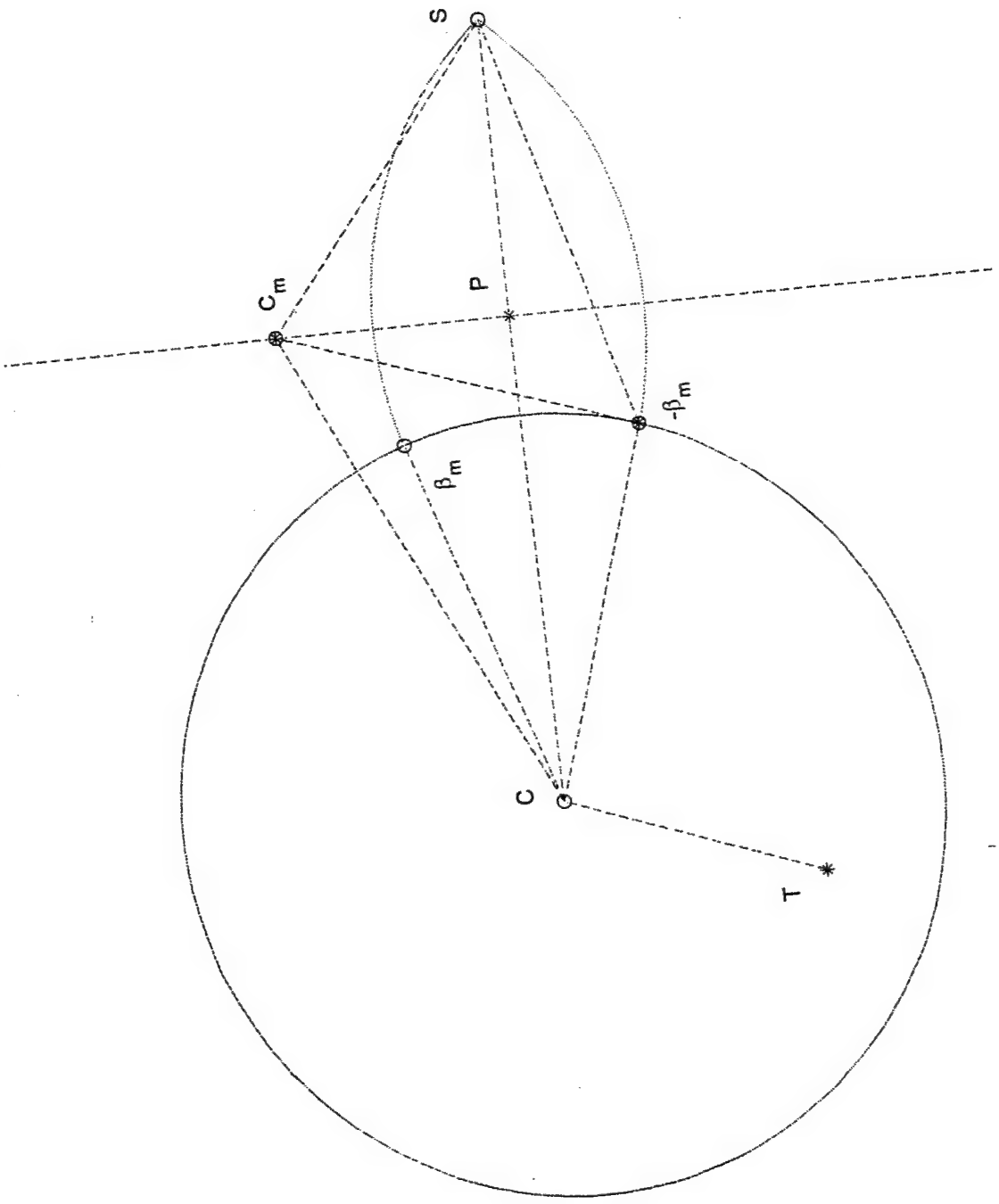

Figure 4.12. The tangency circle and limiting secondary arcs determined by the HE constraint.

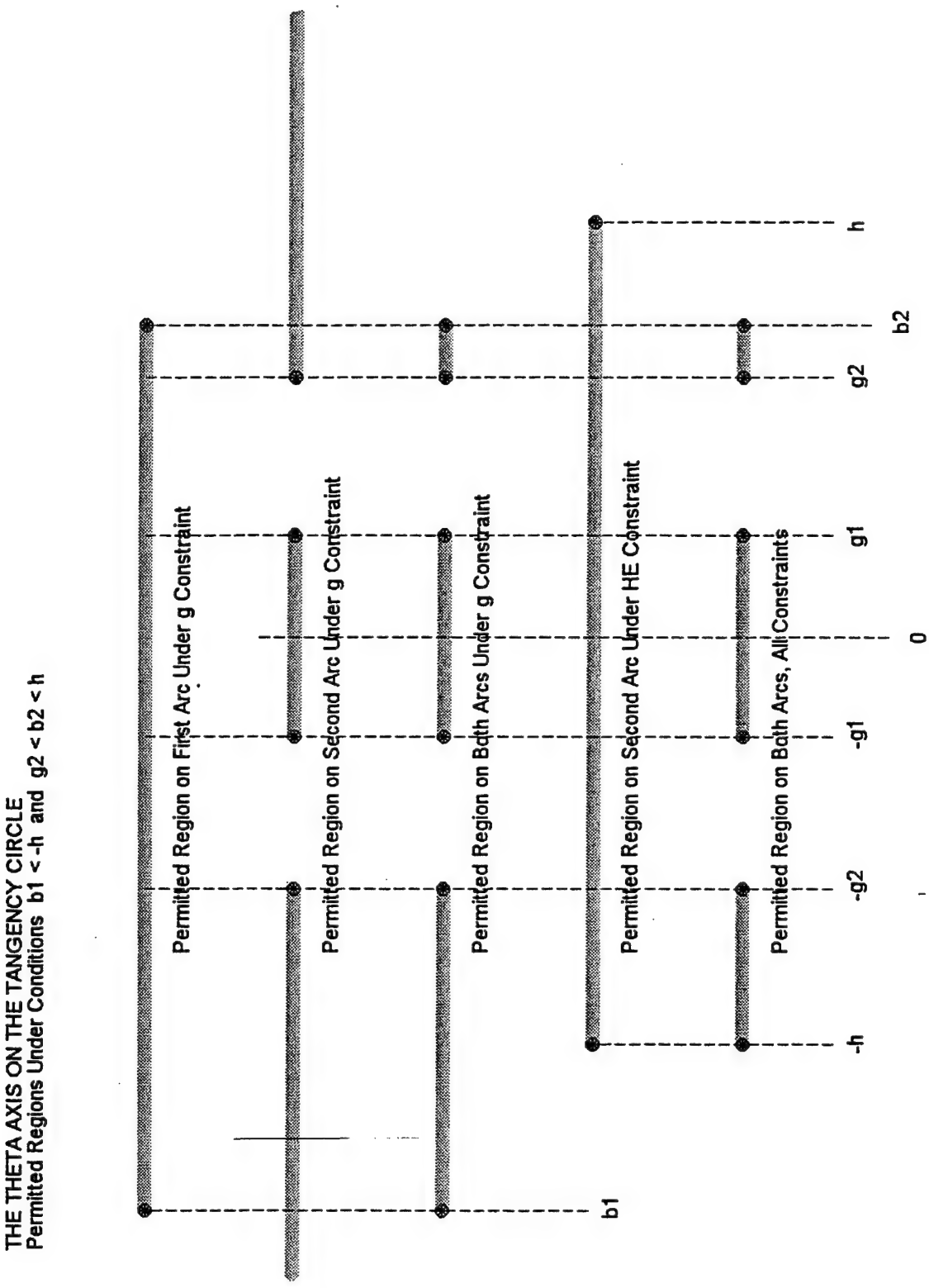

Figure 4.13. Regions of validity along the θ axis.

CHAPTER 5

REGIONS OF ASCM ACCESSIBILITY

In accordance with the assumptions defining the simplified ASCM trajectory, the threat is not allowed to reach points whose heading error exceeds ϕ_m, nor requiring a turn of radius less than b_m. The first requirement restricts the Region of Accessibility (RA) to the interior of a circular cone whose vertex is at the current expected threat position and whose axis is directed along the expected threat velocity. The second condition excludes from the RA the interior of a torus to be described below.

It should be emphasized that the current RA relates to the current threat state. One might think that the RA at a subsequent time would be contained within the earlier RA, but this is not necessarily so. At any time the RA only represents the region accessible to simplified trajectories determined by the threat state at that time.

Consider the conical region. A point $\vec{r}_s$ is in the allowed conical region of the RA, as in Figure 5.1, if

$$\frac{\dot{\vec{r}} \cdot (\vec{r}_s - \vec{r})}{V|\vec{r}_s - r|} \geq \cos\phi_m \tag{5.1}$$

where $\vec{r} = (x, y, z)$ and $\dot{\vec{r}} = (u, v, w)$ are the current expected position and velocity of the threat and $V = |\dot{\vec{r}}|$. For a point on the sea surface, $\vec{r}_s = (x_s, y_s, 0)$, the condition (5.1) imposes the constraint

$$A\xi_1^2 + B\xi_1\eta_1 + C\eta_1^2 + D\xi_1 + E\eta_1 + F \geq 0 \tag{5.2}$$

where

$$\begin{aligned} \xi_1 &= x_s - x \\ \eta_1 &= y_s - y \end{aligned} \tag{5.3}$$

and

$$\begin{aligned} A &= u^2 - V^2\cos^2\phi_m & D &= -2uwz \\ B &= 2uv & E &= -2vwz \\ C &= v^2 - V^2\cos^2\phi_m & F &= z^2(w^2 - V^2\cos^2\phi_m) \end{aligned} \tag{5.4}$$

The terms linear in ξ_1 and η_1 can be eliminated by the substitution

$$\begin{aligned} \xi_1 &= a\xi + b\eta + e \\ \eta_1 &= c\xi + d\eta + f \end{aligned} \tag{5.5}$$

and setting

$$\begin{aligned} 2Aae + B(af + ec) + 2Ccf + Da + Ec &= 0 \\ 2Abe + B(bf + ed) + 2Cdf + Db + Ed &= 0 \end{aligned} \tag{5.6}$$

These relations underdetermine the coefficients a, b, c, d, e, f. Unless the transformation (5.5) is degenerate we can set $b = 0$ and $c = 0$ to get

$$\begin{aligned} 2Ae + Bf &= 0 \\ Be + 2Cf + E &= 0 \end{aligned} \tag{5.7}$$

to determine e and f. The coefficients a and d are left undetermined, and for convenience they can be set equal to one. Then (5.2) becomes

$$A\xi^2 + B\xi\eta + C\eta^2 + G \geq 0 \tag{5.8}$$

where

$$G = Ae^2 + Bef + Cf^2 + De + Ef + F \tag{5.9}$$

The case where (5.7) does not provide valid values for e and f requires special treatment that is not described here.

The matrix of the quadratic form (5.8) is

$$X = \begin{pmatrix} A & \frac{1}{2}B \\ \frac{1}{2}B & A \end{pmatrix} \tag{5.10}$$

Let V be the matrix whose columns are the normalized eigenvectors of X. Then the transformation

$$\begin{pmatrix} x_p \\ y_p \end{pmatrix} = V \begin{pmatrix} \xi \\ \eta \end{pmatrix}, \qquad \begin{pmatrix} \xi \\ \eta \end{pmatrix} = V^T \begin{pmatrix} x_p \\ y_p \end{pmatrix} \tag{5.11}$$

gets rid of the product term and gives

$$Hx_p^2 + Jy_p^2 + G \geq 0 \tag{5.12}$$

where

$$\begin{aligned} H &= AV_{11}^2 + BV_{11}V_{12} + CV_{12}^2 \\ J &= AV_{21}^2 + BV_{21}V_{22} + CV_{22}^2 \end{aligned} \tag{5.13}$$

Consider the toriodal region. This is the region inaccessible to the threat because it cannot turn sharp enough to enter. This toroidal region is determined by given values of $\vec{r}$, $\dot{\vec{r}}$, and b_m. The axis of the torus is a circle of radius b_m lying on the plane perpendicular to $\dot{\vec{r}}$ with the point $\vec{r}$ at its center. Each point on this axial circle is the center of another circle of radius b_m that lies on the surface of the torus in the plane perpendicular to the axial circle. These circles generate the torus.

If $\vec{r}_a$ is a point on the axial circle of the torus, then the relations

$$\begin{aligned} |\vec{r}_a - \vec{r}| &= b_m \\ \dot{\vec{r}} \cdot (\vec{r}_a - \vec{r}) &= 0 \end{aligned} \tag{5.14}$$

must be satisfied. It is convenient to define two special points ($\vec{r}_{a0}$ and $\vec{r}_{a1}$) lying on the axial circle. Let $\vec{r}_{a0}$ lie at the top of the axial circle, and $\vec{r}_{a1}$ lie on the axial circle ninety degrees clockwise from $\vec{r}_{a0}$ relative to the direction of $\dot{\vec{r}}$. The point $\vec{r}_{a0}$ is represented by

$$\vec{r}_{a0} = \vec{r} + \alpha\dot{\vec{r}} + \beta\vec{k} \tag{5.15}$$

and must satisfy (5.14). Accordingly, the constants α and β must satisfy

$$\begin{aligned} V^2\alpha + w\beta &= 0 \\ V^2\alpha^2 + 2w\alpha\beta + \beta^2 &= b_m^2 \end{aligned} \tag{5.16}$$

The point $\vec{r}_{a1}$ is represented by

$$\vec{r}_{a1} = \vec{r} + \alpha\vec{i} + \beta\vec{j} \tag{5.17}$$

redefining α and β, which are now determined by the relations

$$\begin{aligned} u\alpha + v\beta &= 0 \\ \alpha^2 + \beta^2 &= b_m^2 \end{aligned} \tag{5.18}$$

It is convient to let γ be a parameter that selects one of the points $\vec{r}_a$ on the axial circle, and we thus set

$$\vec{r}_a = \vec{r} + (\vec{r}_{a0} - \vec{r})\cos\gamma + (\vec{r}_{a1} - \vec{r})\sin\gamma \tag{5.19}$$

Then every $\gamma \in [0, 2\pi)$ generates a circle on the toroidal surface. Each circle can intersect the sea surface at zero or two points. If $\vec{r}_\gamma$ is one of these points, there is the relation

$$\begin{aligned} |\vec{r}_\gamma - \vec{r}_a| &= b_m \\ \vec{r}_{ap} \cdot (\vec{r}_\gamma - \vec{r}_a) &= 0 \\ \vec{r}_\gamma &= x_b\vec{i} + y_b\vec{j} \end{aligned} \tag{5.20}$$

(defining x_b and y_b), where $\vec{r}_{ap}$ is a unit vector at $\vec{r}_a$ along the axial circle. It can be found by taking the derivative of (5.19), giving

$$\vec{r}_{ap} = [-(\vec{r}_{a0} - \vec{r})\sin\gamma + (\vec{r}_{a1} - \vec{r})\cos\gamma]/b_m \tag{5.21}$$

Figure 5.2 illustrates the RA in a typical case. The expected threat position is indicated by the star (between the two circles), and its velocity is directed along the dashed line, which is the axis of revolution of the figure. The HE restriction defines the conical surface represented by the two lines that would intersect at the threat position. The toroidal region, represented by the two circles, is inaccessible to the threat because of limitation on its lateral acceleration magnitude (the "g" limitation).

Figure 5.3 illustrates the intersection of the RA of Figure 5.2 and the sea surface for a typical case where the threat is initially diving. The region of the sea surface in the torus

is shaded. The expected threat position is indicated by the star. The projection of the axial circle of the torus onto the sea surface is dashed. The array of dots lying just inside the dashed curve are those points on the sea surface where the simplified ASCM trajectory would arrive at a point of tangency. The dots are at equal increments of the turning rate in the hypothetical simplified trajectory. The outer solid curve indicates the boundary of the conical region. The RA consists of the unshaded region inside this solid curve. However, this RA includes a subregion reachable only if the threat is able to fly under water. The simplified trajectories reaching this subregion would lie under the torus. The boundary of this "wet trajectory" subregion is not indicated.

For a given threat it is interesting to consider those regions of the sea surface where the threat can and cannot fly. For a given threat state and the given "g" and HE constraints, the preceding sections give rules that can indicate whether a given point on the sea surface can be reached.

Figure 5.4 shows several regions on the plane of the sea surface for a threat with an initial altitude of 1600 yds, horizontal velocity of 500 yd/sec, and vertical velocity of -600 yd/sec. The dive angle is arctan(600/500) or approximately 70 deg. The maximum allowed lateral acceleration is taken to be 15.8 "g" units, giving a minimum allowed arc radius of 3600 yd. The maximum allowed HE (ϕ_m) is taken as 50 deg. The asterisk shows the projection of the initial threat position onto the sea surface. The solid circle is the "Tangency Circle" of the seaskimming trajectories.

Regions 3 and 6 are inaccessible because of the "g" constraint, and together represent the intersection of a torus with the sea surface. Regions 6 and 7 are inaccessible because of the HE constraint, and together are bounded by a conic section. Regions 1 and 2 are accessible by the "Simple Trajectories" described in Chapter 3. Regions 2 and 5 are accessible by the "Seaskimming" trajectories described in Chapter 4. The region accessible under the stated assumptions and constraints therefore consists of the union of regions 1, 2, and 5.

Regions 4 and 5 would be accessible by a "Simple Trajectory" if flight under water were allowed. Region 7 is accessible under the "g" constraint, but violates the HE constraint and the condition that flight must occur only in air (the "dry" constraint).

Figure 5.5 represents the same conditions as Figure 5.4 except that ϕ_m is 50 deg. The regions identified in Figure 5.4 are present in Figure 5.5, but now there is a new region. Region 8 is accessible under the "g" constraint and satisfies the "dry" condition but violates the HE constraint.

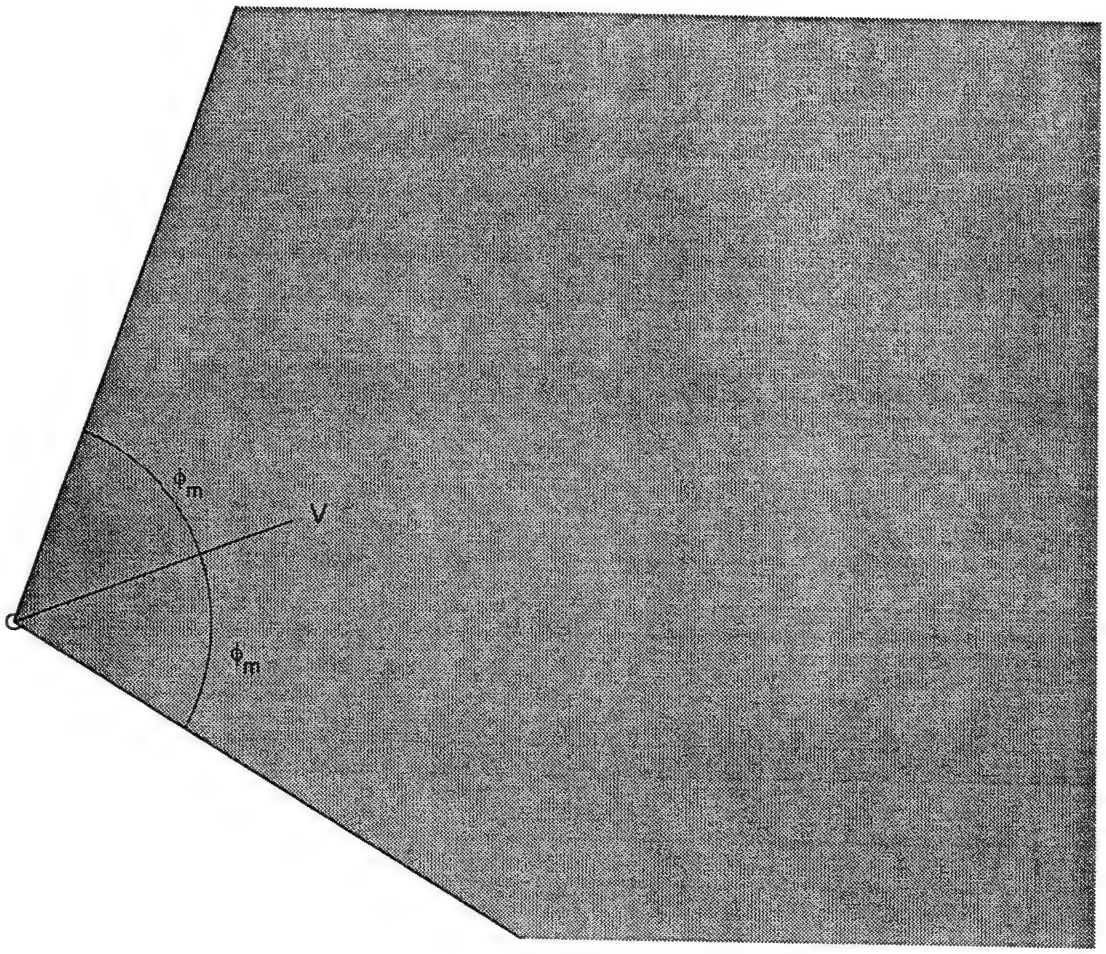

Figure 5.1. Region satisfying the HE constraint: the cone radially symmetric about the velocity vector V indicated by shading.

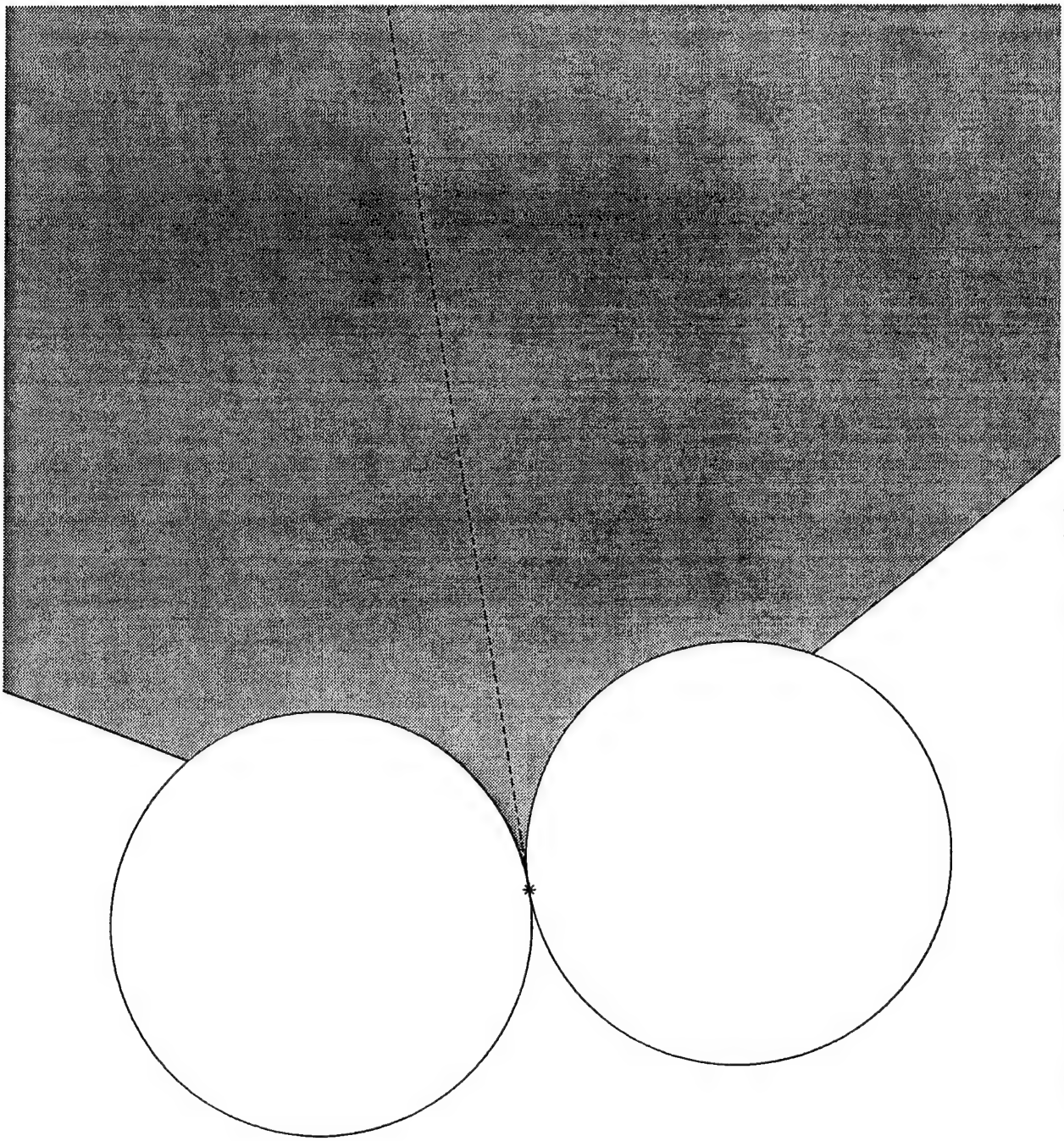

Figure 5.2. The region satisfying both the HE and the "g" constraints is radially symmetric about the velocity vector. The shadowing shows a section of this region about the axis of symmetry.

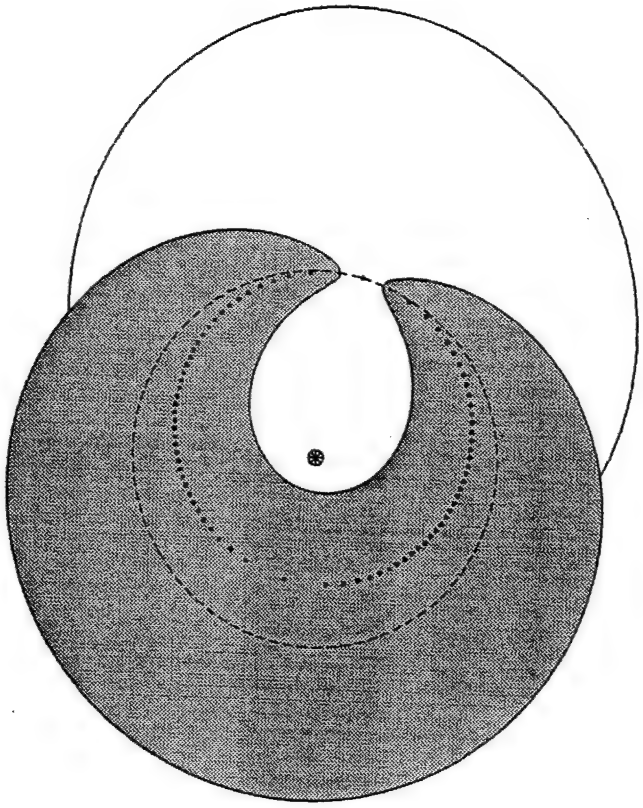

Figure 5.3. The Accessible Region on the Sea Surface.

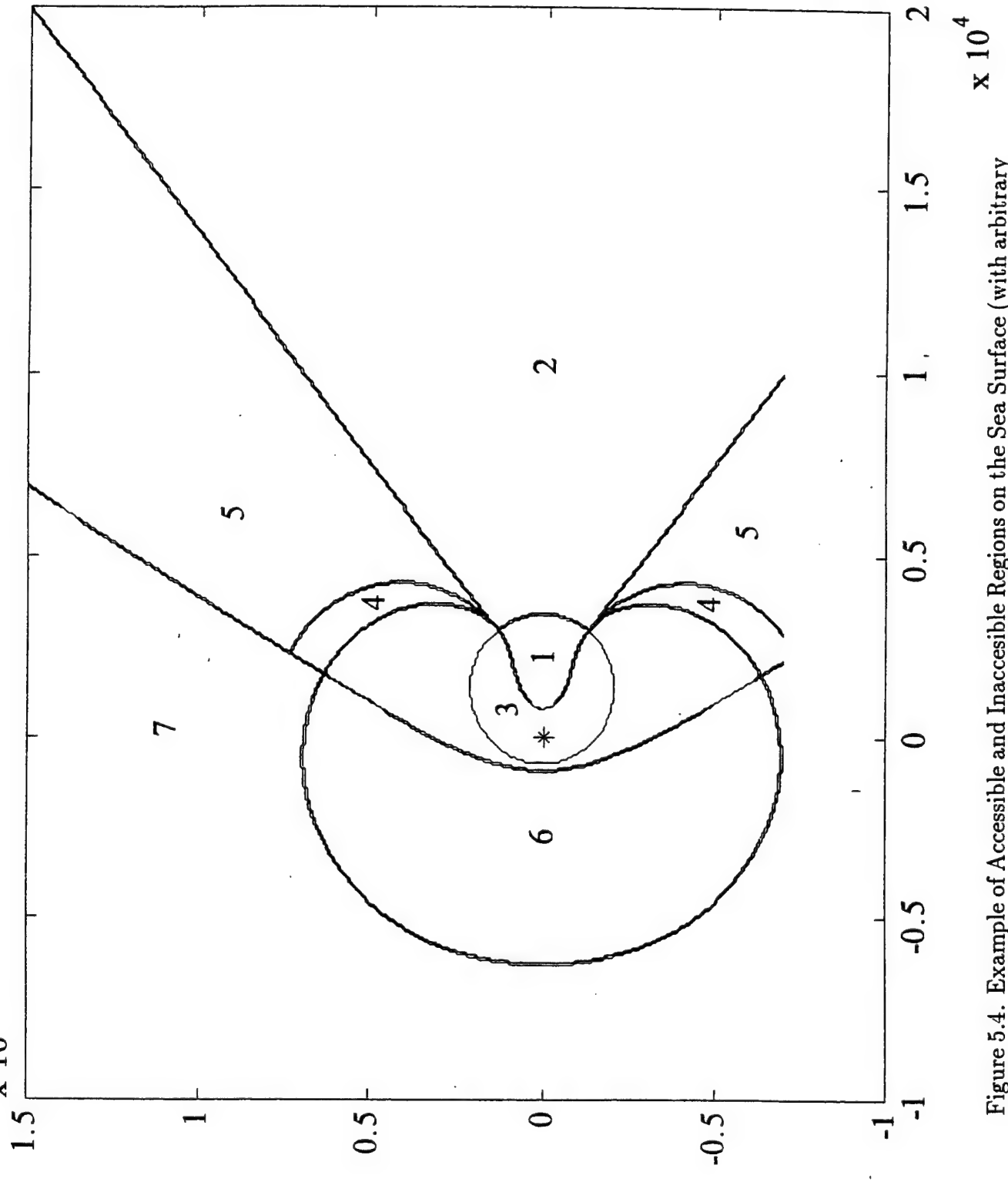

Figure 5.4. Example of Accessible and Inaccesible Regions on the Sea Surface (with arbitrary scale).

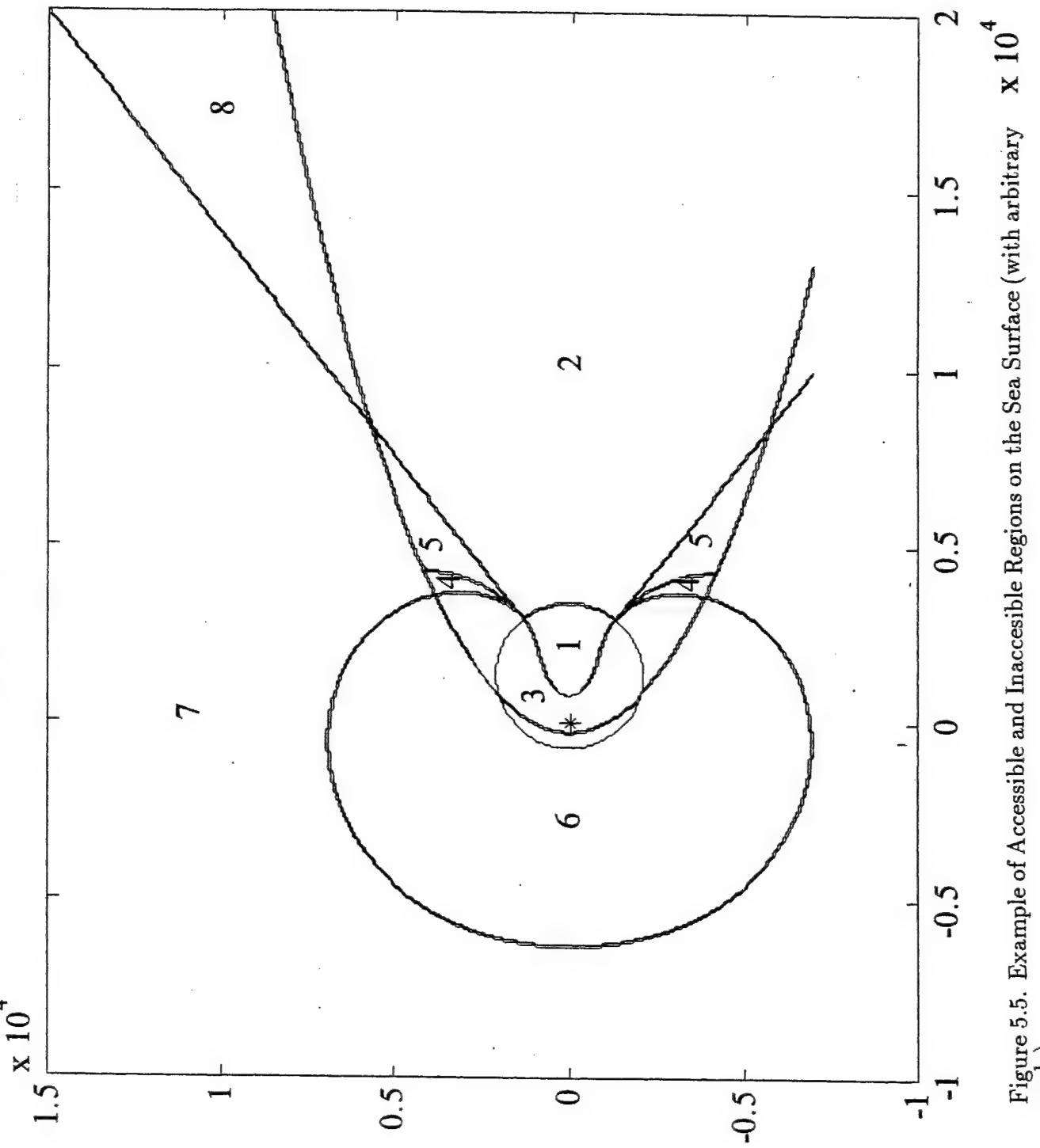

Figure 5.5. Example of Accessible and Inaccesible Regions on the Sea Surface (with arbitrary scale).

CHAPTER 6

ASCM DRAG LOSS

The simplified threat trajectories being used for threat evaluation consist of CV and CTR segments. The drag and lift are approximated by

$$F_D = \kappa V_t^2 (C_{D0} + K C_L^2), \quad F_L = \kappa V_t^2 C_L \tag{6.1}$$

(see, for example, Etkin, 1972) where κ is $\frac{1}{2}\rho S$. The balance of forces on the threat body is represented by

$$m\ddot{\vec{r}} = \vec{F}_D + \vec{F}_L + \vec{T}_h + m\vec{g} \tag{6.2}$$

where

$$\vec{F}_D = -F_D \dot{\vec{r}}/V_t, \quad \vec{F}_L = F_L \vec{u}, \quad \vec{T}_h = T_h \dot{\vec{r}}/V_t, \quad \vec{g} = -g\vec{k} \tag{6.3}$$

The lift is in the direction of the unit vector, $\vec{u}$, which at the moment is undetermined. However, it must be perpendicular to $\dot{\vec{r}}$ in addition to having unit length, and therefore is specified by only one additional constant.

The thrust, T_h, needed to keep the threat speed constant is just an artifact of the simplified dynamics and has no meaningful importance. It is approximated by taking it in the direction of the threat velocity instead of along the body axis. The purpose of this term is to avoid the necessity of considering the body orientation. The effect of thrust is neglected because in the first place it is unknowable, and secondly because the gain in energy resulting from any actual powered flight incurs a corresponding cost to the threat.

It may seem plausible to omit gravity in (6.2) since it would seem to contribute equally to a gain in kinetic energy and a loss in potential energy as the threat descends. However, these two effects do not cancel. Gravity requires a compensating lift, which is obtained by an appropriate angle of attack that also affects the drag. Accordingly, gravity must be included in (6.2). Furthermore, it is not necessary to account for the gravitational loss in potential energy because this loss is independent of the trajectory shape.

The problem is to determine the total drag loss from a threat trajectory with given $\dot{\vec{r}}(t)$ and $\ddot{\vec{r}}(t)$. The drag as well as the other quantities can be found from (6.2) and (6.3) by scalar

multiplication of (6.2) successively by $\dot{\vec{r}}$, $\ddot{\vec{r}}$, $\vec{u}$, and $\vec{k}$ to get

$$0 = -\kappa V_t^3(C_{D0} + KC_L^2) + T_h V_t - mgv_z \tag{6.4a}$$

$$m|\ddot{\vec{r}}|^2 = \kappa V_t^2 C_L(\vec{u} \cdot \ddot{\vec{r}}) - mga_z \tag{6.4b}$$

$$m(\vec{u} \cdot \ddot{\vec{r}}) = \kappa V_t^2 C_L - mgu_z \tag{6.4c}$$

$$ma_z = -\kappa V_t(C_{D0} + KC_L^2)v_z + \kappa V_t^2 C_L u_z + T_h V_t^{-1} v_z - mg \tag{6.4d}$$

where the v_z, a_z, and u_z represent the z components of $\dot{\vec{r}}$, $\ddot{\vec{r}}$, and $\vec{u}$. The quantities not yet determined are T_h, u_z, $(\vec{u}\cdot\ddot{\vec{r}})$, and C_L. Only three of the four equations (6.4) are independent, but also only three of the four undetermined quantities are independent.

6.1 The CV Segment

The acceleration is set equal to zero and only three of the equations (6.4) are meaningful. Because of the loss of one of the equations (6.4) the CV case is not a special case of CTR and is treated separately. The quantities T_h and $(\vec{k} \cdot \vec{u})$ are eliminated from (6.4) to obtain

$$C_L^2 = \frac{mg[1 - (v_z/V_t)^2] - 2\kappa C_{D0} V_t v_z}{2\kappa K V_t v_z + \kappa^2 (mg)^{-1} V_t^4} \tag{6.5}$$

The drag is then

$$F_D = \kappa V_t^2 (C_{D0} + KC_L^2) \tag{6.6}$$

with C_L as given by (6.5). The quantity (6.6) is constant if variation in air density is neglected. The total drag loss is just F_D times the length of the segment.

6.2 The CTR Segment

The quantities $(\vec{u} \cdot \ddot{\vec{r}})$, T_h, and $(\vec{k} \cdot \vec{u})$ are eliminated from (6.4) to obtain

$$C_L^2 = \frac{m^2}{\kappa^2 b^2 V_t^4} \left(V_t^4 + 2gb^2 a_z + g^2 b^2 \left[1 - \frac{v_z^2}{V_t^2} \right] \right) \tag{6.7}$$

A real solution is obtained if (6.7) is positive. Note that

$$\text{sign}(C_L^2) = \text{sign} \left\{ V_t^4 \left[1 + \frac{2ga_z}{a^2} \right] + g^2 b^2 \left[1 - \frac{v_z^2}{V_t^2} \right] \right\} \tag{6.8}$$

where a is the acceleration magnitude. The second bracket is always non-negative. While the vertical component a_z is often negative, there is a wide range of circumstances where

the first bracket is non-negative, or if it is negative it could be dominated by the positive second bracket. However, the exact criterion for a real solution seems complicated.

The drag is then given by

$$F_D = \kappa V_t^2 C_{D0} + \frac{m^2 K}{\kappa b^2 V_t^2}\left(V_t^4 + 2gb^2 a_z + g^2 b^2\left[1 - \frac{v_z^2}{V_t^2}\right]\right) \tag{6.9}$$

The energy lost during the entire trajectory is

$$L_o = \int F_D \, ds \tag{6.10}$$

where $ds = d\theta/b$ is the incremental path length and the integration is over the entire CTR arc.

In a CTR segment the threat position is given by (3.5), from which the velocity and acceleration are seen to be

$$\begin{aligned} \dot{\vec{r}} &= \dot{\vec{r}}_0 \cos\omega t + \omega(\vec{r}_c - \vec{r}_0)\sin\omega t \\ \ddot{\vec{r}} &= -\omega\dot{\vec{r}}_0 \sin\omega t + \omega^2(\vec{r}_c - \vec{r}_0)\cos\omega t \end{aligned} \tag{6.11}$$

The total loss is obtained by the integral (6.10) over θ from 0 to θ_t. Neglecting the variation in air density (keeping κ constant), the integrals of the time-varying parts of (6.9) are

$$\int_0^{t_t} a_z \, dt = v_{z0}(\cos\omega t_t - 1) + \omega(z_c - z_0)\sin\omega t_t \tag{6.12}$$

and

$$\begin{aligned} \int_0^{t_t} v_z^2 dt = {} & \tfrac{1}{2}[v_{z0}^2 + \omega^2(z_c - z_0)^2]t_t + \tfrac{1}{4}\omega^{-1}[v_{z0}^2 - \omega^2(z_c - z_0)^2]\sin 2\omega t_t \\ & + \tfrac{1}{2}v_{z0}(z_c - z_0)(1 - \cos 2\omega t_t) \end{aligned} \tag{6.13}$$

CHAPTER 7

THE TBM TRAJECTORY

7.1 Introduction

ASCMs are evaluated by estimating an Objective Probability for each threat-objective pair by constructing a simplified trajectory from the initial threat position to the objective. Many alternative simplified trajectories were possible because ASCMs can maneuver by using aerodynamic forces. On the other hand, our treatment considers a TBM as incapable of maneuver. Its impact point is therefore predetermined by its initial threat state and its physical characteristics such as drag coefficient, etc. The uncertainty of its impact point arises from uncertainties in these physical characteristics and errors in the estimation of its initial state.

The length of TBM trajectories is not negligible compared to the Earth radius, and consequently it is advisable to use geographic rather than Cartesian coordinates. The time interval between establishment of firm track and impact is long enough that earth rotation needs to be considered. This could be accomplished by bringing the Coriolis force into the dynamics. Here, we use the simpler approach of using nonrotating coordinates and allowing the earth to rotate under the trajectory during the time in flight. To do this, the initial E velocity component is adjusted for Earth rotation to obtain the threat velocity relative to an inertial (nonrotating) system.

Assignment of Objective Probabilities is effected by determining an impact "footprint" on the Earth's surface. This footprint is the two-dimensional PDF of the impact point. To simplify the calculations, the expected impact point is determined by the *expected* initial threat state along with the best estimates of the threat's physical characteristics. The footprint is assumed to be a Gaussian function whose covariance is determined by several simplifying assumptions.

Oblateness of the Earth is neglected and we use the right-handed spherical geographic coordinates (ϕ, L, r) representing East Longitude, North Latitude, and radial distance. The threat velocity is expressed by components (u, v, w) having the dimensions of L/T in the three coordinate directions. Note that these components are neither covariant nor contravariant. Also, it is understood that u has been adjusted for earth rotation. That is, (u, v, w) are the

components in the celestial (inertial) system. The only difference between the celestial and the geographic coordinates is in the longitudinal or E components, which are related by

$$\phi = \phi_g + \Omega t, \qquad u = u_g + a\Omega \cos L \tag{7.1}$$

where the subscript "g" denotes the geographic coordinate or component, and Ω is the angular speed of the Earth rotation, equal to 2π per sidereal day. The celestial longitude ϕ is referred to a datum fixed on the celestial sphere. At the initial time the celestial and geographic coordinate systems coincide.

The complication of atmospheric reentry on a rotating, spherical Earth, is avoided by adjusting a Keplerian orbit. Instead of introducing the Coriolis force into the dynamics, Earth rotation is considered by carrying out the calculations in the celestial (inertial) frame. The effect of aerodynamic drag on a planar trajectory with a flat Earth is used to adjust the impact point and flight time.

The following steps are performed:

- Use the expected initial threat state relative to an inertial system. This is done by just adding $a\Omega \cos L$ to the Eastward velocity component relative to the rotating Earth. Calculate the arc length, θ_c, and flight time, T, to the impact point on the surface of the spherical Earth assuming a Keplerian orbit. Drag and Earth rotation are not considered.
- Carry out the same calculation in Cartesian Coordinates on a plane with a flat Earth. Find the distance X_0 and flight time T_0 to the impact point assuming a parabolic trajectory. Drag and Earth rotation are again neglected.
- Carry out the same calculation in Cartesian Coordinates on a plane with a flat earth, but this time consider the drag force in an exponential atmosphere. Integrate the dynamic equations numerically to find the distance X_a and flight time T_a to the impact point. The lift force is considered to be zero.
- The quantities $X_a - X_0$ and $T_a - T_0$ provide a correction for drag that would be cumbersome to obtain in spherical coordinates. Find the corrected arc distance and time of flight,

$$\begin{aligned} \theta &= \theta_c + a^{-1}(X_a - X_0) \\ T &= T_c + (T_a - T_0) \end{aligned} \tag{7.2}$$

- Calculate the impact point in the Celestial Coordinate system based on the expected initial threat state relative to an inertial system, using the corrected flight distance θ and flight time T.

- Get the (rotating) geographic coordinates of the impact point. This is done by just subtracting $a\Omega T \cos L_i$ from the Celestial East longitude of the impact point.
- Use Cartesian coordinates on a nonrotating, flat Earth and parabolic orbits to calculate the (2 by 2) covariance matrix of the footprint PDF on the Earth surface from the (6 by 6) covariance matrix of the initial threat-state errors. Uncertainties in knowledge of the threat characteristics (drag coefficient, etc.) are included to increase the footprint covariance.
- Assume a Gaussian footprint on the Earth's surface having the expected position and covariance as obtained above.

The last two steps are described in Chapter 8.

7.2 The Keplerian Orbit

Refer to Figure 7.1. With the simplifications described above the arc length θ between the initial threat geographic position (ϕ_0, L_0) and the impact point (ϕ_i, L_i) depends only on the initial threat speed V_0 and flight-path angle γ_0. This relation is given by Regan and Anandakrishnan (1993, equation (6.34)) as

$$\lambda = \frac{1 - \cos\theta}{(r_0/R_e)\cos^2\gamma_0 - \cos(\theta + \gamma_0)\cos\gamma_0} \tag{7.3}$$

where $r_0 = a + z_0$ is the initial threat radial distance, a is the Earth radius, $R_e = a + z_i$ is the radial distance of the impact point, and

$$\lambda = \frac{V_0^2 r_0}{\mu}, \quad \mu = g_0 a^2 \tag{7.4}$$

where g_0 is the acceleration of gravity at the Earth surface. The parameter λ determines the trajectory type. For the suborbital trajectories of interest, $\lambda \in (0, 1)$. Solving this equation for θ by representing the cosine in terms of the sine leads to the equation

$$A\sin^2\theta + B\sin\theta + C = 0 \tag{7.5}$$

where

$$\begin{aligned} A &= \lambda^2\cos^2\gamma_0 - 2\lambda\cos^2\gamma_0 + 1 \\ B &= -2\lambda\cos\gamma_0\sin\gamma_0(1 - \lambda\sigma\cos^2\gamma_0) \\ C &= \lambda(\sigma - 1)\cos^2\gamma_0[(\sigma + 1)\lambda\cos^2\gamma_0 - 2] \end{aligned} \tag{7.6}$$

where σ is r_0/R_e. It should be noted that there are cases where the trajectory may intersect the Earth surface behind the initial threat position, or may not intersect the Earth surface

at all. These cases are rejected, and the solution of interest is the smallest positive value θ obtained.

The unadjusted time of flight is given by Regan and Anandakrishnan (1993, equation (6.41b)), and is

$$T_F = \frac{r_0}{V_0 \cos\gamma_0}\left\{\frac{\tan\gamma_0(1-\cos\theta)+(1-\lambda)\sin\theta}{(2-\lambda)\{[(1-\cos\theta)/(\lambda\cos^2\gamma_0)]+[\cos(\gamma_0+\theta)/\cos\gamma_0]\}}\right\} + \frac{2r_0}{V_0\lambda[(2/\lambda)-1]^{3/2}}\arctan\left[\frac{[(2/\lambda)-1]^{1/2}}{\cos\gamma_0\,\mathrm{ctn}(\theta/2)-\sin\gamma_0}\right] \tag{7.7}$$

7.3 Correction for Drag

It is assumed that the reentry vehicle is subjected to drag but not to any lift force. The simplified aerodynamic equations are

$$\begin{aligned}\frac{dx}{dt} &= V\cos\gamma\\ \frac{dz}{dt} &= V\sin\gamma\\ \frac{d\zeta}{dt} &= -2V[\delta\zeta e^{-z/h}+g\sin\gamma]\\ \frac{d\gamma}{dt} &= -gV^{-1}\cos\gamma\end{aligned} \tag{7.8}$$

where

$$\zeta = V^2, \qquad \delta = \frac{\rho_0 C_D S}{2m} \tag{7.9}$$

with ρ_0 being the air density at the Earth's surface, C_D the drag coefficient, S a cross-sectional area, and m the threat's mass. These equations, which have been adapted from Regan and Anandakrishnan (1993), are integrated numerically to obtain the time of flight, T_a, and horizontal distance traversed, X_a, by a body falling through the exponential atmosphere.

Modification of the Keplerian trajectory is made by comparing the cases of falling through air, as in the previous paragraph, and falling through a vacuum. For the latter case the time of flight and horizontal distance traversed are given by

$$T_0 = \frac{\dot z_0 + \sqrt{\dot z_0^2 + 2g(z_0 - z_i)}}{g}, \qquad X_0 = \dot x_0 T_0 \tag{7.10}$$

to provide the quantities needed in (7.2) for this modification. An example is shown in Figure 7.2.

7.4 Impact Point

The foregoing formulas are for determining the impact point for a threat whose initial position and velocity are given. Consider the spherical triangle NOS where N is the North Pole, O is the subthreat point, and S is the subimpact point, where "sub" means projected radially onto a sphere of radius a (see Figure 7.3). From the previous definitions it is seen that $\frac{\pi}{2} - L_0$ is the arc NO, θ is the arc OS, and $\frac{\pi}{2} - L_i$ is the arc NS. Let the angle NOS be denoted by α, where

$$\tan \alpha = -u_0/v_0 \tag{7.11}$$

Then the celestial coordinates (ϕ_i, L_i) of the impact points are given by

$$\sin L_i = \sin L_0 \cos \theta + \cos L_0 \sin \theta \cos \alpha \tag{7.12}$$

and

$$\sin(\phi_0 - \phi_i) = \frac{\sin \theta \sin \alpha}{\cos L_i} \tag{7.13}$$

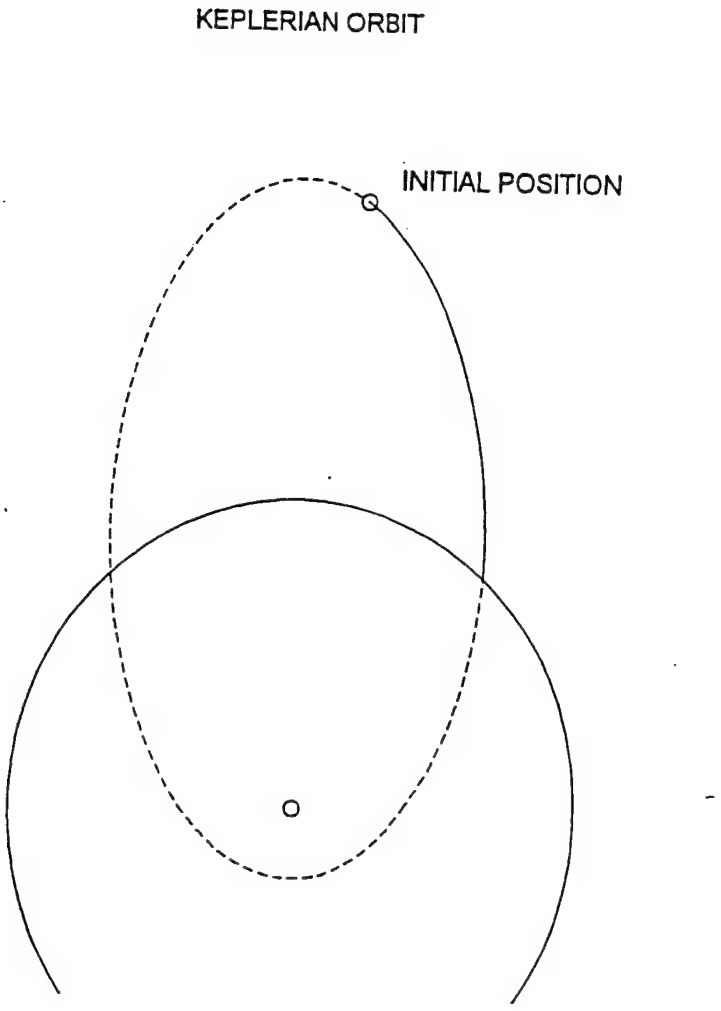

Figure 7.1. The Keplerian orbit. The flight plane passes through the threat initial position, the Earth center, and the initial velocity vector. This figure is viewed in an inertial reference frame, in which the Earth is rotating.

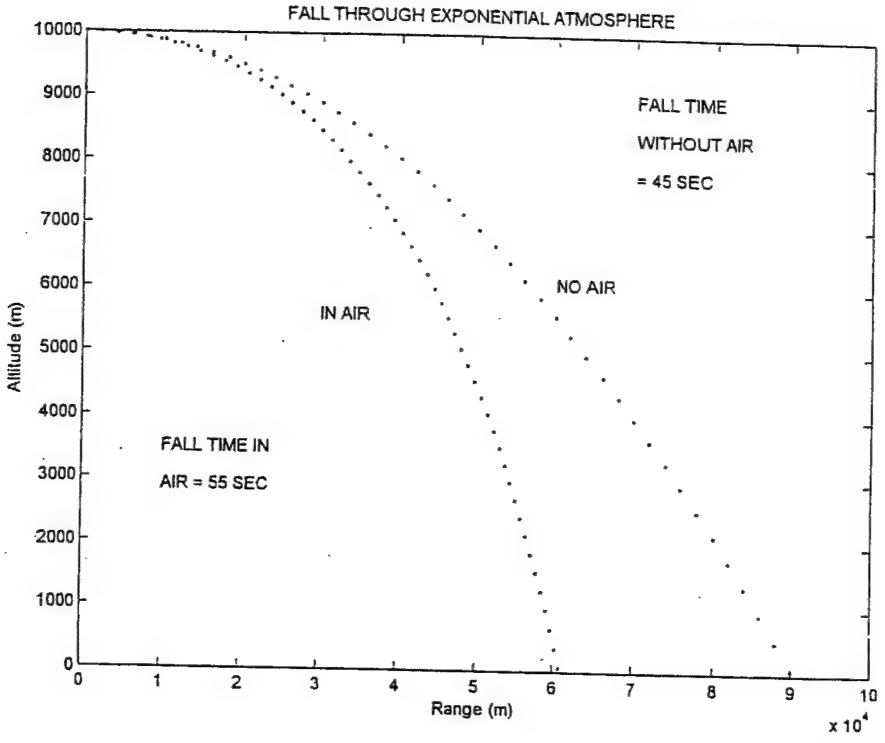

Figure 7.2. Example of fall through exponential atmosphere, and through vacuum. The points are at equal time intervals. In general, the air resistance increases the flight time while decreasing the horizontal range.

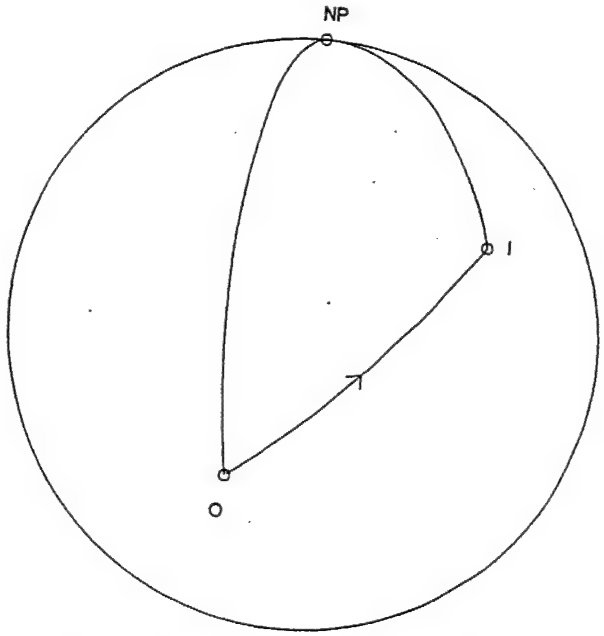

Figure 7.3. Location of the impact point "I" on the spherical Earth, where "O" is the projection of the initial threat position onto the Earth surface and "NP" is the North Pole. This picture is as viewed in an inertial reference frame, with the Earth rotating.

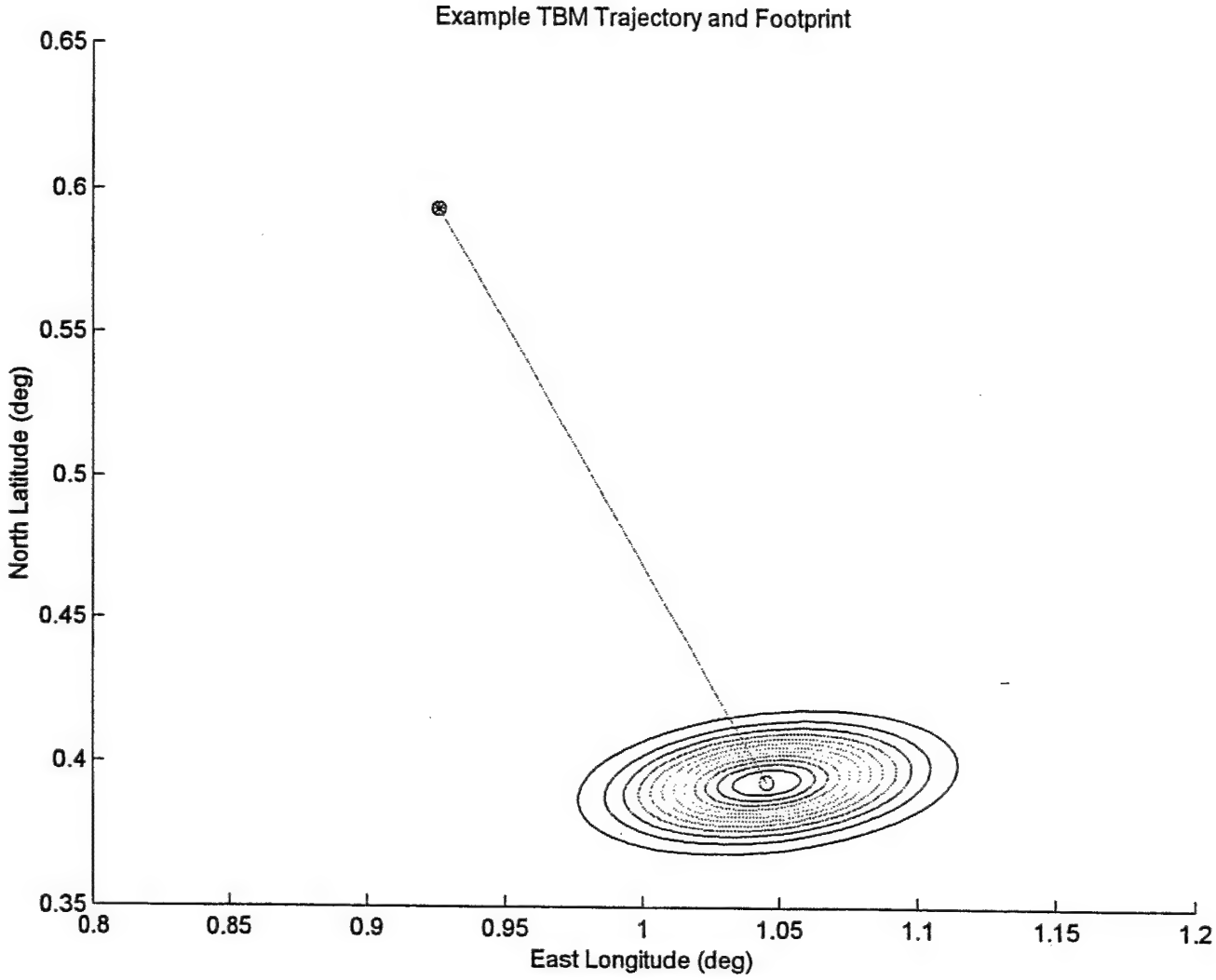

Figure 8.1. Example TBM Trajectory Projected onto Sea Surface and Footprint.

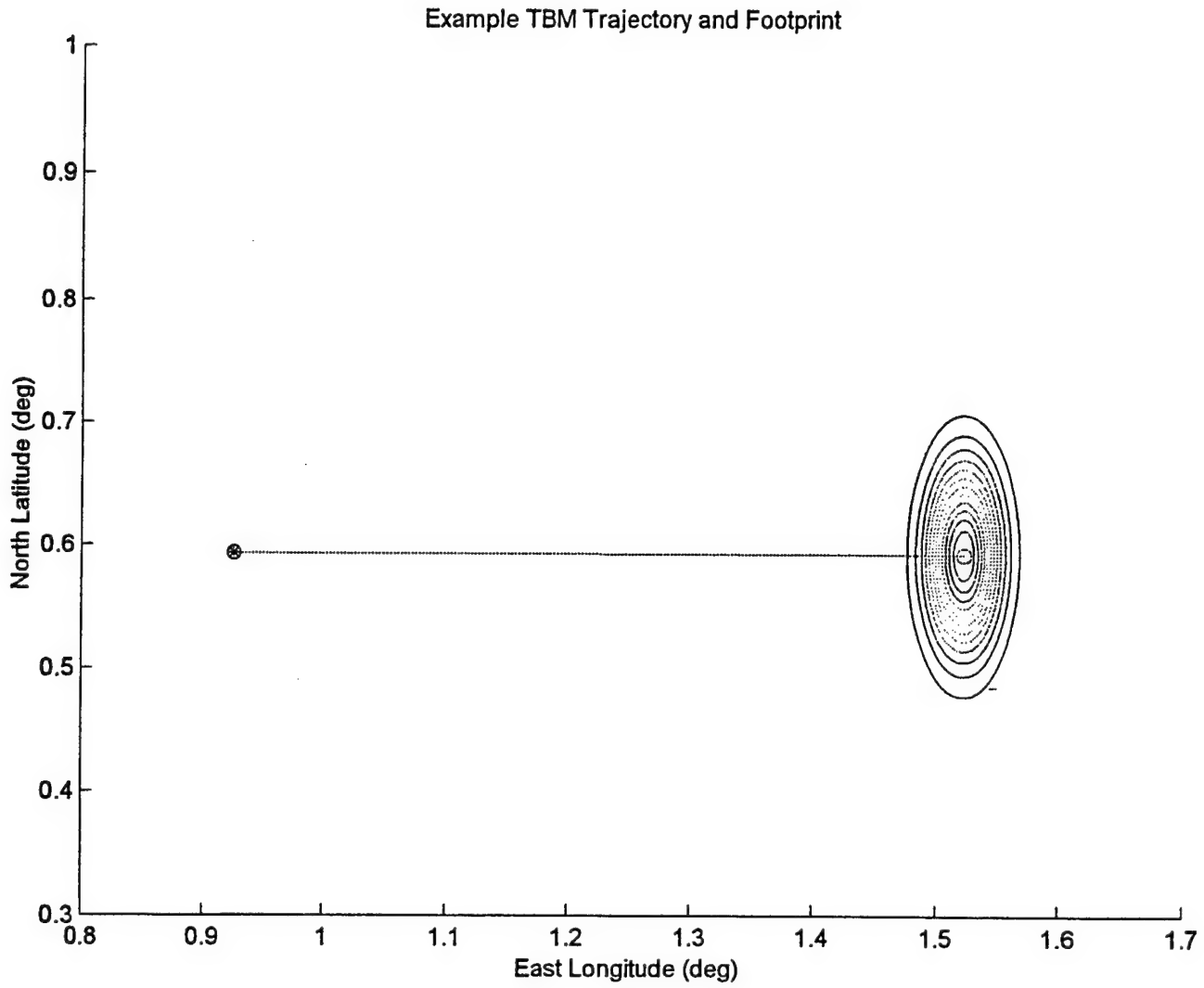

Figure 8.2. Example TBM Trajectory Projected onto Sea Surface and Footprint.

CHAPTER 8

THE TBM FOOTPRINT

8.1 Covariance of Impact Position Error

The geometry of Keplerian trajectories in spherical coordinates is more complicated than necessary for the estimation of the impact position error. For this estimate we consider a parabolic trajectory on a plane Earth in a right-handed Cartesian system (x, y, z) in the direction of the local (ϕ, L, r) (with z directed upward), and corresponding velocity components $(\dot{x}, \dot{y}, \dot{z})$. Also, the acceleration of gravity, g, is assumed constant. The flight time and the impact point at elevation z_i are given by

$$T_F = g^{-1}\left[\dot{z}_0 + \sqrt{\dot{z}_0^2 + 2g(z_0 - z_i)}\right], \quad x_i = x_0 + \dot{x}_0 T_F, \quad y_i = y_0 + \dot{y}_0 T_F \tag{8.1}$$

Even if the initial state error is Gaussian the joint PDF of the position error of the impact point is a complicated function because of the nonlinearity of (8.1). To simplify the analysis, the initial state errors are now taken to be infinitessimal quantities. To relate the initial state errors with the impact position errors we need the (2 by 6) Jacobian matrix J, where

$$J^T = \left(\frac{\partial(x_i, y_i)}{\partial(x_0, y_0, z_0, \dot{x}_0, \dot{y}_0, \dot{z}_0)}\right)^T$$

$$= \begin{pmatrix} 1 & 0 \\ 0 & 1 \\ \dot{x}_0\left[\dot{z}_0^2 + 2g(z_0 - z_i)\right]^{-1/2} & \dot{y}_0\left[\dot{z}_0^2 + 2g(z_0 - z_i)\right]^{-1/2} \\ g^{-1}\left[\dot{z}_0 + \sqrt{\dot{z}_0^2 + 2g(z_0 - z_i)}\right] & 0 \\ 0 & g^{-1}\left[\dot{z}_0 + \sqrt{\dot{z}_0^2 + 2g(z_0 - z_i)}\right] \\ g^{-1}\dot{x}_0\left(1 + \dot{z}_0[\dot{z}_0^2 + 2g(z_0 - z_i)]^{-1/2}\right) & g^{-1}\dot{y}_0\left(1 + \dot{z}_0[\dot{z}_0^2 + 2g(z_0 - z_i)]^{-1/2}\right) \end{pmatrix} \tag{8.2}$$

The (2 by 2) covariance of the impact position error C_s due to uncertainty in the threat state is related to the (6 by 6) covariance of the initial threat state error C_0 by

$$C_s = JC_0J^T \tag{8.3}$$

8.2 Uncertainty in the Drag Coefficient

If the threat classification is unknown, there may be appreciable uncertainty in the appropriate value of the drag parameter δ. This uncertainty will widen the extent of the TBM footprint and needs to be taken into account. There are ways to estimate the drag and its uncertainty from previous state estimates. A few such methods are outlined in Appendix A. The following is a simplified procedure for estimating the TBM footprint variance assuming that the expected value and standard error of δ are given.

Let $\overline{\delta}$ and σ_δ be the mean and standard deviation of the hypothetical PDF of δ representing our ignorance of its correct value. Carry out the numerical integration of the equations (7.8) for two values of δ and denote the results as follows:

$$\begin{aligned} T_{F1},\ \theta_1 \quad & \text{for } \delta = \overline{\delta} - \sigma_\delta \\ T_F,\ \theta \quad & \text{for } \delta = \overline{\delta} \end{aligned} \tag{8.4}$$

Denote the geographic coordinates of the two impact points by (ϕ_1, L_1) and (ϕ, L). The uncertainty in local Cartesian coordinates due to the error in δ is represented by the covariance matrix

$$C_d = a^2 \begin{pmatrix} (\phi_1 - \phi)^2 \sin^2 L & (\phi_1 - \phi)(L_1 - L)\sin L \\ (\phi_1 - \phi)(L_1 - L)\sin L & (L_1 - L)^2 \end{pmatrix} \tag{8.5}$$

The total error covariance in the impact point is given by

$$C_i = C_s + C_d \tag{8.6}$$

The impact "footprint" resulting from the initial state vector and error covariance is taken to be a Gaussian PDF with mean given by the geographic impact location ((7.12) and (7.13)) of the expected threat state, and covariance given by (8.6). Some examples are shown in Figures 8.1 and 8.2. When the TBM footprint overlaps a defended area, as it always does to some extent, as in Figure 8.3, the probability that the TBM will impact within the defended area is the integral of the footprint PDF over the defended area, and represented by $\hat{P}_{km}$, as discussed in Section 9.3.

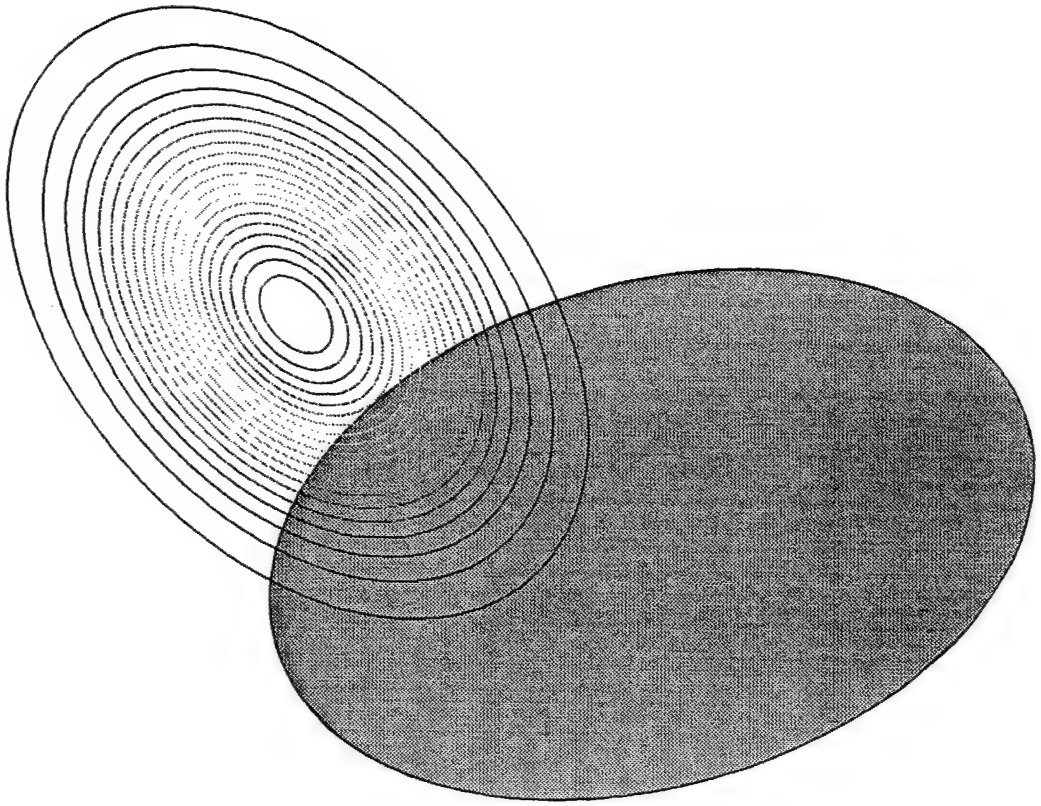

Figure 8.3. Example TBM Footprint and Defended Area.

CHAPTER 9

DETERMINATION OF EVALUATION PARAMETERS

9.1 Objective Probabilities

The immediate problem is to determine the objective of each threat in a battle situation. An "objective" is any surface unit or other defended point/region that may be the objective of an enemy attack. In situations where there are a large number of defended positions that might be under attack, as in the case of a task force, there is uncertainty as to which position is the objective of any given threat. This suggests the assignment of an "Objective Probability" to each threat-objective pairing. Let P_{kj} denote the probability that objective j is the target of threat k. Then for a threat capable of reaching any of the objectives

$$\sum_j P_{kj} = 1 \quad \text{for all } k \tag{9.1}$$

Otherwise

$$P_{kj} = 0 \quad \text{for all } j \tag{9.2}$$

for those threats k incapable of reaching any objective. Then we can use a Markov update model to assess probability that a state will be reached by a threat k.

9.2 ASCMs

The targets of ASCMs are assumed to be defended points, each having a specified position. Some of these positions may change during an engagement. The probability that a given threat is targeting a given objective would seem to depend on several circumstances: (1) the perceived value of the objective, (2) the flight time to the objective, and (3) the energy requirement to reach the objective.

Each defended point is assigned a Perceived Value $V_j^{(p)}$ and an Actual Value $V_j^{(a)}$. The value $V_j^{(p)}$ determines the probability of its being targeted, while $V_j^{(a)}$ determines the effort to be expended in its defense. These values are not necessarily equal, because the defender may have some knowledge about the objective that the attacker lacks.

The flight time and energy requirement depend on the unknown threat trajectory. Ways to hypothesize the trajectory of an ASCM and arrive at plausible values of the flight time

and energy requirement are discussed in Chapters 3, 4, and 6. Let T_{kj} be the ETA flight time of threat k to objective j. Similarly, let L_{kj} be the drag loss incurred by threat k in its ETA flight to objective j. These values are used to calculate a preliminary objective probability $\tilde{P}_{kj}$. It seems reasonable to assume that the probability of targeting an objective increases both with flight time and drag loss. Accordingly, the formula

$$\tilde{P}_{kj} = \frac{V_j^{(p)}}{\sqrt{T_{kj} L_{kj}}} \left(\sum_j \frac{V_j^{(p)}}{\sqrt{T_{kj} L_{kj}}} \right)^{-1} \tag{9.3}$$

9.3 TBMs

For each threat its initial state estimate determines a "TBM footprint" in terms of the PDF of its impact point, as described in Chapters 7 and 8. The assignment of values of P_{kj} to the defended positions is different for defended points and defended areas. Consider first the defended points. Each defended point lying within this footprint is assigned a preliminary value of $\tilde{P}_{kj}$ in proportion to the footprint density at its position.

Each defended region is assigned a Perceived Value per Unit Area $W_j^{(p)}$ and an Actual Value per Unit Area $W_j^{(a)}$. The reason for defining the values of defended areas differently from those for defended points is explained below. Defended areas have the complication that the radius of destruction about the impact point depends on the yield of the threat, which may not be known. The simplified procedure described here considers this effect only through values of the "Threat Menace" M_k, which are assumed specified along with other features of threat classification in advance of the "Threat Evaluation" being described here.

Each defended region lying within or overlapping the footprint is assigned a preliminary value of $\hat{P}_{kj}$ in proportion to the probability that the TBM will impact within the area. This probability is a surface integral of the footprint PDF over the defended area.

The values obtained need to be normalized, noting that the dimensions of the preliminary values for the defended points are different than those for the defended areas. However, the product of the preliminary values $\hat{P}_{kj}$ with the corresponding $W_j^{(p)}$ have the same dimensions as the preliminary $\tilde{P}_{kj}$ values for the defended points. Accordingly, values $\tilde{P}_{kj} = W_j^{(p)} \hat{P}_{kj}$ are defined.

9.4 Normalization

Now that the dimensions of the $\tilde{P}_{kj}$ are the same for defended points and defended areas, these are all normalized together so that their sum over all defended positions is unity for

each threat. That is,

$$P_{kj} = \tilde{P}_{kj} \left(\sum_j \tilde{P}_{kj} \right)^{-1} \qquad \text{for all } k \tag{9.4}$$

9.5 Time-Ordered Evaluation Parameters

It would be great if the threats could be adequately characterized by a single parameter each. However, it is easy to visualize situations in which such a simple characterization fails. Consider two threats, "A" and "B", where threat "A" reaches a low-valued asset quickly, while "B" reaches a more valuable asset later. Even in this simplistic scenario it is evident that the Weapons Control System (WCS) needs information that includes times of arrival. In addition, the optimal use of defensive assets (missiles) requires additional types of information, such as estimates of kill probabilities for the various threats, shooting platforms, launch times, etc., not to mention the scheduling of illuminators and magazine limitations.

The problem addressed here is to provide an evaluation of the threats based solely on the current estimates of their states and properties, along with the positions and values of the defended assets. The evaluation parameters provided by this study are insufficient for prioritization of the threats, which is expected to be carried out subsequently. Defense consists of the following steps:

THREAT EVALUATION → PRIORITIZATION → ENGAGEMENT

Consider now the product that "THREAT EVALUATION" should provide to "PRIORITIZATION". Two alternative characterizations are proposed: (1) The "Maximum Possible Value Loss" (MPVL), and (2) the "Maximum Expected Value Loss" (MEVL).

The MPVL, for each threat, is a monotonic function of time beginning with the current time. At any given time the MPVL is equal to the value ($V^{(a)}$) of the most valuable asset that the threat could reach by means of an ETA trajectory. At this time the threat is capable of reaching a definite set of assets. This set includes the assets belonging to previous sets. Since the MPVL is the maximum $V^{(a)}$ in the set, it monotonically increases with time.

The earliest arrival time of threat k to defended asset j is T_{kj}. For each threat k these values are reordered to obtain a set of ordered arrival times $\hat{T}_{ki}$, where

$$\hat{T}_{k1} \leq \hat{T}_{k2} \leq \hat{T}_{k3} \leq \ldots \tag{9.5}$$

where every i corresponds to one of the asset indices j for the given threat k. Having ordered

the arrival times to obtain the pairings

$$(k,i) \sim (k,j) \tag{9.6}$$

the ordered Actual Asset Values $\hat{V}_{ki}^{(a)}$ are obtained from the original $V_j^{(a)}$ by the pairing (9.6). The MPVL values are then obtained by taking

$$\tilde{E}_{ki} = \max(E_{k1}, E_{k2}, ..., E_{ki}) \tag{9.7}$$

The MEVL is obtained in the same way, by replacing the $V_j^{(a)}$ values by $V_j^{(a)} P_{kj}$. Note that the pairings (9.6) and the $\hat{T}_{ki}$ are the same as before. However, the $\tilde{E}_{ki}$ values may be different than in the MPVL case.

The implementation of threat evaluation is capable of providing both the MPVL and the MEVL. Neither is voluminous or not very computer intensive. It is suggested that simulation with various scenarios be performed in order to decide which of the two is preferable.

9.6 Algorithm

The determination of the Objective Probabilities proceeds in the following order:

- Determine the positions, and the $V_j^{(p)}$ and $V_j^{(a)}$ values of all defended points, and the locations, extents, and the $W_j^{(p)}$ and $W_j^{(a)}$ values for all defended areas.
- Obtain from the Track Server the estimated initial states and covariance matrices for all active threats.
- Obtain or hypothesize classification data on each threat. If an ASCM, specify its M_k, $\phi_k^{(m)}$, and $b_k^{(m)}$. If a TBM, specify its M_k, δ_k, and $\Delta\delta_k$.
- For each ASCM, k, determine the simplified trajectory to each defended point j and the values T_{kj}, L_{kj}, and P_{kj}.
- For each TBM, k, determine its footprint, and the values T_{kj} and P_{kj} for each defended point and area.
- Determine the T_k and $\tilde{E}_{ki}$ values.

9.7 Example

A task force consists of six units deployed on a two by three rectangular array as in Figure 9.1 (on an arbitrary scale), with separation of three kilometers between adjacent units. A

threat is initially observed at an altitude of five kilometers, at a distance of five kilometers downrange. The threat is initially in horizontal flight and arrives in a circular arc, targeting unit number five. The relative values of the units ($V_j^{(p)}$ values) are (1,5,2,2,4,2), respectively.

The variation with time of the "Time to Go" for the ETA trajectory to each unit (T_j values) is displayed in Figure 9.2 on an arbitrary scale. These values for all units decrease as the threat approaches, but finally only the T_j for unit five (the targeted unit) decreases to zero, as the threat arrives after 13 seconds. The variation with time of the "Objective Drag Loss" for the ETA trajectory to each unit (L_j values) is displayed in Figure 9.3 on an arbitrary scale. These values exhibit about the same trends as the Time to Go values.

The variation with time of the Objective Probabilities for each unit (P_j values) is shown in Figure 9.4 on an arbitrary scale. These values were computed according to equations (9.3) and (9.4). The defenders at first would assume that it is more probable that the threat is targeting unit 2 because of its higher value. But after about three seconds, the Objective Probability of unit 5 (the true target) becomes higher, as the Time to Go and Objective Drag Loss to all other units become great enough to depress their Objective Probabilities in comparison to that for unit 5, the true targeted unit.

The evaluation parameters MPVL and MEVL, as described in Section 9.5, are illustrated in another example described in Appendix B.

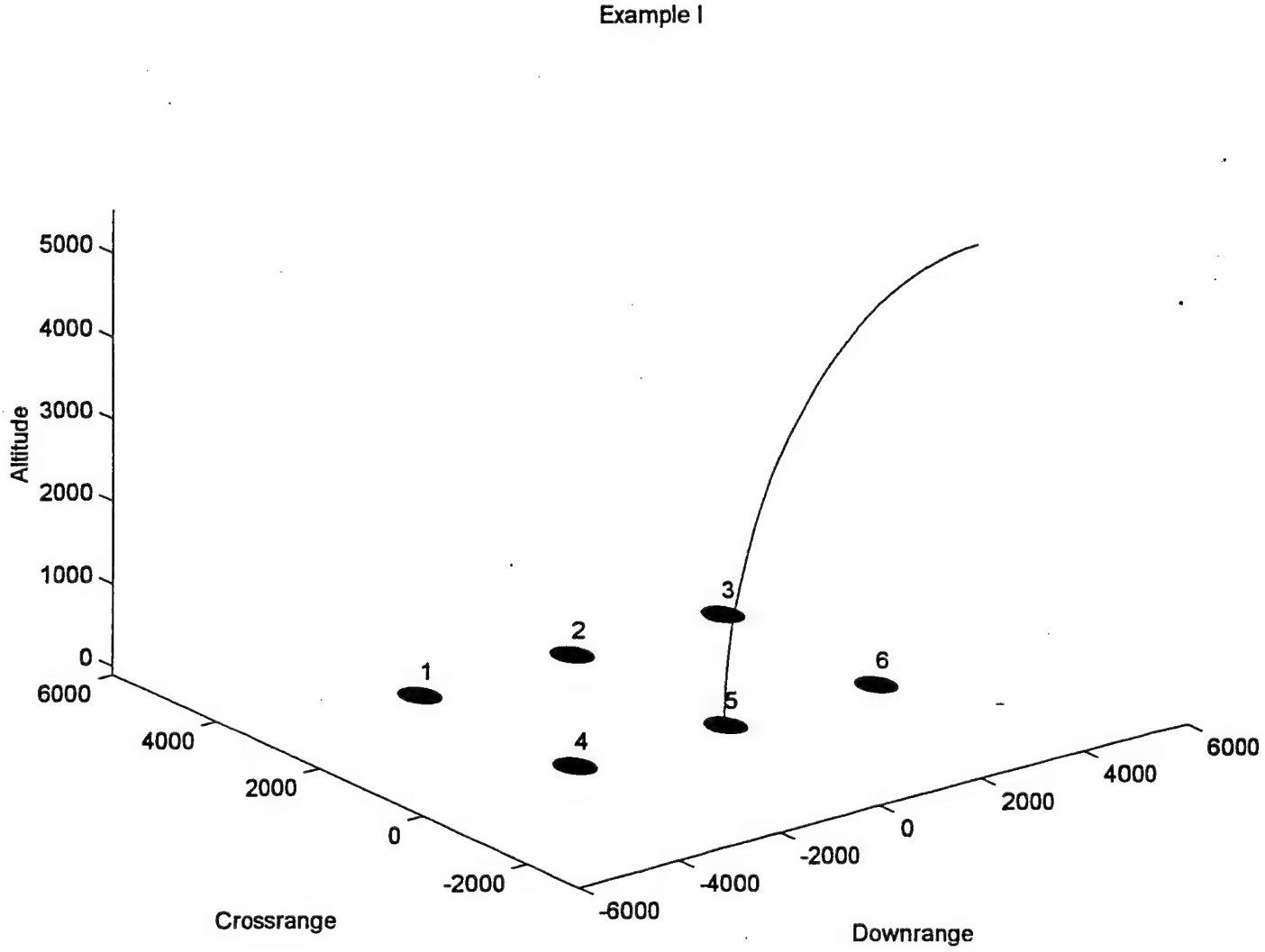

Figure 9.1. Scenario with six defended points and one ASCM threat. Defended Point #5 is the threat's target, initially unbeknownst to the defenders.

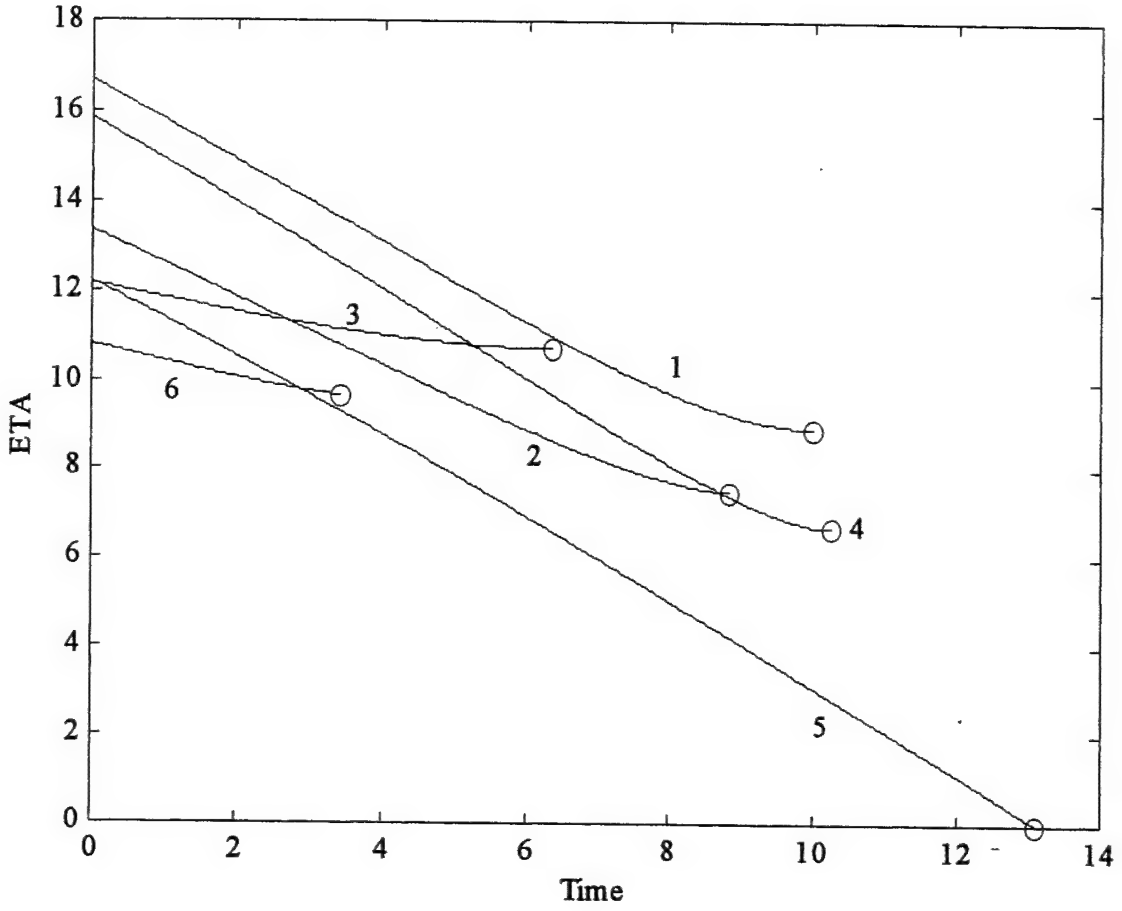

Figure 9.2. Evolution of the ETA arrival times for the scenario of Figure 9.1.

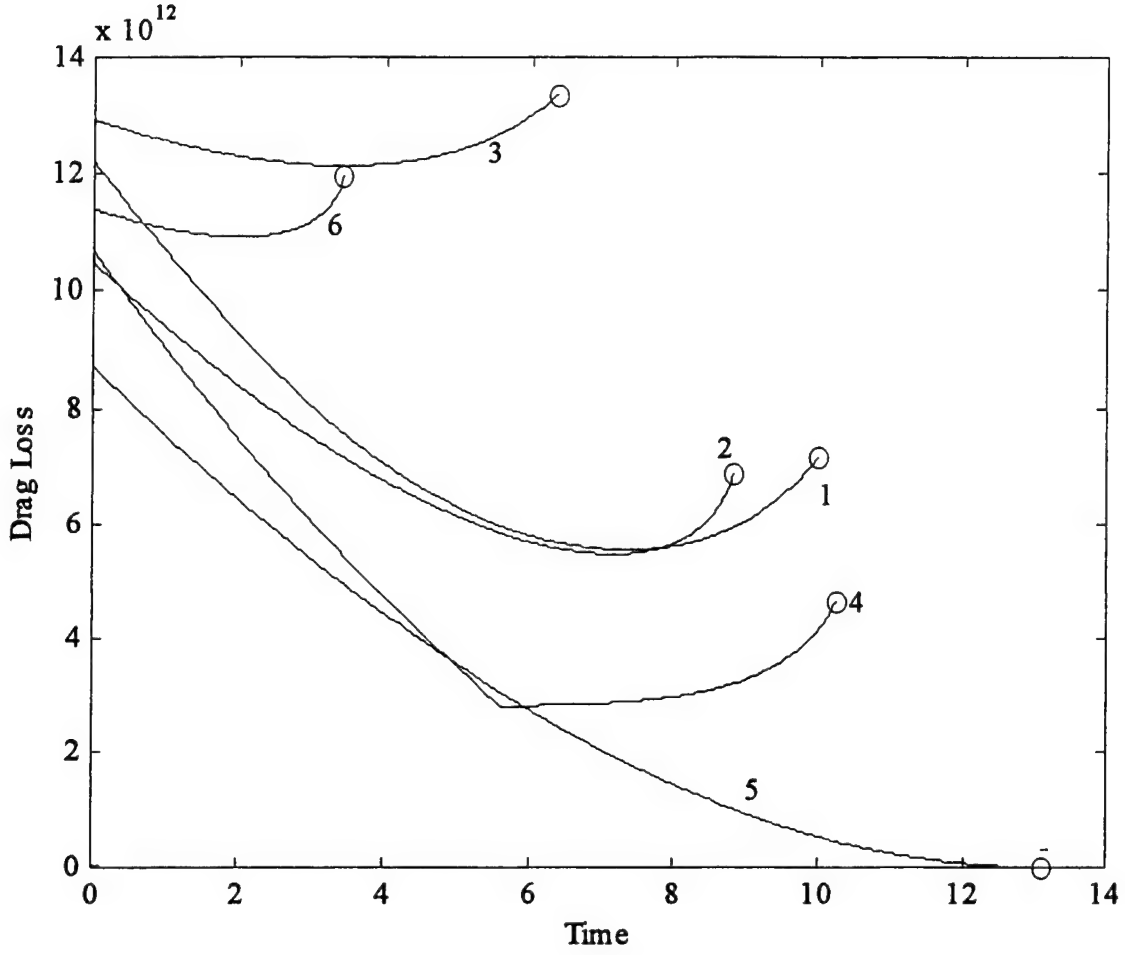

Figure 9.3. Evolution of the ETA drag loss for the scenario of Figure 9.1.

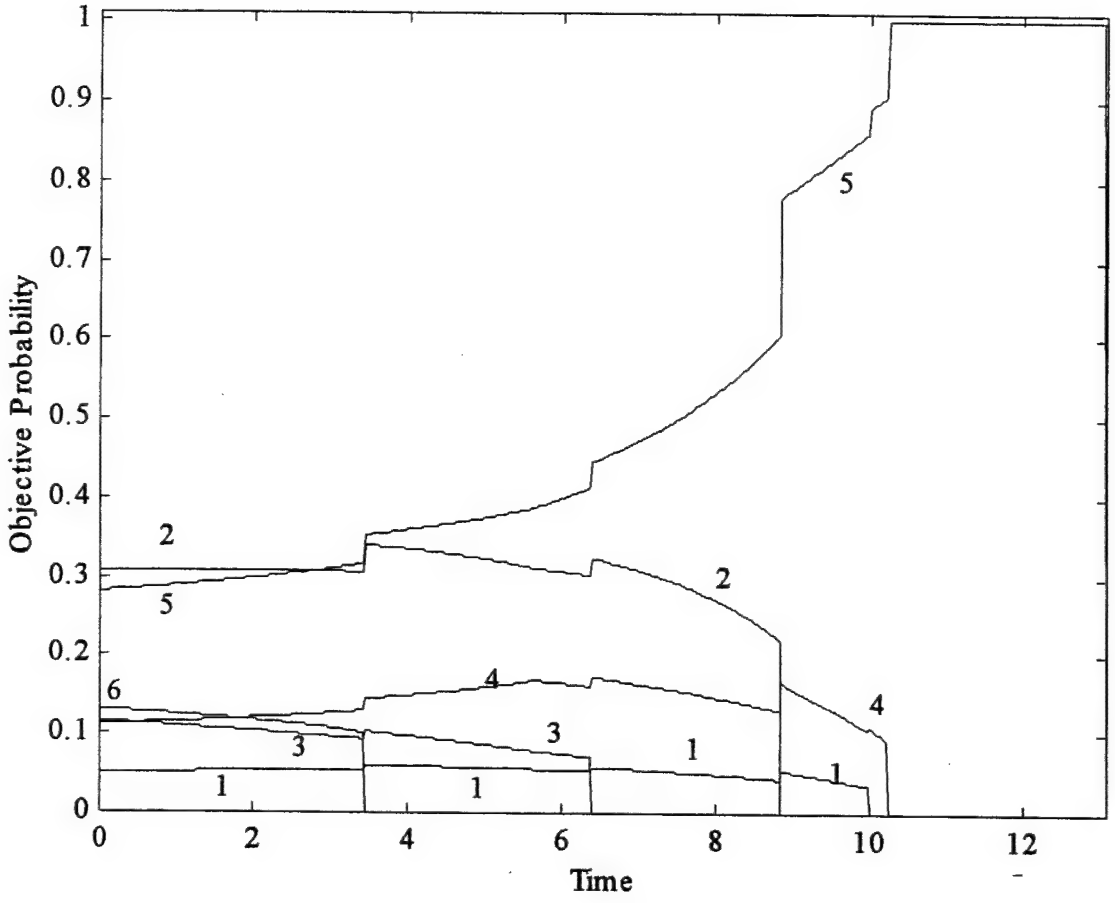

Figure 9.4. Evolution of the Objective Probabilities for the scenario of Figure 9.1.

CHAPTER 10

ORGANIZATION OF THE COMPUTATIONS

10.1 Background

The algorithm described in this chapter considers two types of threat – ASCMs and TBMs – as well as two kinds of defended positions – Points (*e.g.* ships) and Shore Areas (*e.g.* cities). Treatment of ASCMs differs from treatment of TBMs in the following respects. Each ASCM is considered potentially able to target any of the Defended Points. These are given "Objective Probabilities" to indicate which are more likely to be targeted.

For simplicity, the Objective Probabilities are based on the *expected* state of the ASCM, regardless of the errors in the state estimation. A maneuver is required for the threat to reach any of the Defended Points. A hypothesized simplified trajectory is proposed for each threat-objective pair, and used to determine the time of arrival and energy usage requirement. The Objective Probability is high for points that can be reached quickly (early time of arrival) and easily (low drag loss). The Objective Probability is zero for those points impossible for the threat to reach under reasonable assumptions regarding its flight capabilities.

In contrast, the trajectory of a TBM is considered determined by the threat characteristics (*e.g.*, mass, drag coefficient, etc.) and initial state. Maneuvers are not considered. If its target were considered determined only by its *expected* state, most likely it would not reach any of the Defended Points. These are possible targets only because the initial threat state and its physical properties are not precisely known. Accordingly, both the covariance matrix of the threat-state estimation errors and uncertainty in the value of the threat's drag coefficient are considered. These determine a "footprint", which is the PDF of the threat's impact point. Defended Points lying within this footprint are assigned Objective Probabilities related to the footprint PDF.

Extended shore areas may be targets of TBMs, but not of ASCMs unless there are Defended Points within the area. The Defended Points are represented by their positions, which may move during the engagement, and by an "Actual Value" (Va), and a "Perceived Value" (Vp). The Perceived Value is used to calculate the Objective Probability, while the Actual Value determines how much effort is to be expended in its defense.

A Defended Area can be represented by a circle, ellipse, or polygon. A TBM generates an Objective Probability determined by the intersection of its footprint onto the Defended Area. There is no structure. A real defended area such as a city would have variation in value from one part to another. This feature can be simulated by placing defended points within the area.

The Objective Probabilities form a two-dimensional matrix whose dimensions equal the number of threats (active at a given time) in one dimension, and the number of Defended Points and Defended Areas in the other. These values, along with the Va values, constitute an important input into the evaluation of the threats.

Engageability of the threat is not considered. The number and positions of the shooting platforms is not included among the data used. No PIPs are generated. The Objective Probabilities are estimated without regard to whether or not the threat can be engaged, or the most favorable launch times, etc.

10.2 Simplified Trajectories

For each (ASCM - Defended Point) pair a trajectory producing the soonest arrival time is determined. The initial threat-state error covariance is ignored, and the trajectory is based entirely on the initial *expected* state. The initial speed is maintained constant throughout the flight. The trajectory producing the earliest arrival time is determined. This lies on the plane determined by the initial threat velocity and the Defended Point. Initially there is a maximum-g turn followed by a CV segment to the Defended Point. Cases where this pattern would require the threat to fly below the sea surface are adjusted if possible.

The initial state estimate of a TBM including the covariance matrix generates a suite of hypothetical trajectories, one for each possible initial state. The flight follows a Keplerian orbit modified for liftless drag in an exponential atmosphere.

10.3 Determination of the Objective Probabilities

At any given time, all the threats that are active at that time are considered one by one. The ASCMs are treated separately from the TBMs.

For an ASCM, all the Defended Points are considered. For each Defended Point the drag loss along the simplified trajectory is approximated on the basis of whatever threat information is at hand. All incomplete threat information is hypothesized in a way that minimizes flight time and drag loss. The Objective Probability for each Defended Point is

based on these two values. After all Objective Probabilities have been approximated in this way, they are normalized so that their sum over all Defended Points is unity for each threat.

For a TBM, the first step is to approximate its footprint on the Earth's surface. The expected initial threat state is used to determine a single Keplerian orbit to the Earth surface. Next, the atmospheric effect is approximated by using a simplified dynamic model of a mass point falling in a planar orbit, without lift, from the expected initial state to the Earth's surface. The resulting flight time and distance provide a correction to the previously-determined Keplerian orbit to give a more accurate impact position and flight time.

The initial state covariance is usually assumed to be Gaussian. But even with this idealization, the complicated nonlinear flight path makes it difficult to get a closed-form footprint PDF. Instead, the impact position covariance is determined by assuming small errors and a parabolic planar trajectory through an airless medium. In addition to the error in impact position due to error in the estimation of the initial threat state, the error due to ignorance of the threat's drag coefficient is estimated. This is done by making drag corrections corresponding to two values of the drag coefficient differing by one standard deviation of the uncertainty. The separation of the two impact points provides an increment to the footprint covariance. This impact covariance is centered on the expected impact point that was previously determined by a somewhat more complete analysis, and is used to generate a two-dimensional Gaussian PDF to represent the impact footprint.

Defended Points lying within the impact footprint are assigned Objective Probabilities related to the Perceived Value and the PDF density at that position. Defended Areas intersecting the footprint are assigned Objective Probabilities related to their Perceived Values and the integrated footprint probability of impact in the intersection.

10.4 Pseudocode for Global Threat Evaluation

Initialize with $n = 0$ (no threats), and $m = 0$ (no defended positions). Actions to be performed are one of the following:

- Add a threat track.
- Drop a threat track.
- Update a threat track.
- Add a defended point.
- Delete a defended point.
- Move a defended point.

- Add a defended area.
- Delete a defended area.
- Calculate the Threat Evaluation Parameters.

perform a new action
update the battle time to the time of the action
if new track added
    $n = n + 1$
    state(n) inputted
    M(n) inputted
elseif track k_d dropped
    if $k_d < n$
        $M_{k_d} = M_n$
        state(k_d) = state(n)
    end
    $n = n - 1$
elseif threat track k_u is updated
    state(k_u) updated
    M_{k_u} updated
elseif a new defended point added
    $m = m + 1$
    position, $V_m^{(p)}$, and $V_m^{(a)}$ inputted
elseif a defended point j_d is deleted
    if $j_d < m$
        position(j_d) = position(m)
        parameters(j_d) = parameters(m)
    end
    $m = m - 1$
elseif defended point j_m is moved
    position(j_m) is changed
elseif a defended area is added
    $m = m + 1$
    position, $W_m^{(p)}$, and $W_m^{(a)}$ inputted
elseif defended area j_d is deleted
    if $j_d < m$

position(j_d) = position(m)
parameters(j_d) = parameters(m)
end
$m = m - 1$
elseif Threat Evaluation Parameters are to be calculated
for $k = 1 : n$
if threat(k)=ASCM
for $j = 1 : m$
if position(j) is a defended point
determine an ETA trajectory from k to j
if the ETA trajectory is valid
calculate T_{kj} and L_{kj}
end
end
end (of j loop)
calculate $\tilde{P}_{kj}$
if threat(k)=TBM
calculate the Keplerian orbit, range and time
correct the Keplerian parameters for drag
calculate the TBM footprint
for $j = 1 : m$
if position(j) is a defended point
calculate $\tilde{P}_{kj}$
elseif position(j) is a defended area
calculate $\hat{P}_{kj}$ and $\tilde{P}_{kj}$
end
end (of j loop)
end (of if ASCM or TBM)
calculate P_{kj}, T_k, and $\tilde{E}_{ij}$
end (of k loop)
end (of action)

The organization of these computations is shown schematically in Figure 10.1.

10.5 Computation Modules

The following numbers are defined:

na	Number of Cruise Missiles (ASCMs)
nt	Number of TBMs
mp	Number of Defended Points
ma	Number of Defended Areas
nd	Number of Data Points in Trajectories

derivs – a function used during Runge-Kutta numerical integration (see Press et al, 1986)

Inputs

t	time (s)
y	(4 by 1) Vector of Dependent Variables
delta	Modified Drag Coefficient (1/m)
hatm	1/e altitude of air density (m)

Outputs

dydt	(4 by 1) Vector of Derivatives

dragloss – a function to calculate the drag loss

Inputs

Cdo	Drag Coefficient at Zero Lift
K	A Coefficient in Drag Relation
r0vec	(3 by 1) Initial Threat Position (m)
rsvec	(3 by 1) Targeted Point Position (m)
r0dotvec	(3 by 1) Initial Threat Velocity (m/s)
bm	Minimum Allowed Turn Radius (m)
kappa	Physical Parameter for Air and Vehicle (kg/m)
m	Vehicle Mass (m)
flag	Flag Indicating Validity of Inputs
etarcvec	(3 by 1) Position of ETA Arc Center (m)
etartvec	(3 by 1) Position of Transition Point (m)
etathetat	Arc Length (rad)

Outputs

etaloss	Drag Loss (kg m^2/s^2)

falltime – a function called for each TBM at desired time

Inputs

hatm	Altitude where air density is 1/e of surface value (m)
delta	Drag Coefficient (1/m)
V0cel	Initial Threat Speed (m/s)
gamq0cel	Initial Flight Angle (rad)
z0	Initial Threat Altitude (m)
zi	Altitude of Impact Area (m)
dt	Time Increment for Numerical Integration (s)
epsi	Parameter Needed in Runge Kutta Integration
h1	Parameter Needed in Runge Kutta Integration
hmin	Parameter Needed in runge Kutta Integration

Outputs

Tfall	Time of Flight thru atmosphere (s)
Xfall	Range (in inertial system) reached during flight (m)

footprin – a function called for each TBM at desired time

Inputs

elong0	Initial Threat East Longitude (rad)
nlat0	Initial Threat North Latitude (rad)
r0dotvec	(3 by 1) Initial Threat Velocity (m/s)
C0	Initial Threat State Error Covariance
z0	Initial Threat Altitude (m)
zi	Altitude of Impact Area (m)
hatm	Altitude where air density is 1/e of surface value (m)
delta	Drag Coefficient (1/m)
dt	Time Increment for Numerical Integration (s)
epsi	Parameter Needed in Runge Kutta Integration
h1	Parameter Needed in Runge Kutta Integration
hmin	Parameter Needed in runge Kutta Integration

Outputs

elongi	Impact Point East Longitude (rad)
nlati	Impact Point North Latitude (rad)

Ci	(2 by 2) Covariance of Impact Position Error (m^2)
TF	Expected Flight Time (s)

gentraj – called at beginning of run

This is supplied by used to generate a number n of threat trajectories. These are used to input initial threat states and covariance matrices at different times.

Inputs

none

Outputs

n	Number of threat trajectories
na	Number of ASCM Trajectories
nt	Number of TBM Trajectories
nd	Maximum number of time steps in trajectories
	(nd by n by 6) Array of threat states
	(nd by n by 6 by 6) Array of covariance matrices
Mvec	(n by 1) Threat Menace parameter

kepler – a function to find the flight time and arc traversed in Keplerian orbit

Inputs

z0	Initial Threat Altitude (m)
zi	Altitude of Targeted Area (m)
r0dotcel	(3 by 1) Velocity Vector in Celestial System

Outputs

thetakep	Arc Distance Traversed in Keplerian Orbit
TFkep	Time of Flight in Keplerian Orbit

makeJ21 – a function that generates the transformation matrix J21

Inputs

phi1,L1	Geographic Position of First Cartesian System (rad)
phi2,L2	Geographic Position of Second Cartesian System (rad)

Output

J21	(3 by 3) Transformation Matrix

overlap – a function that computes TBM impact probability

Inputs

x0,y0	Coordinates of Center of Defended Area (m)
asemi	Semimajor Axis of Elliptical Region (m)
bsemi	Semiminor Axis of Elliptical Region (m)
phia	direction of line of apsides (rad)
xi,yi	Coordinates of Center of TBM Footprint (m)
Ci	Covariance Matrix of Footprint PDF (m^2)

Output

prob	Probability of Impact Within Defended Area

simptraj – a function called for each (ASCM - Defended Point) pair at desired time

Inputs

r0vec	(3 by 1) Initial threat position (m)
r0dotvec	(3 by 1) Initial threat velocity (m/s)
bm	Minimum allowed turn radius (m)
phim	Maximum allowed heading error (rad)
rsvec	(3 by 1) targeted point coordinates (m)

Outputs

flag	Indicator of ETA trajectory validity
etarcvec	(3 by 1) Position of turn arc center (m)
etartvec	(3 by 1) Position of transition point (m)
etathetat	length of turn arc (rad)
eta	ETA arrival time (s)
s	Length of CV segment (m)

taskfors – to be written by user and called at desired times

Inputs

none

Outputs

m	Number of Defended Assets
mp	Number of Defended Points

ma	Number of Defended Areas
rsvec	(mp by 3) Positions of Defended Points (m)
r0vec	(ma by 3) Centers of Defended Areas (m)
avec	(ma by 1) Semimajor axes of Defended Areas (m)
bvec	(ma by 1) Semiminor axes of Defended Areas (m)
phiavec	(ma by 1) Directions of Lines of Apsides (rad)
Vavec	(m by 1) Actual Values of Defended Assets
Vpvec	(m by 1) Perceived Values of Defended Assets

timorder – a function that orders the ETA arrival times

Inputs

k	threat index
m	(or numit) Number of Defended Assets
T(1:n,1:m)	ETA Times of Arrival
Va(1:m)	True Values of Defended Assets
E(1:n,1:m)	Expected Loss of Value

Outputs

That(1:n,1:m)	Ordered ETA Times of Arrival (s)
Vhat(1:n,1:m)	Ordered True Values of Defended Assets
Ehat(1:n,1:m)	Ordered Expected Loss of Value
Etil(1:n,1:m)	Maximum Possible Value Loss

For computation of Maximum Expected Value Loss, Va*P is inputted instead of VA, and the outputted Etil contains MEVL values.

twoarc – a script file for displaying two-arc trajectories

Inputs

r0vec	(3 by 1) Initial Threat Position (m)
r0dotvec	(3 by 1) Initial Threat Velocity (m/s)
rsvec	(3 by 1) Targeted Point Position (m)
nomega	(or na) Number of Turning Rates

Outputs

none

uodeint – a function based on the Runge Kutta ODE solver, "odeint" (see Press et al, 1986)

Inputs

yinout	(4 by 1) Vector of Dependent Variables
t1,t2	Beginning and End Times of Stepped Interval
epsi	Parameter Governing Integration Process
h1,hmin	Parameters Governing Integration Process

Outputs

yinout	(4 by 1) Vector of Dependent Variables
nok,nbad	Parameters Displaying Result of Step

urkqc – a function used in Runge Kutta process, based on "rkqc" (see Press et al, 1986)

Inputs

yin	(4 by 1) Vector of Dependent Variables
tin	(4 by 1) Independent Variable
delta	Modified Drag Coefficient
hatm	Altitude where Air Density is 1/e of Surface Value
epsi,yscal	Parameters Governing Stepping Process

Outputs

yout	Vector of Dependent Variables
tout	Independent Variable
hdid	Parameter Displaying Result of Step
hnext	Parameter Displaying Result of Step

urk4 – function used in Runge Kutta process, based on "rk4" (see Press et al, 1986)

Inputs

yin	(4 by 1) Vector of Dependent Variables
tin,tout	Times at Beginning and End of Step
delta	Modified Drag Coefficient
hatm	Altitude where Air Density is 1/e of surface Value

Outputs

yout	Vector of Dependent Variables

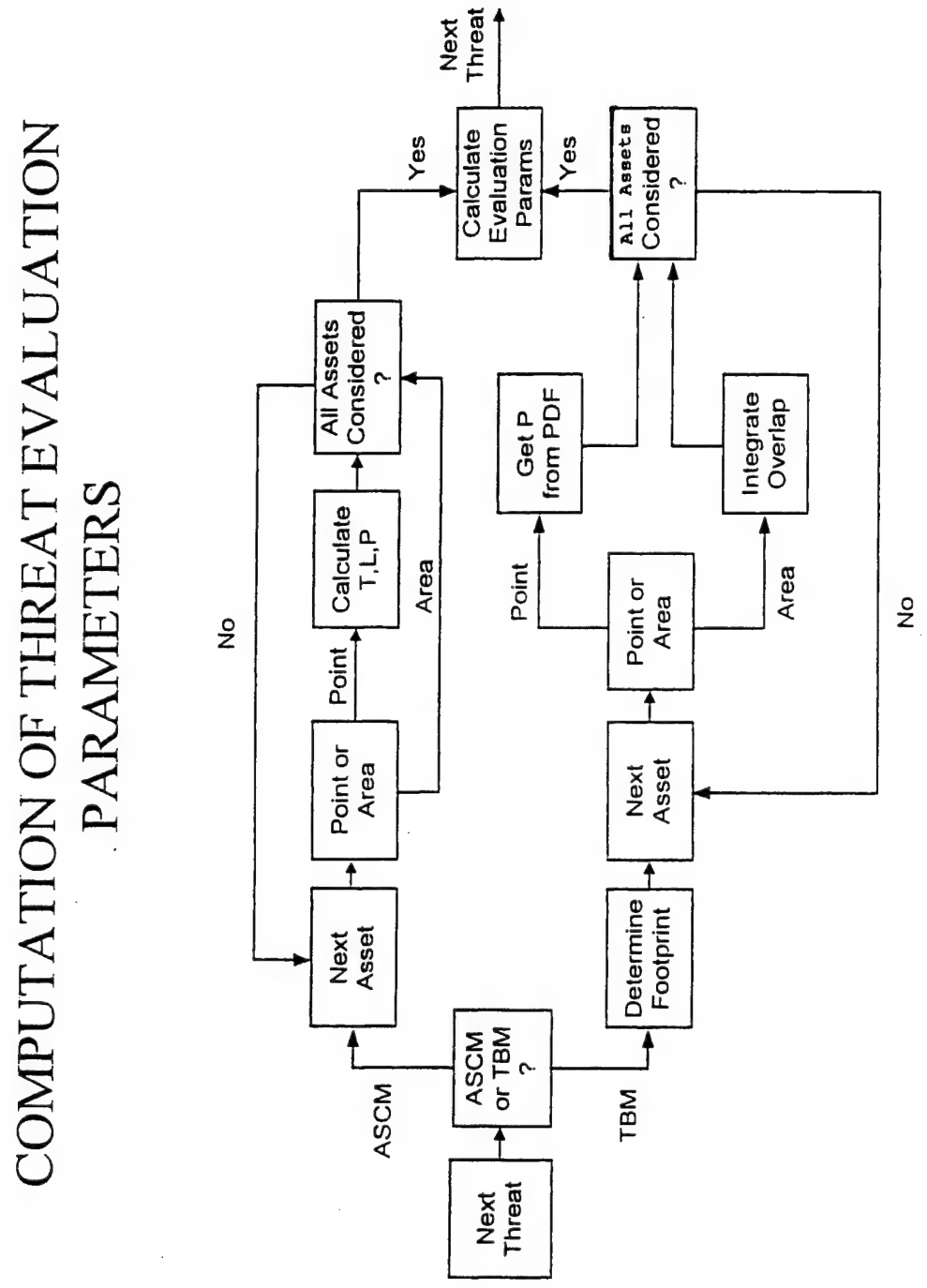

Figure 10.1. Organization of the Computations for Threat Prioritization.

CHAPTER 11

SUMMARY AND CONCLUSIONS

This report considers the case where a number of airborne threats may be targeting a number of defended assets. The threats are assumed to be one of two types: Anti-Ship Cruise Missiles (ASCMs) or Theater Ballistic Missiles (TBMs). The defended assets are of two types: points (*e.g.*, ships) or areas (*e.g.*, cities). Each threat is evaluated to provide parameters to be passed to the Weapons Control System to aid in prioritization and engagement. The threat evaluation is usually based on the latest state estimate and whatever classification information is available.

ASCMs are treated by constructing a simplified constant-speed trajectory to each defended asset to estimate the Earliest Time of Arrival (ETA). These trajectories obey constraints limiting the lateral acceleration magnitude and heading error. Objective Probabilities are estimated for each ASCM-asset pairing, based on the asset's value, ETA, and the energy requirement for reaching the asset.

TBMs are assumed unable to maneuver. Uncertainty in the impact point arises because of state estimation errors and lack of knowledge of the physical characteristics of the vehicle. This uncertainty is estimated to produce an impact Probability Density Function (PDF), or "footprint", representing the place where the TBM might land. Objective Probabilities for each TBM-asset pairing are estimated on the basis of the asset's value and the footprint PDF at the asset's position.

The evaluation of each threat is expressed in terms of two functions of time: the Maximum Expected Value Loss (MEVL) and the Maximum Possible Value Loss (MPVL). The Objective Probabilities, asset values, ETAs, and other information are used to calculate the MEVL and the MPVL. At any time the MEVL and the MPVL for a given threat express in slightly different ways the value loss that would be incurred if the threat were to leak.

It is recognized that the assumptions upon which the hypothesized predictive trajectories are based may not be universally applicable. The main assumptions have been (a) constant speed, (b) a limited HE, and (c) a limited "g" capability. Constant speed results from neglect of transfer between potential and kinetic energy upon descent or ascent, as well as from disregard of drag losses and the possibility of powered flight. A limited HE assumes that

the threat must continually be in a homing (seeking) mode. It is likely that less restrictive predictive models will provide better estimates of ETA and a more useful threat prioritization algorithm.

CHAPTER 12

ACKNOWLEDGEMENTS

The authors are grateful to Harry Lambertson for his encouragement to undertake this study, to Hugh McCabe for help in preparing figures, and to Gary Hild for presenting a synopsis of this report (Groves and Gray, 2001) at the National Fire Control Symposium 2001.

CHAPTER 13

REFERENCES

Becker, R. A., 1954: *Introduction to theoretical mechanics*, McGraw-Hill Book Company.

Etkin, B., 1972: *Dynamics of atmospheric flight.* John Wiley and Sons, Inc., New York, 579 pp.

Groves, G. W., W. D. Blair, and J. E. Gray, 1992: Some new approaches to trajectory prediction for maneuvering targets. *Proc. Symp. on Command and Control Research*, Naval Postgraduate School, Monterey, CA, 10-11 June 1992, pp. 302-317.

Groves, G. W., W. D. Blair, and J. E. Gray, 1994: Some concepts for trajectory prediction. NSWCDD TR-92/445, Naval Surface Warfare Center, Dahlgren Division, Dahlgren, VA.

Groves, G. W., and J. E. Gray, 2001: Threat prioritation in a multithreat, multiship scenario. *Proc. National Fire Control Symposium 2001*, Lihue, HI, August 2001.

Press, W. H., B. P. Flannery, S. A. Teukolsky, and W. T. Vettering, 1986: *Numerical Recipes*, Cambridge University Press, New York, 818 pp.

Regan, F., J., and S. M. Anandakrishnan, 1993: *Dynamics of atmospheric re-entry*, American Institute of Aeronautics and Astronautics, Inc., Washington, DC, 588 pp.

APPENDIX A

ESTIMATION OF TBM DRAG

A.1 Introduction

Air has a negligible effect on a Theater Ballistic Missile (TBM) during most of its flight. Only the initial and final phases of flight are influenced by aerodynamic effects. During the initial phase the TBM is usually subject to a large thrust force that makes it difficult to estimate the aerodynamic effects. Therefore, the concepts discussed here apply only during the final seconds of flight when it may be too late to take defensive action.

For aerodynamic forces on a body, the force is a function of the speed. If the force is a function of the speed alone, the force law can be expressed as

$$F_0 + F(v) = m\frac{dv}{dt} \tag{A.1}$$

or,

$$F_0 + F(v) = mv\frac{dv}{dx} \tag{A.2}$$

F_0 is any constant force that doesn't depend on v. For fluid resistance a fair approximation to $F(v)$ is

$$F(\vec{v}) = -c_1\vec{v} - c_2\vec{v}\,|\vec{v}| \tag{A.3}$$

where c_1 and c_2 are constants that depend on the size and shape of the object. For spherical objects, the approximate values of the constants in (A.3) are $c_1 = \hat{c}_1 D$ and $c_2 = \hat{c}_2 D^2$ where D is the diameter of the sphere and $\hat{c}_1 = 1.55 \times 10^{-4}$ kg/sec and $\hat{c}_2 = .22$ kg/m. For two cases, there is a limiting form of the drag problem depending on whether the speed is large or small. For small v the limiting form is

$$F(\vec{v}) = k\rho\vec{v} - mg\vec{z} \tag{A.4}$$

($\vec{z}$ is the upward unit vector) while for large v, the limiting form is

$$F(\vec{v}) = k\rho\,|\vec{v}|\,\vec{v} - mg\vec{z} \tag{A.5}$$

The third alternative for the friction law is

$$F(v) = k\rho v^2 \tag{A.6}$$

for the x and y components, while the z component is

$$F(v) = k\rho v^2 - mg \tag{A.7}$$

Closed form solutions can be obtained for (A.4) and for (A.6-A.7) but not for (A.5). An alternative to (A.4) that is sometimes used is to multiply $\vec{v}$ by $e^{-z/h}$ in (A.4). What we are interested in determining is estimators of the ballistic coefficient. For the dynamics laws that have closed form solutions to the equations of motion can be used as a means for estimating the ballistic coefficient. For other dynamics, alternative estimators are derived.

A.2 Solution of Equations of Motion

For motion along the z axis, in the quadratic case there are two differential equations to consider: upward motion (positive v, minus sign) and downward motion (negative v, plus sign)

$$-mg \pm c_2 v^2 = m\frac{dv}{dt} \tag{A.8}$$

The solution to (A.8) is

$$t - t_0 = \int_{v_0}^{v} \frac{m\,dv}{-mg - c_2 v^2} = \tau\left(\arctan\left(\frac{v_0}{v_t}\right) - \arctan\left(\frac{v}{v_t}\right)\right) \; (ris) \tag{A.9}$$

$$t - t_0' = \int_{v_0}^{v} \frac{m\,dv}{-mg + c_2 v^2} = \tau\left(\operatorname{arctanh}\left(\frac{v_0}{v_t}\right) - \operatorname{arctanh}\left(\frac{v}{v_t}\right)\right) \; (fal) \tag{A.10}$$

where $\tau = \sqrt{m/c_2 g}$ and $v_t = \sqrt{mg/c_2}$. Solving these equations for v gives

$$v = v_t \tan\left[\frac{t_0 - t}{\tau} + \arctan\frac{v_0}{v_t}\right] \; (ris) \tag{A.11}$$

$$v = -v_t \tanh\left[\frac{t - t_0'}{\tau} - \operatorname{arctanh}\frac{v_0}{v_t}\right] \; (fal) \tag{A.12}$$

The position as a function of time is therefore

$$z - z_0 = v_t \tau \log\left(\cos\left(\frac{t_0 - t}{\tau} + \arctan\frac{v_0}{v_t}\right)\right) \; (ris) \tag{A.13}$$

and

$$z - z_0 = v_t \tau \log\left(\cosh\left(\frac{t_0' - t}{\tau} - \operatorname{arctanh}\frac{v_0}{v_t}\right)\right) \; (fal) \tag{A.14}$$

Note for both of these cases, the x and y positions are the same as those in (A.11-A.12). Expanding (A.13-A.14) using the standard identities gives

$$(z - z_0)/(v_t \tau) = -\log\sqrt{v_t^2 + v_0^2} + \log\left[v_t \cos\left(\frac{t_0 - t}{\tau}\right) - v_0 \sin\left(\frac{t_0 - t}{\tau}\right)\right] \tag{A.15}$$

$$(z - z_0)/(v_t \tau) = -\log\sqrt{v_t^2 - v_0^2} + \log\left[v_t \cosh\left(\frac{t_0' - t}{\tau}\right) - v_0 \sinh\left(\frac{t_0' - t}{\tau}\right)\right] \tag{A.16}$$

For the x and y positions, the equations of motion follow from solving (A.5), which gives

$$x - x_0 = \frac{1}{b_x} ln\left(b_x v_R \sin(\alpha) t + 1\right) \tag{A.17}$$

and

$$y - y_0 = \frac{1}{b_y} ln\left(b_y v_R \cos(\alpha) t + 1\right) \tag{A.18}$$

We will now assume both t_0 and t_0' are both zero for the sake of simplicity. The second order expansions for rising and falling objects, (A.15-A.16), become

$$z - z_0 = v_t \tau \log\left(\frac{v_t}{\sqrt{v_t^2 + v_0^2}}\right) + v_0 t + \frac{t^2}{\tau}\left(\frac{v_0^2}{v_t} - \frac{v_t}{2}\right) \ (ris) \tag{A.19}$$

and

$$z - z_0 = v_t \tau \log\left(\frac{v_t}{\sqrt{v_t^2 - v_0^2}}\right) + v_0 t + \frac{t^2}{2\tau}\left[v_t + 2\frac{v_0^2}{v_t}\right] \ (fal) \tag{A.20}$$

Thus, the effect of a quadratic drag term is to induce an 'acceleration' whose magnitude using the relationship $v_t/\tau = g$, becomes either $2v_0^2/g\tau^2 \pm g$. Approximating the solutions for the x and y components gives

$$x - x_0 = \frac{1}{b_x}\left[v_R b_x \sin(\alpha) t - \tfrac{1}{2} v_R^2 b_x^2 \sin^2(\alpha) t^2 + ...\right], \tag{A.21}$$

and

$$y - y_0 = \frac{1}{b_y}\left[v_R b_y \cos(\alpha) - \tfrac{1}{2} v_R^2 b_y^2 \cos^2(\alpha) t^2 + ...\right] \tag{A.22}$$

Note if we retain first order terms only, the slant range is

$$R_H(t) = \sqrt{(x - x_0)^2 + (y - y_0)^2} = v_R t \tag{A.23}$$

Thus, under the circumstance that the drag is small, one could ignore the effects of drag on the slant range velocity. Thus it suffices to design a two state filter to handle the slant range when this approximation is true. A more realistic assumption is to keep the second order term because b is in the range 50-500. For this situation, with the assumption $b_x = b_y$, it is better to go to third order filter.

A.3 Ballistic Estimators

These formulas enable one to determine the ballistic coefficient from tracking data, they do not work for the types of drag functions that do not have analytic solutions. The method is general enough to work for any dispersive system of the type we are discussing. An

estimator can be derived based on the following observation: *Any dispersive system that can be written as*

$$\frac{d}{dt}(T+V) = \frac{d}{dt}E_c = F'v \tag{A.24}$$

where F' is the portion not derivable from a potential, $T+V$ is kinetic plus potential energy or the total conservative energy E_c, and F' is the portion of the force not derivable from a potential or the power delivered by an effective force F'.

For our application, the normalized E_c is

$$E_c = \tfrac{1}{2}v^2 + gz \tag{A.25}$$

There are several possibilities for the effective force,. depending on the circumstances. An estimator can be determined independent of the details of what $F'(v)$ functional form provided it is assumed that

$$F'(v) = k\rho f(v) \tag{A.26}$$

Substituting (A.25) and (A.26) into (A.24) gives

$$\frac{d}{dt}(\tfrac{1}{2}v^2 + gz) = k\rho v f(v)$$

or

$$d(\tfrac{1}{2}v^2 + gz) = k\rho v f(v)dt \tag{A.27}$$

To derive an estimator from (A.27), the derivatives and the variables are made discrete.

$$d \rightarrow \Delta_i = (\delta_i - \delta_{i-1})$$

so (A.27) becomes

$$E_i - E_{i-1} = k_i\rho_i v_i f(v_i)(t_i - t_{i-1}) \tag{A.28}$$

Summing over i gives

$$E_n - E_0 = \sum_{i=1}^{n} k_i\rho_i v_i f(v_i)(t_i - t_{i-1}) \tag{A.29}$$

If one defines $\hat{D}$ as the negative of the right side of (A.29), and recognizes that the variables are measurements, the energy loss estimator LE is formed

$$L\hat{E} = \hat{D} + \hat{E}_n - \hat{E}_0 \tag{A.30}$$

which can be used as ones' test statistic for a hypothesis test. General Electric (Reifler) has attempted this. There are other alternatives to the energy estimator in (A.35) besides those already mentioned.

Another method is to solve the equation of motion for the drag coefficient, obtaining

$$\delta = v^{-2} e^{z/h} \left[-\frac{dv}{dt} - g \sin\gamma \right] \tag{A.31}$$

The change in threat speed Δv is observed a number n of times along the TBM trajectory, resulting in a set of values

$$\Delta v_j, \quad \Delta t_j, \quad j = 1, ..., n \tag{A.32}$$

At each observation an estimate of the drag coefficient

$$\hat{\delta}_j = \delta + v_j^{-2} e^{z_j/h} \left[-\frac{\Delta v_{ej}}{\Delta t_j} \right] \tag{A.33}$$

is obtained, where δ is the true value and Δv_{ej} are the errors in the observed speed increments with standard error $\sigma_{\Delta v}$. The weighted mean of these estimates is

$$\bar{\delta} = \frac{\sum \hat{\delta}_j v_j^2 e^{-z_j/h} \Delta t_j}{K} = \delta - \frac{\sum \Delta v_{ej}}{K}, \qquad K = \sum v_j^{2-z_j/h} \Delta t_j \tag{A.34}$$

This weighting provides an unbiased estimate of the drag coefficient. To find the standard error of this estimate it is necessary to find the standard error in the speed estimate. This is cumbersome in general even when the error in the estimates of the threat state are assumed Gaussian. However, usually the threat speed greatly exceeds its error. Accordingly, it is assumed that

$$|\vec{v} - \langle \vec{v} \rangle| \ll |\vec{v}| \tag{A.35}$$

where the angle brackets denote expected value. The threat speed $v = |\vec{v}|$ is expressed by

$$v = \sqrt{[\langle \vec{v} \rangle + (\vec{v} - \langle \vec{v} \rangle)]^T [\langle \vec{v} \rangle + (\vec{v} - \langle \vec{v} \rangle)]} \tag{A.36}$$

where the magnitude of the vector within the parentheses is assumed small. To first order in the small quantity this becomes

$$v = \langle v \rangle \sqrt{1 + 2\langle v \rangle^{-2} \langle \vec{v} \rangle^T (\vec{v} - \langle \vec{v} \rangle)} = \frac{\langle \vec{v} \rangle^T \vec{v}}{\langle v \rangle} \tag{A.37}$$

and

$$\langle v \rangle = |\langle \vec{v} \rangle| \tag{A.38}$$

Thus, since v is a linear combination of the components of $\vec{v}$, v is Gaussian if $\vec{v}$ is Gaussian. The error in the speed estimates is

$$\sigma_v^2 = \left\langle [v - \langle v \rangle]^2 \right\rangle = \frac{\langle \vec{v} \rangle^T C \langle \vec{v} \rangle}{\langle v \rangle^2} \tag{A.39}$$

where C is the error covariance of the velocity estimates,

$$C = \left\langle [\vec{v} - \langle \vec{v} \rangle][\vec{v} - \langle \vec{v} \rangle]^T \right\rangle \tag{A.40}$$

Estimates of the speed increments are not independent even when the speed errors are independent. If one increment is overestimated, the following increment is likely to be underestimated. However, the error in a speed increment is independent of the errors in all the non-contiguous speed increments. The correlation between contiguous increment errors has little effect, and the relation between them and those of the speed estimates is

$$\sigma_{\Delta v}^2 = 2\sigma_v^2 \tag{A.41}$$

The error in the drag estimate is then

$$\sigma_\delta^2 = \langle [\bar{\delta} - \langle \bar{\delta} \rangle]^2 \rangle = \left\langle \left[-\frac{\sum \Delta v_{ej}}{K} \right]^2 \right\rangle = K^{-2}\sigma_{\Delta v}^2 = \frac{2\langle \vec{v} \rangle^T C \langle \vec{v} \rangle}{K^2 \langle v \rangle^2} \tag{A.42}$$

The foregoing analysis is based on a number of assumptions, some of which have been discussed previously. One is that the air density is a simple exponential function of altitude. A more refined approach would be to take the actual density profile existent at the place and time. Another is that the speed errors are independent of time (and altitude), whereas in actuality these errors are likely to increase as the air density and drag increase. Still another is that the expected velocity varies little during the time the observations are made.

APPENDIX B

EXAMPLE

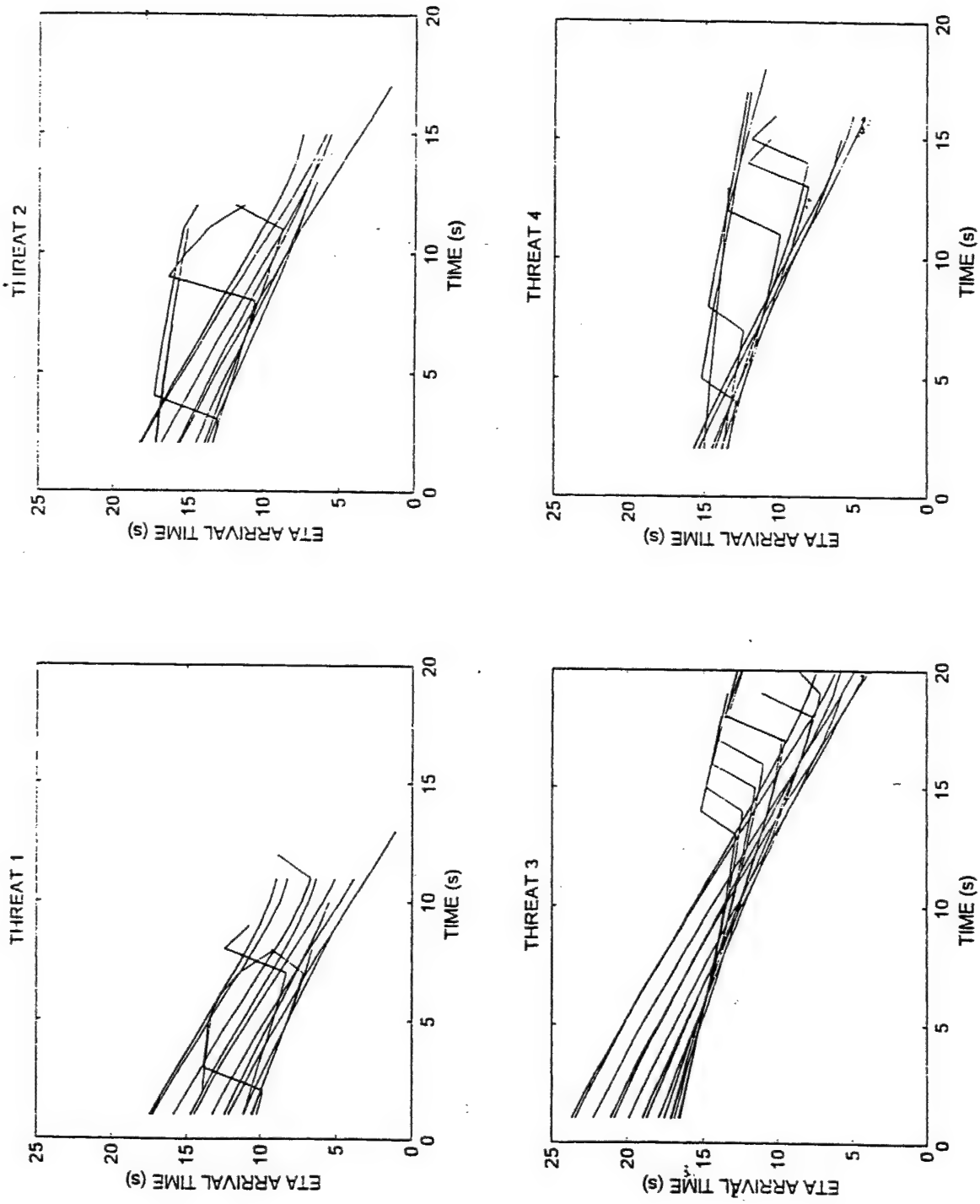

Figure B.2. Evolution of ETA arrival times for the fifteen defended assets of scenario of Figure B.1.

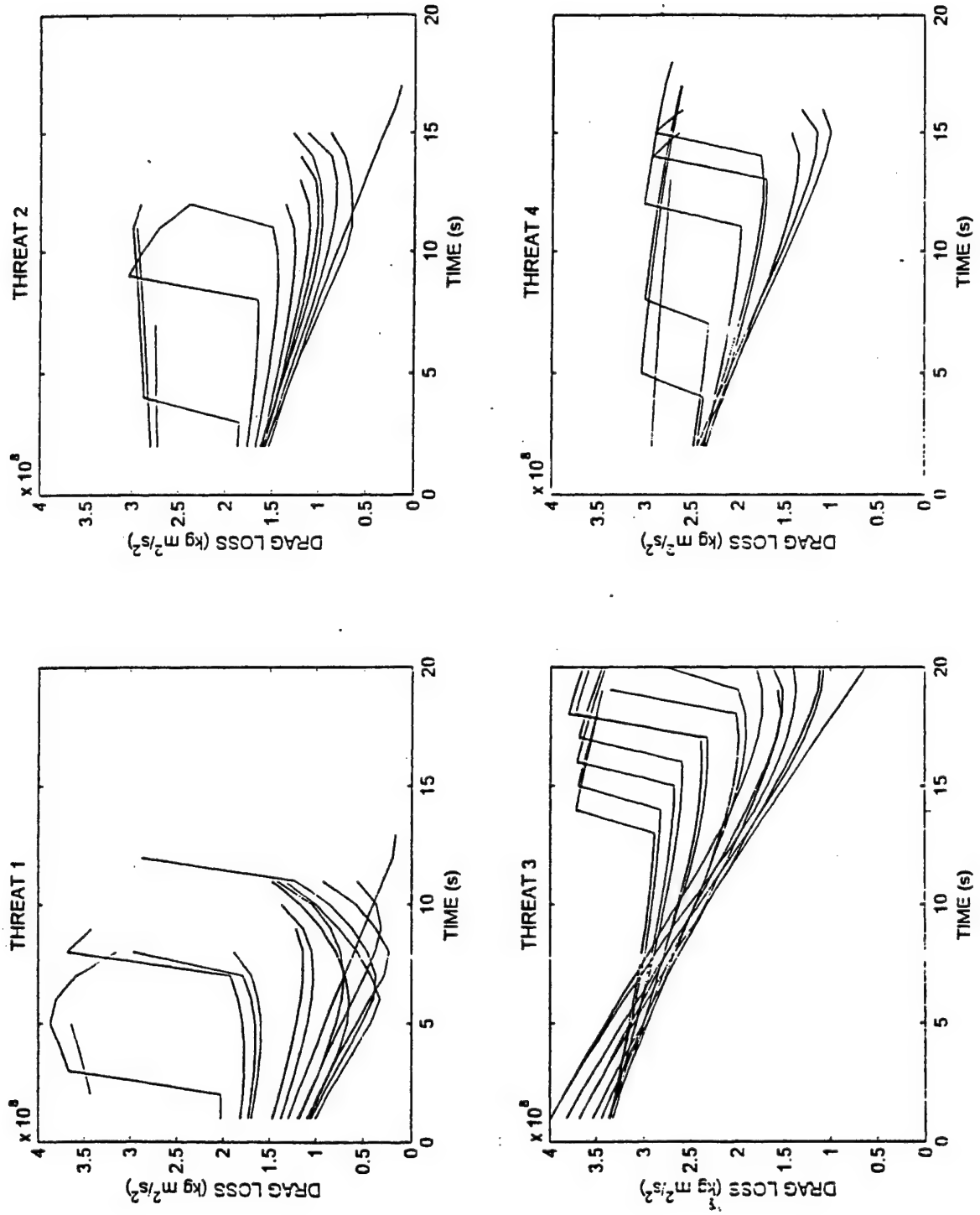

Figure B.3. Evolution of ETA drag loss for the fifteen defended assets of the scenario of Figure B.1.

This scenario illustrates the time-ordered threat evaluation parameters, the Maximum Possible Value Loss (MPVL) and the Maximum Expected Value Loss (MEVL), defined in Section 9.5 of the main text. There is a task force consisting of fifteen defended points and four Anti-Ship Cruise Missile (ASCM) trajectories, as shown in Figure B.1. The size of each dot representing a defended point is proportional to its value. Here, there is no distinction between actual and perceived value. The ASCM trajectories are numbered at the point representing their initial position. The trajectories are shown in plan view, the threat positions being projected vertically onto the horizontal plane.

The evolution of the Earliest Times of Arrival (ETAs) is shown in Figure B.2 for each of the four threats. There are fifteen curves, one for each of the defended points. The curve for each defended point terminates after the threat is no longer able to reach it. These curves generally decrease with increasing actual time, but there is sometimes a rather abrupt increase in arrival time when the threat progresses into a position less favorable for reaching that target.

The evolution of ETA drag loss is shown in Figure B.3 for each of the four threats. These curves generally display the same nature as those for the arrival times. The rate of drag loss increases with decreasing radius of curvature, and thus the curves rise whenever the threat needs to pull a higher lateral acceleration to reach the targeted point.

The evolution of the Objective Probabilities for Threat #1 is shown in Figures B.4a-e at five different times. The size of the dots representing the defended points is proportional to the Objective Probability. Points no longer reachable by the threat are indicated by their absence from the figure. The Objective Probabilities for Threat #2 are shown at three different times in Figure B.5a-c, and for Threats #3 and #4 in Figures B.6a-b and B.7a-c.

The MPVL is displayed for the four threats at three different times in Figures B.8a-c. The MEVL is similarly displayed in Figures B.9a-c. The amount of information represented in these displays is small, as only the coordinates of the corner points of the staircase representation are needed.

Figure B.10 displays the comprehensive MPVL and MEVL functions for all the threats.

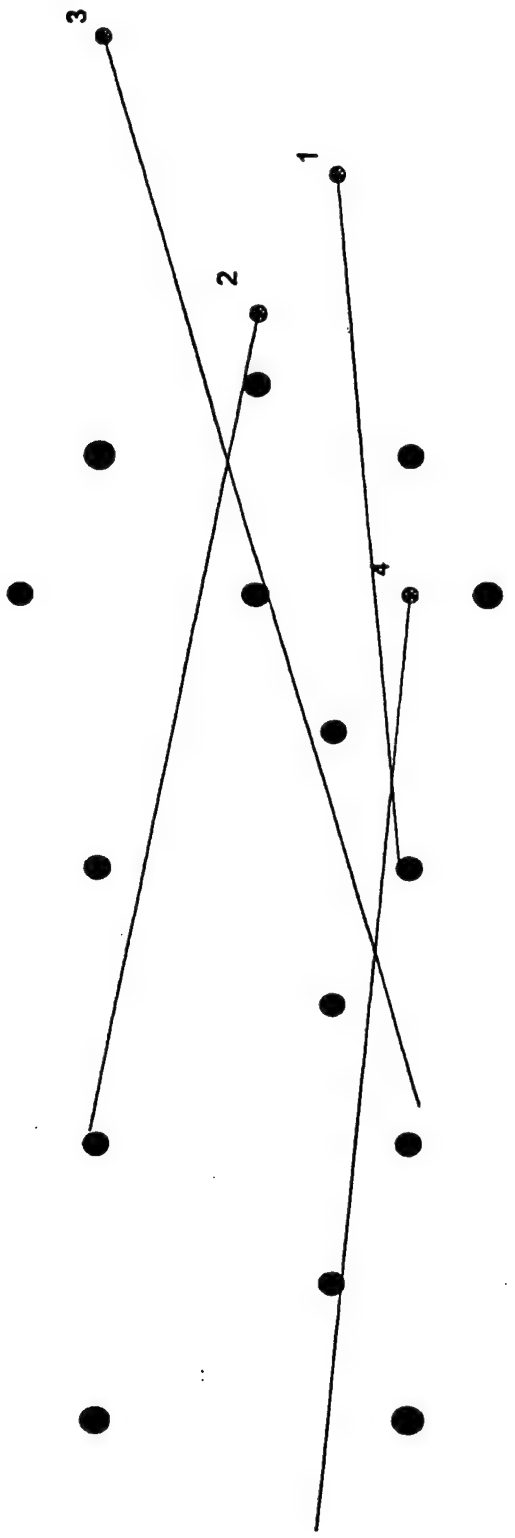

Figure B.1. An example scenario of fifteen defended points and four ASCM trajectories in plan view. The trajectories are projected vertically onto the sea surface. The size of the dots representing the defended points is proportional to their actual values.

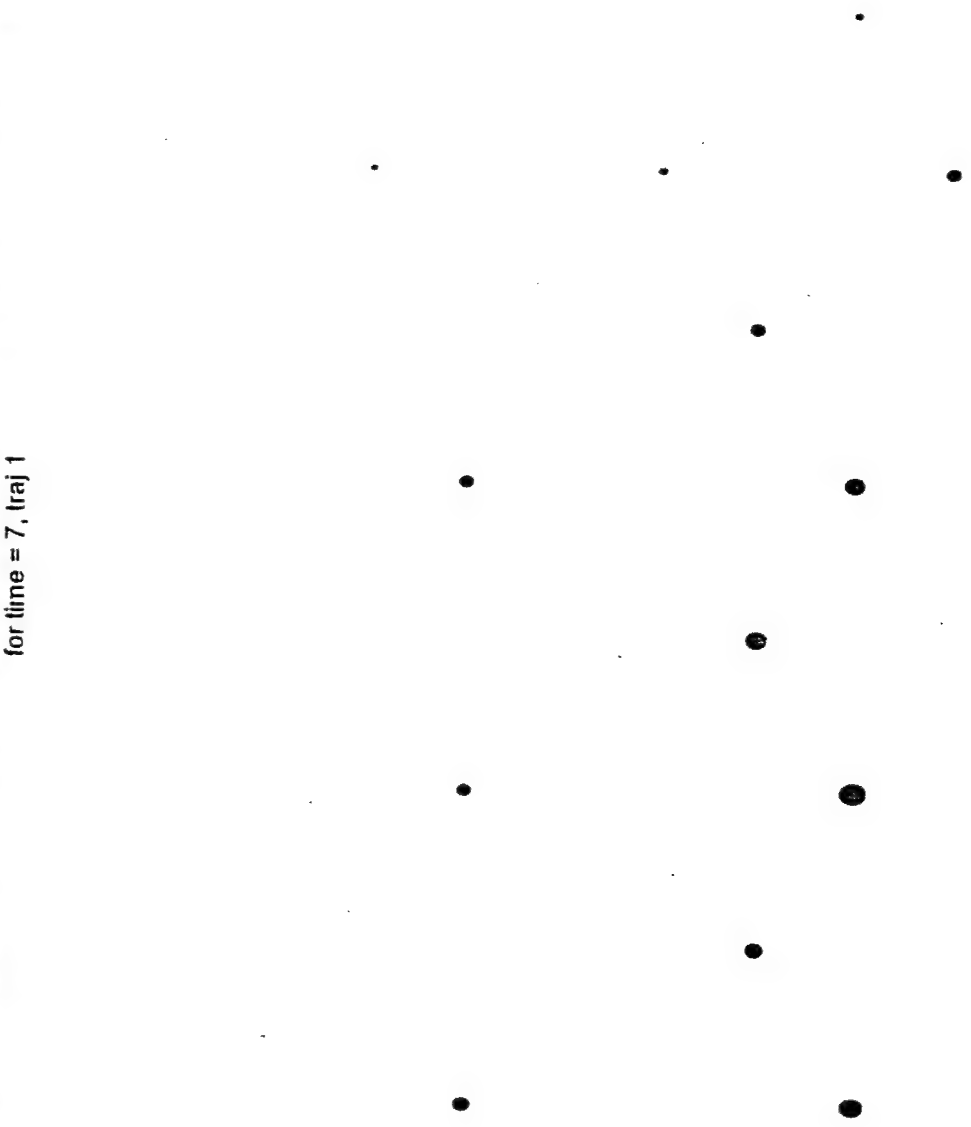

Figure B.4a. Objective Probabilities for the fifteen defended points, indicated by size of the dots, for threat #1 at time 7 sec.

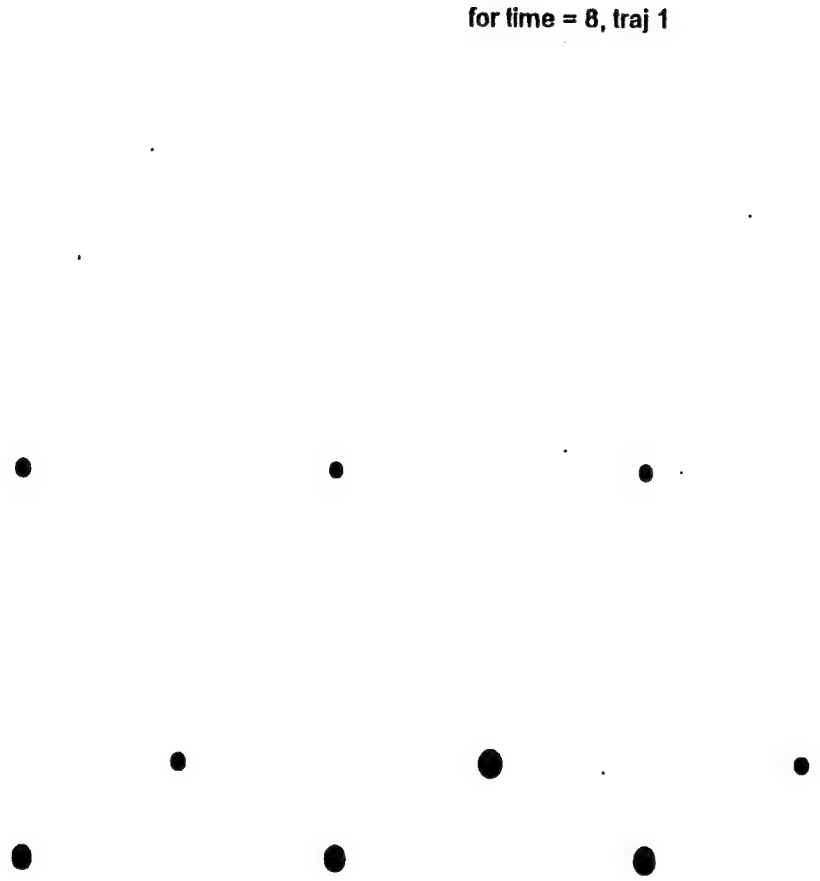

Figure B.4b. Objective Probabilities for the fifteen defended points, indicated by size of the dots, for threat #1 at time 8 sec.

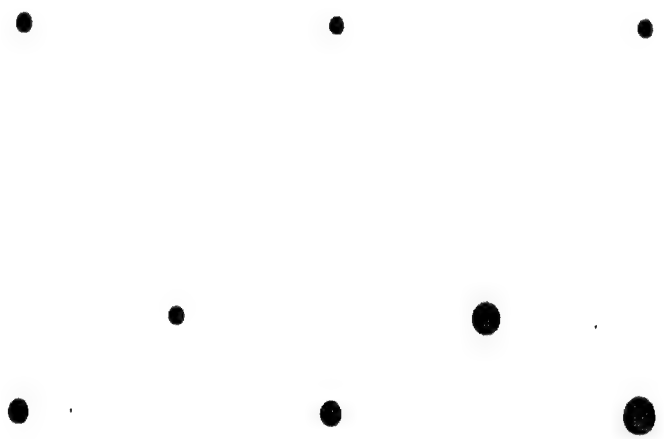

Figure B.4c. Objective Probabilities for the fifteen defended points, indicated by size of the dots, for threat #1 at time 9 sec.

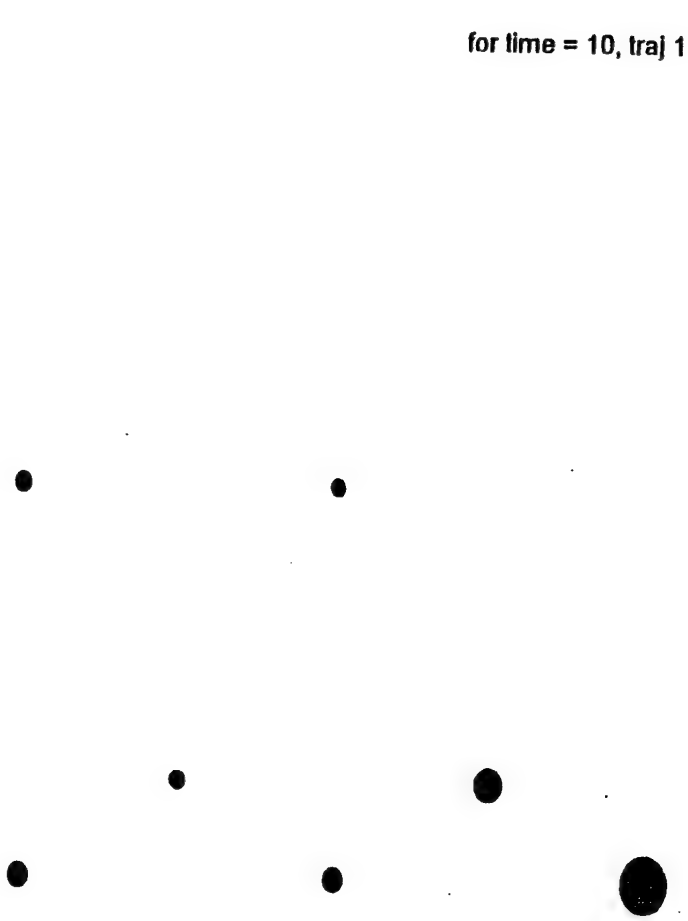

Figure B.4d. Objective Probabilities for the fifteen defended points, indicated by size of the dots, for threat #1 at time 10 sec.

Figure B.4e. Objective Probabilities for the fifteen defended points, indicated by size of the dots, for threat #1 at time 11 sec.

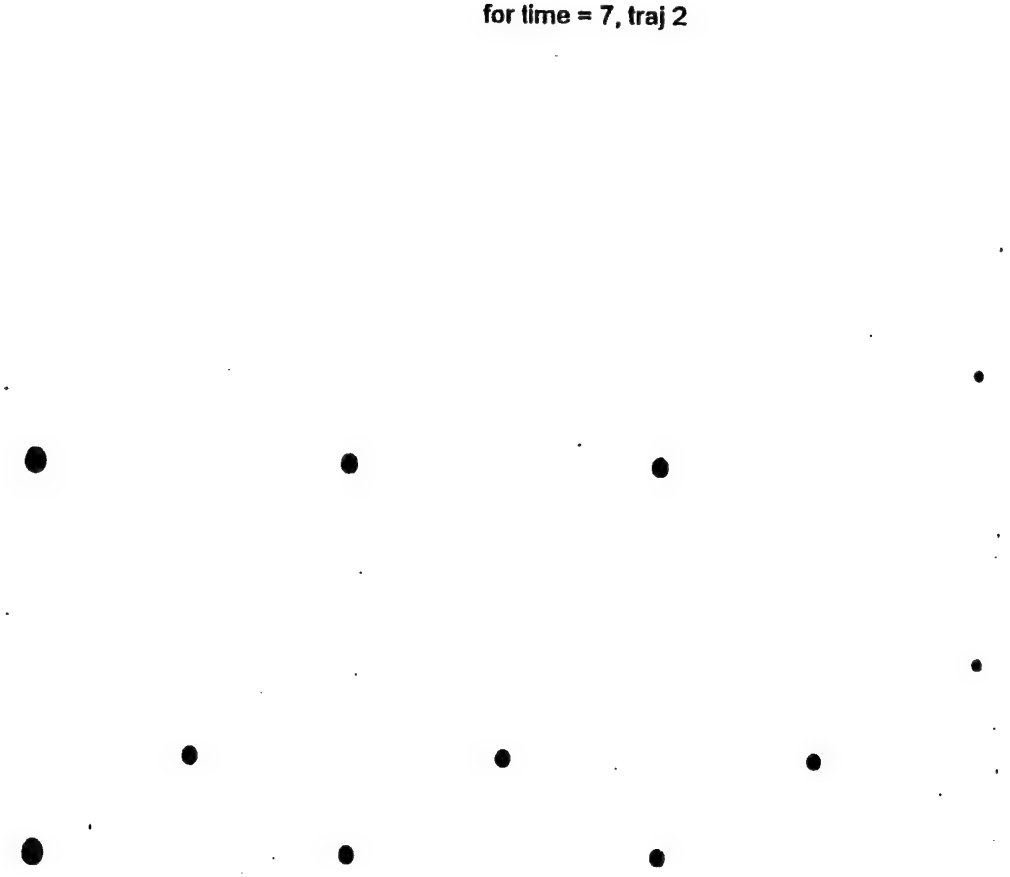

Figure B.5a. Objective Probabilities for the fifteen defended points, indicated by size of the dots, for threat #2 at time 7 sec.

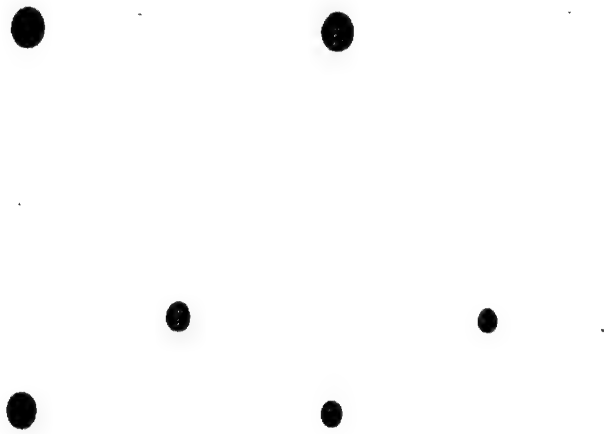

Figure B.5b. Objective Probabilities for the fifteen defended points, indicated by size of the dots, for threat ,#2 at time 12 sec.

Figure B.5c. Objective Probabilities for the fifteen defended points, indicated by size of the dots, for threat #2 at time 13 sec.

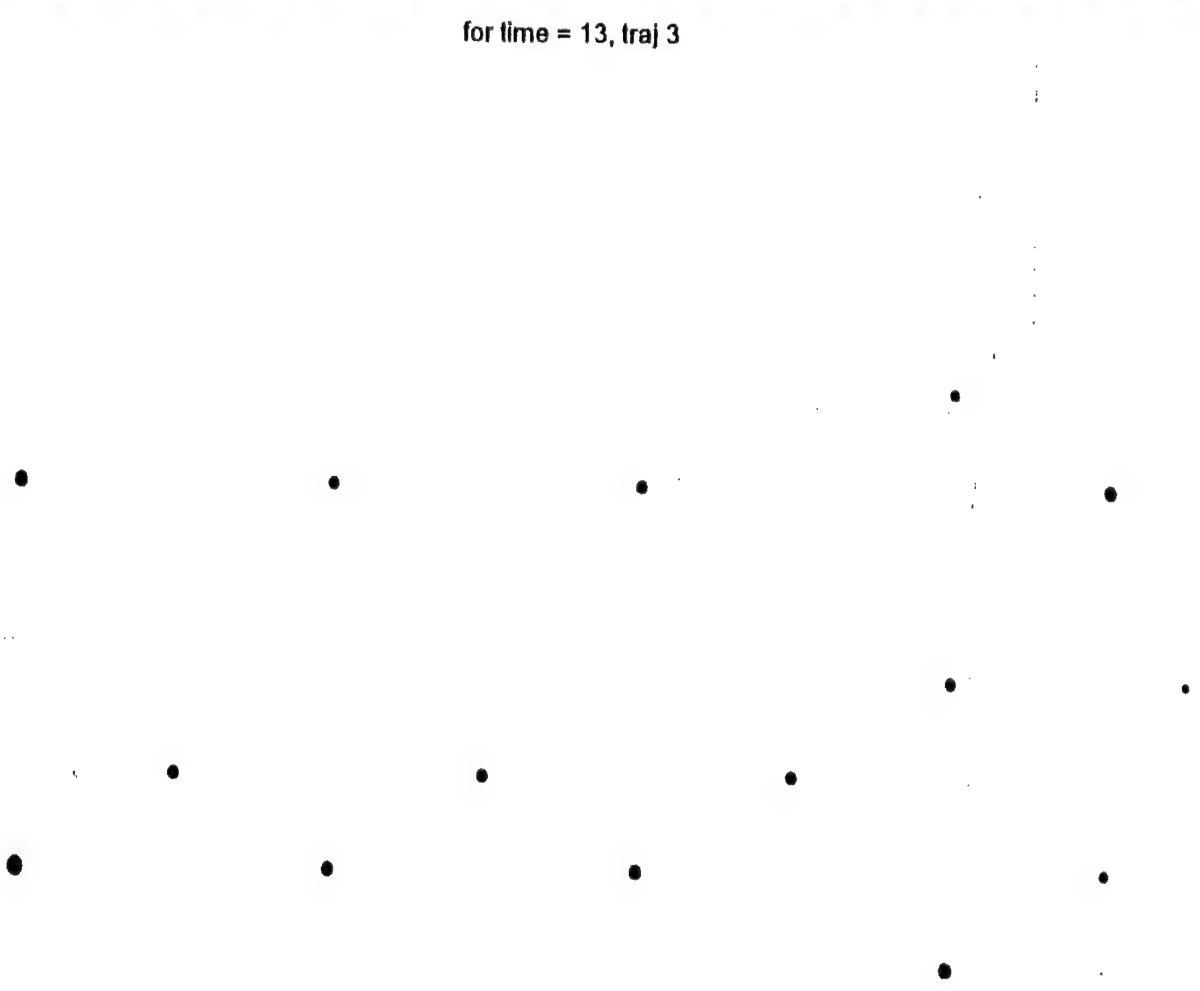

Figure B.6a. Objective Probabilities for the fifteen defended points, indicated by size of the dots, for threat #3 at time 13 sec.

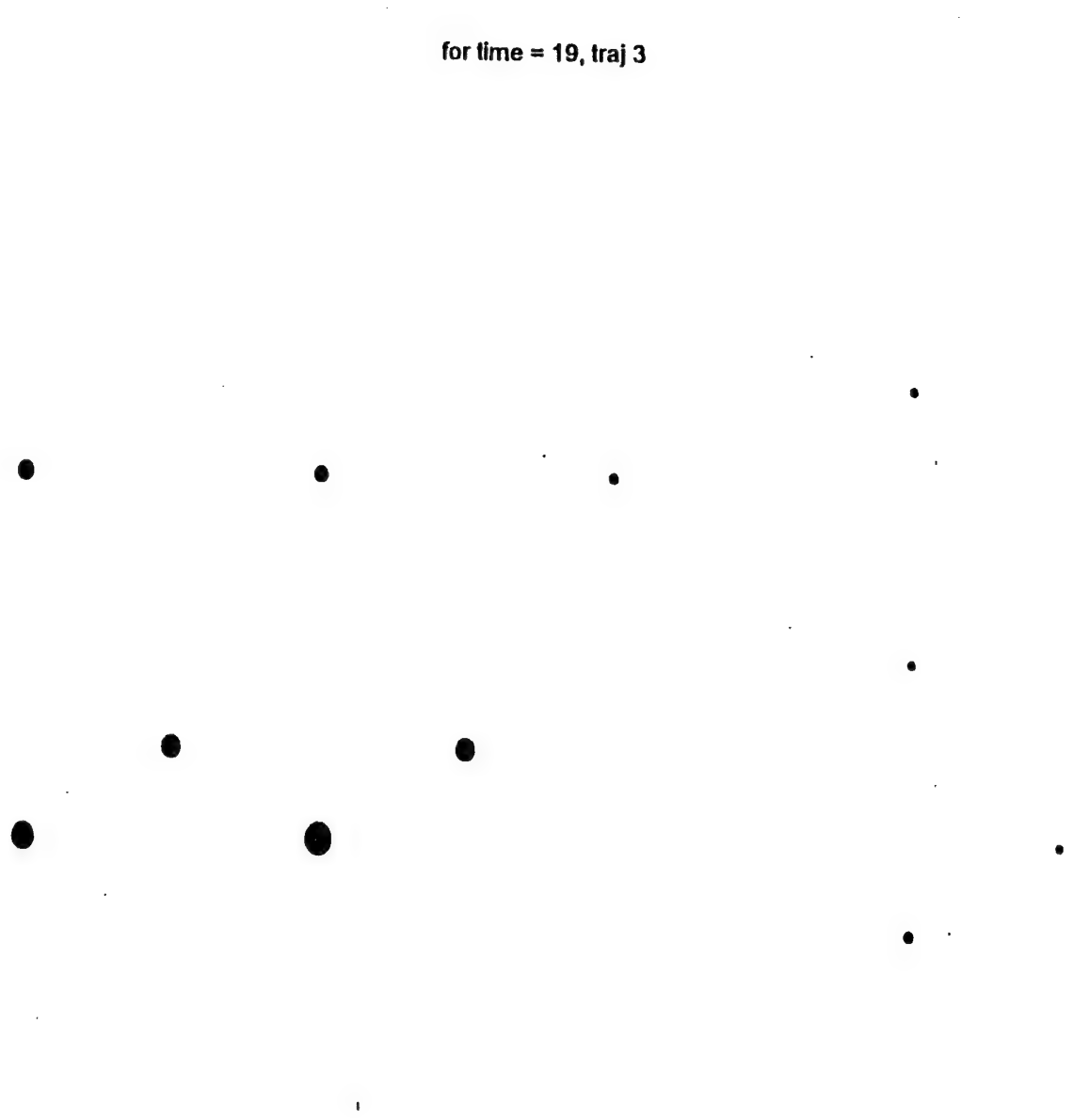

Figure B.6b. Objective Probabilities for the fifteen defended points, indicated by size of the dots, for threat #3 at time 19 sec.

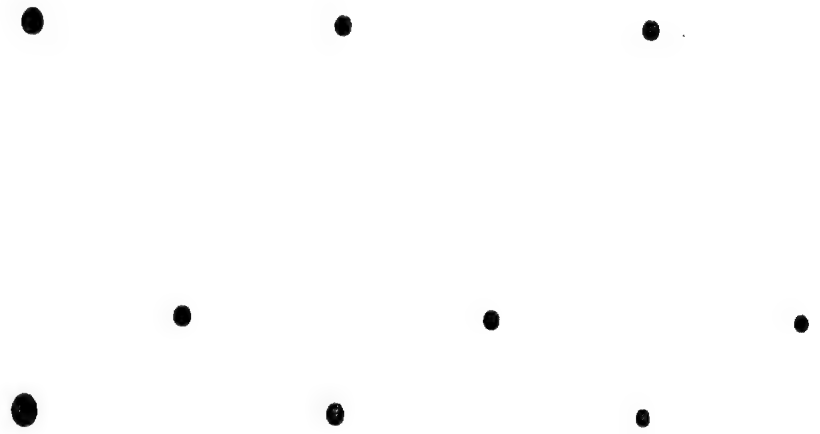

Figure B.7a. Objective Probabilities for the fifteen defended points, indicated by size of the dots, for threat #4 at time 4 sec.

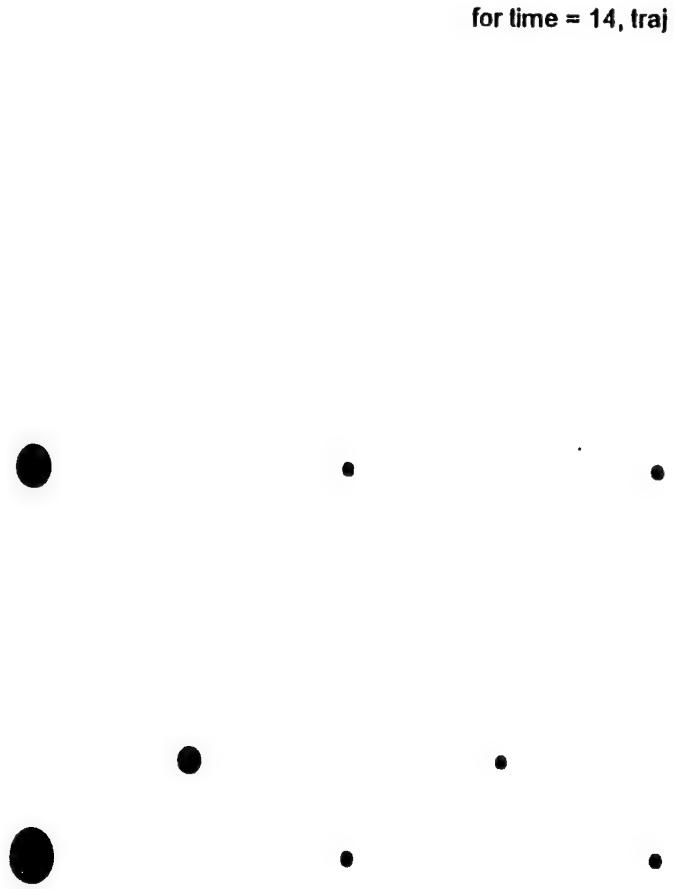

Figure B.7b. Objective Probabilities for the fifteen defended points, indicated by size of the dots, for threat #4 at time 14 sec.

Figure B.7c. Objective Probabilities for the fifteen defended points, indicated by size of the dots, for threat #4 at time 16 sec.

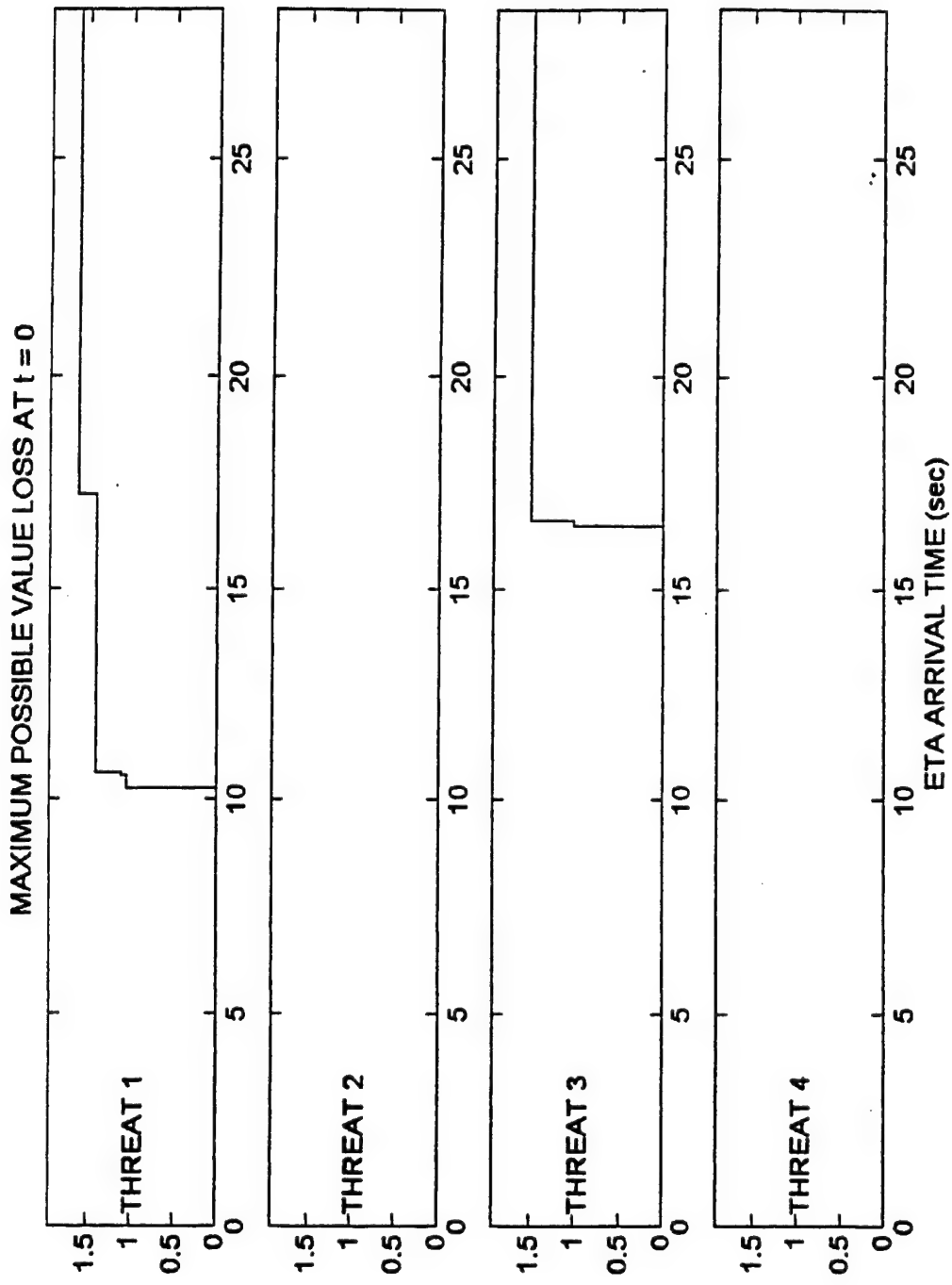

Figure B.8a. The Maximum Possible Value Loss (MPVL) for the four threats of the scenario of Figure B.1 at time t = 0.

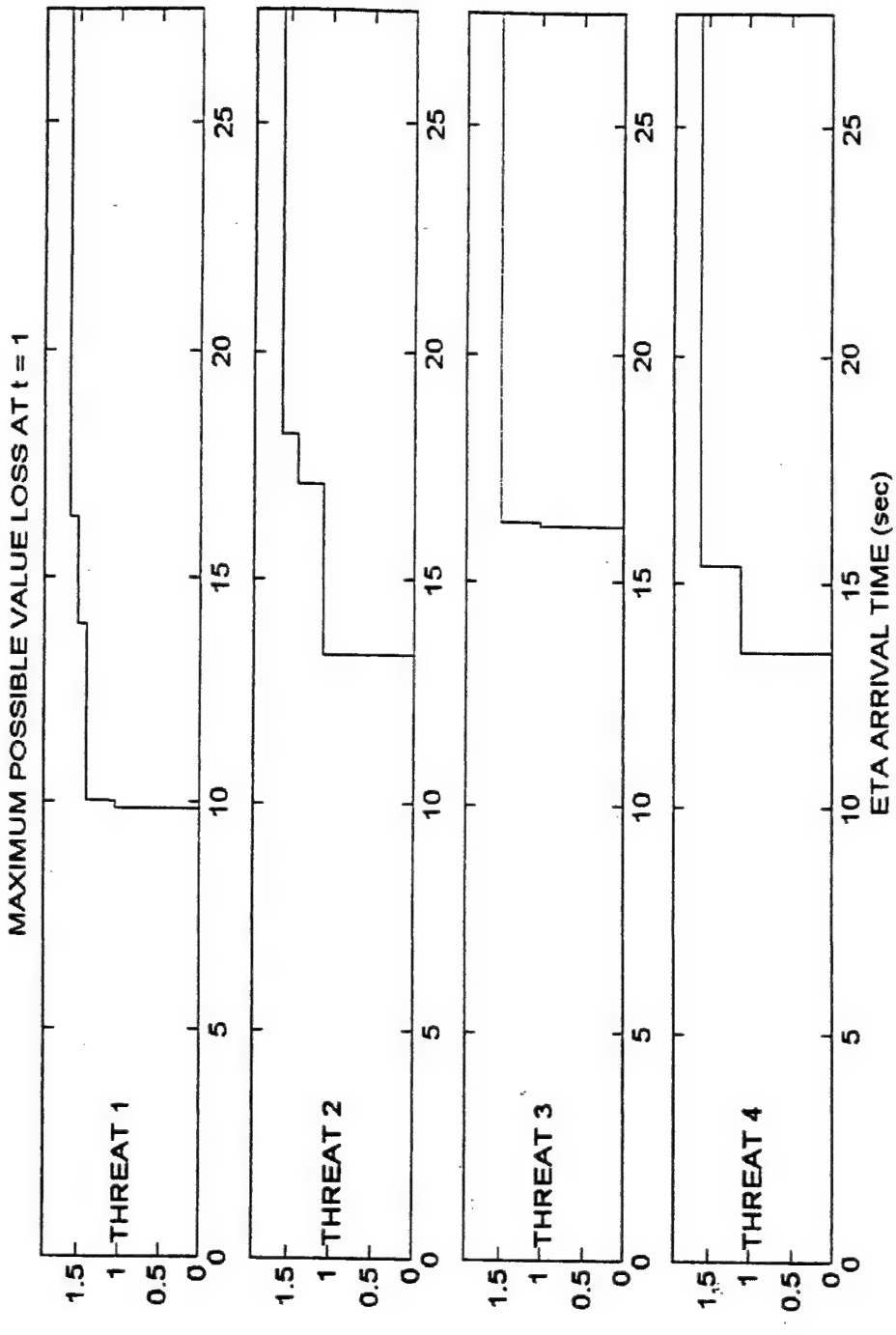

Figure B.8b. The Maximum Possible Value Loss (MPVL) for the four threats of the scenario of Figure B.1 at time t = 1.

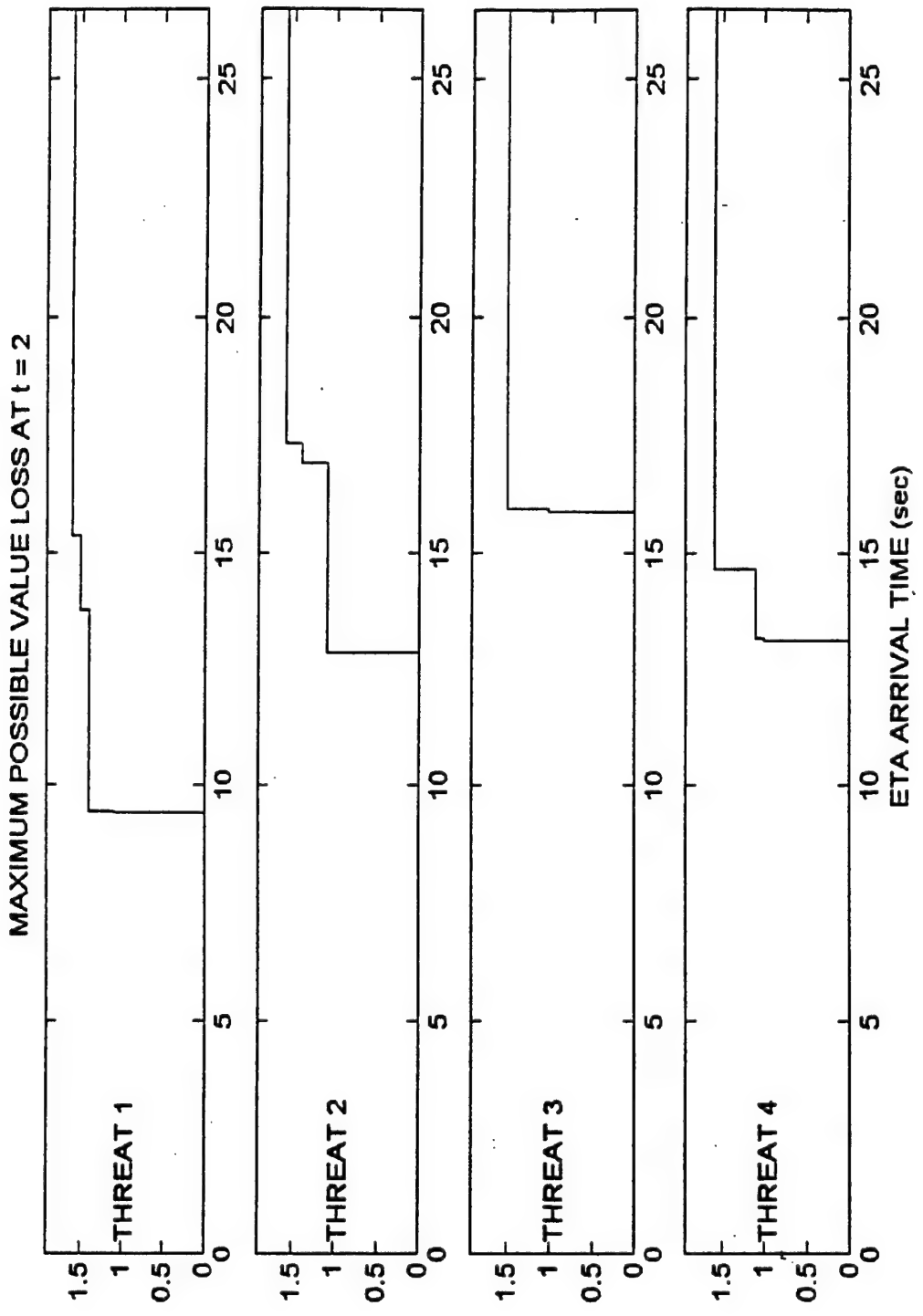

Figure B.8c. The Maximum Possible Value Loss (MPVL) for the four threats of the scenario of Figure B.1 at time t = 2.

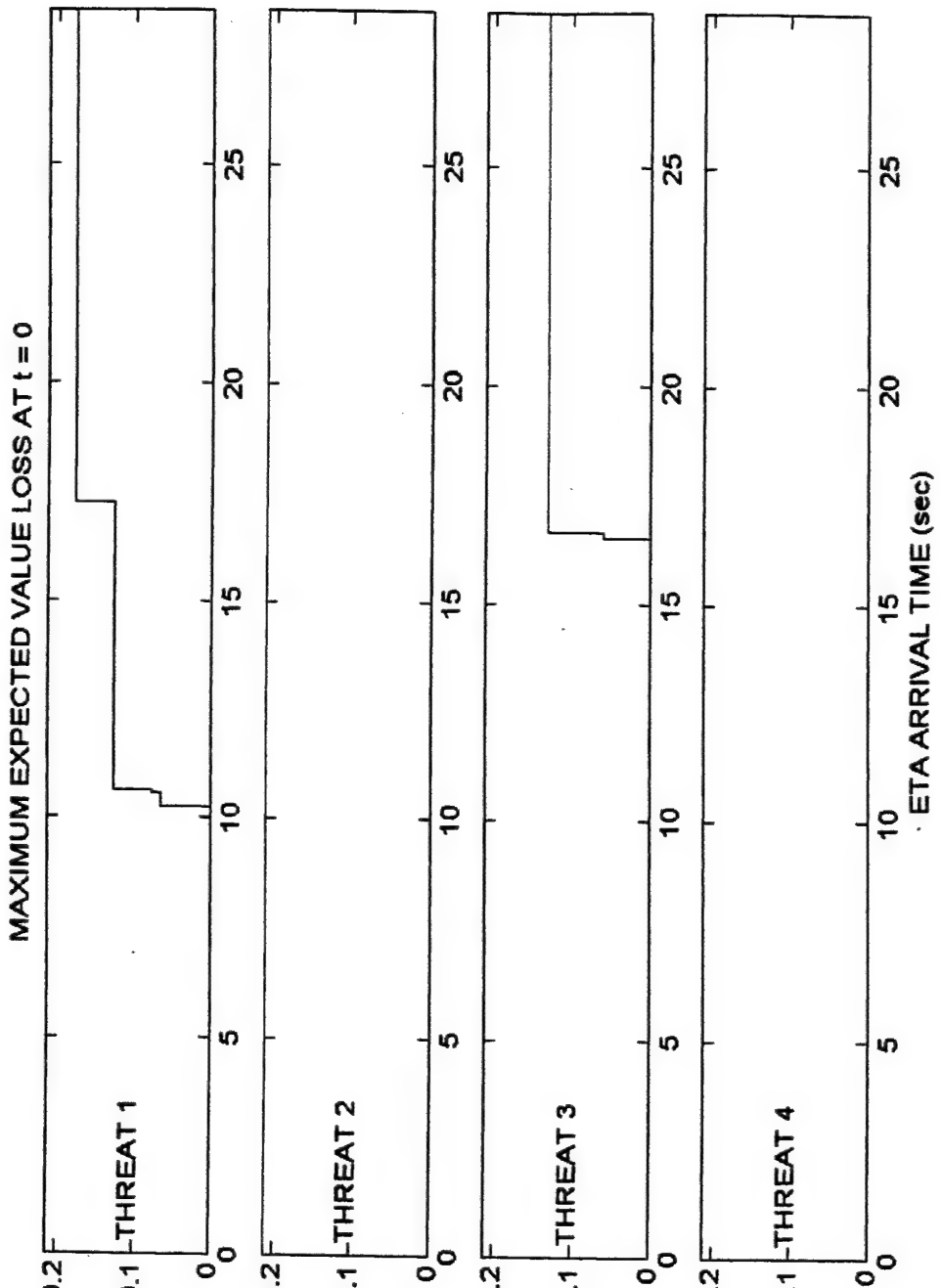

Figure B.9a. The Maximum Expected Value Loss (MEVL) for the four threats of the scenario of Figure B.1 at time t=0.

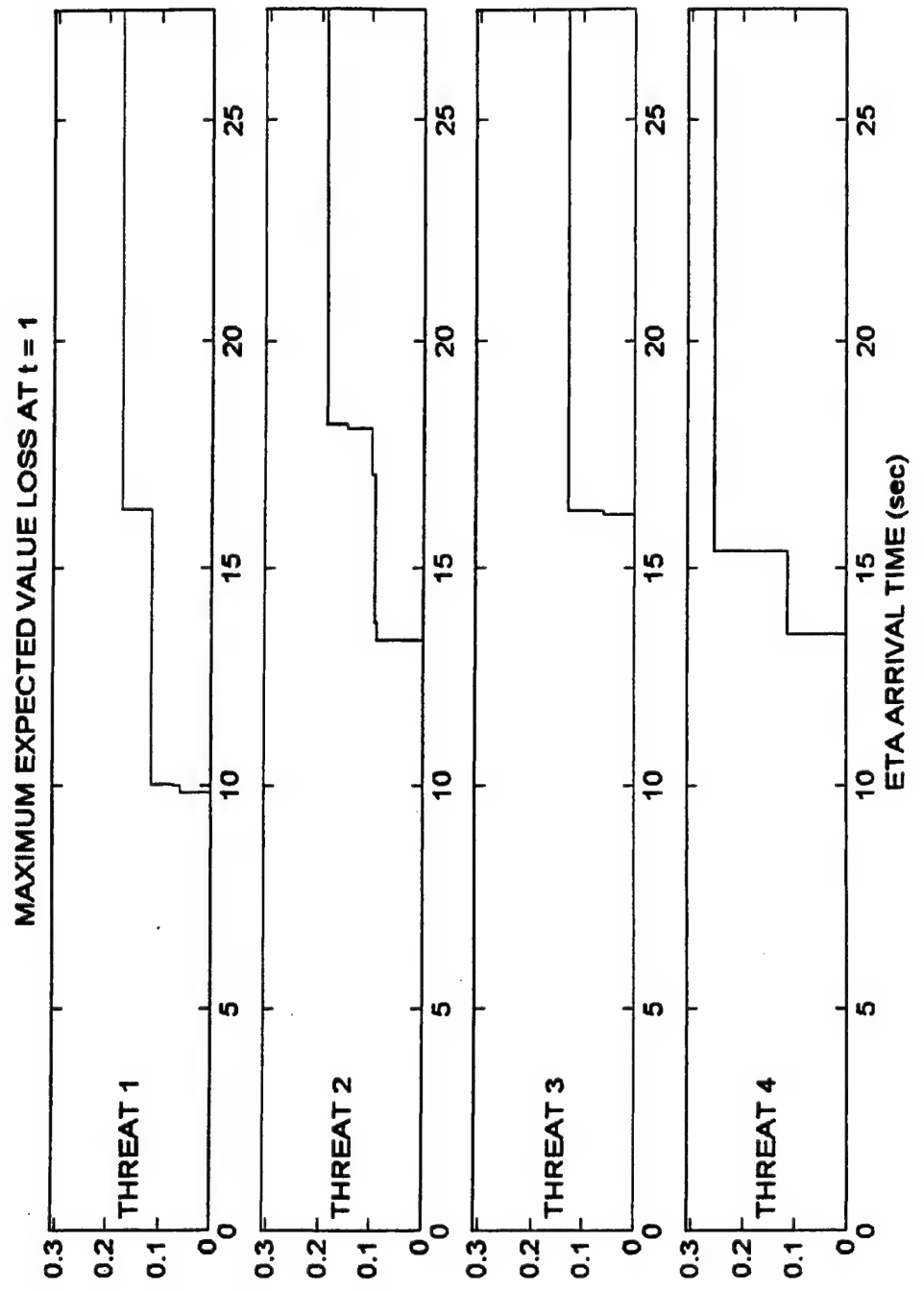

Figure B.9b. The Maximum Expected Value Loss (MEVL) for the four threats of the scenario of Figure B.1 at time t=1.

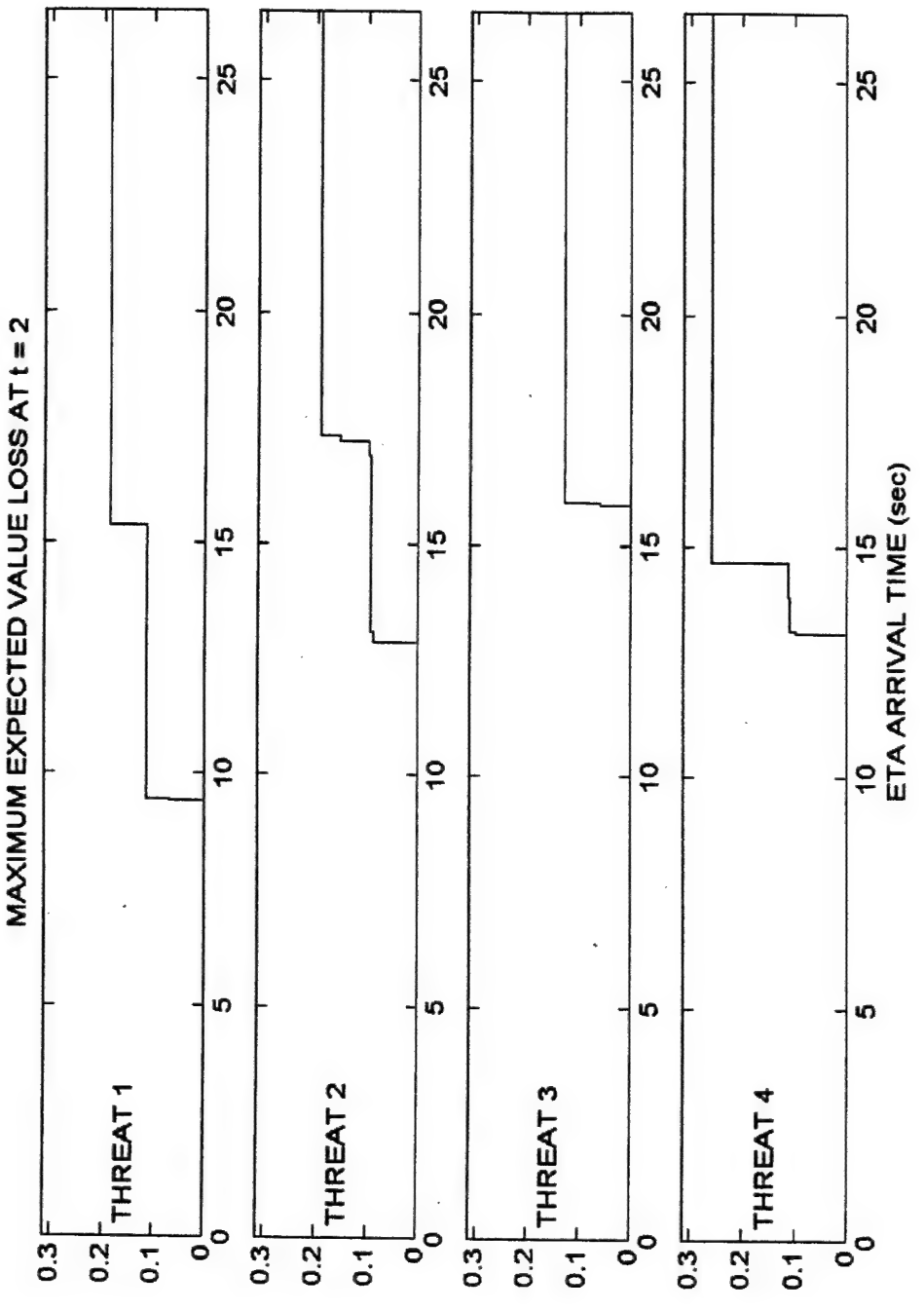

Figure B.9c. The Maximum Expected Value Loss (MEVL) for the four threats of the scenario of Figure B.1 at time t=2.

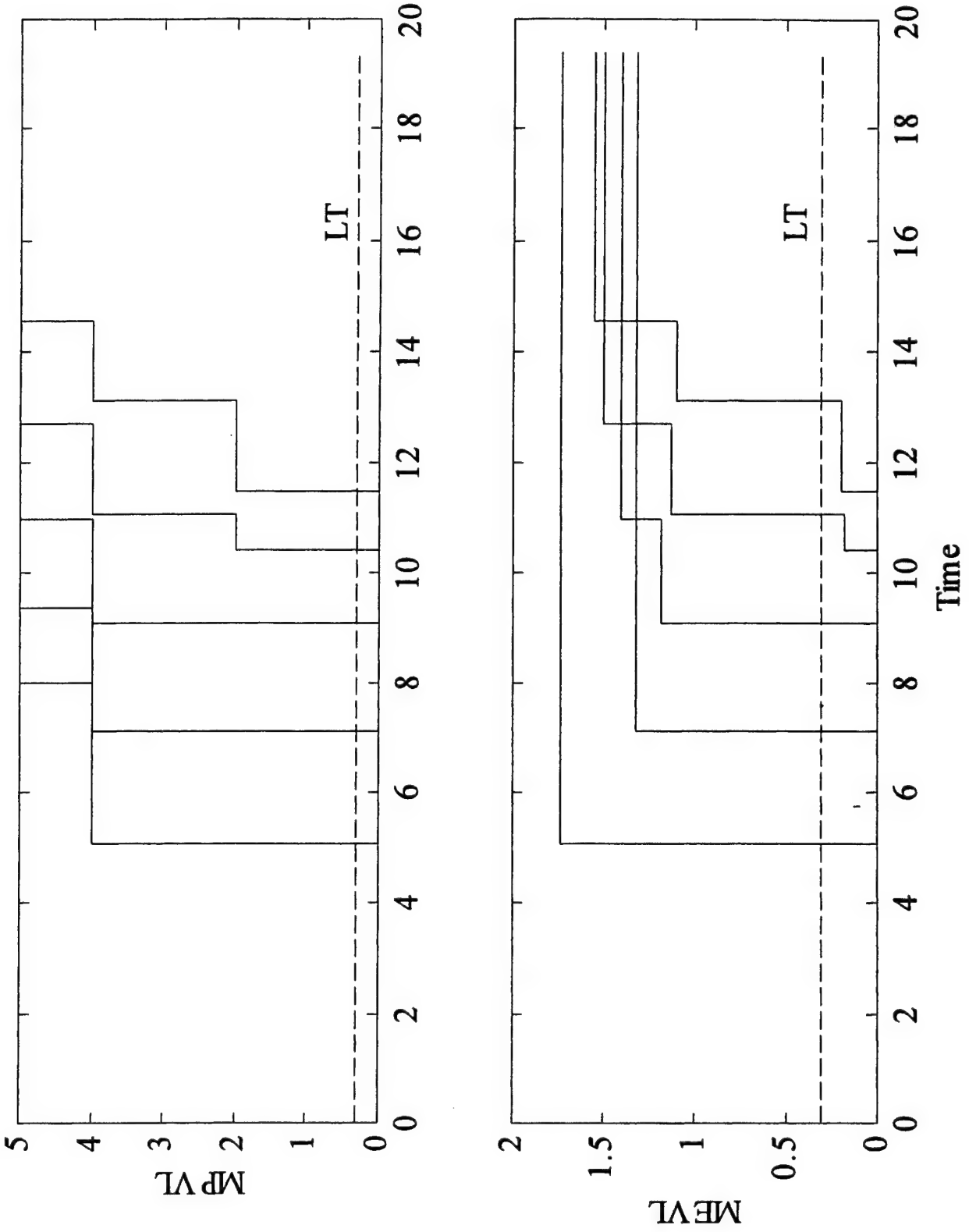

Figure B.10. Evolution in time of the Comprehensive MPVL and MEVL.

APPENDIX C

VARIABLE NAMES

Comprehensive List of Variable Names

The units indicated apply only to the variable name in the computer program.

Chapter 2

$V_j^{(a)}$	Va	actual value of a defended asset (ndim)
$V_j^{(p)}$	Vp	perceived value of a defended asset (ndim)
ϕ	elong	East longitude (rad)
L	nlat	North latitude (rad)
r	r	radial coordinate (m)
ϕ_0	elong0	East longitude of point of tangency (rad)
L_0	nlat0	North latitude of point of tangency (rad)
u	u	East velocity component (m/s)
v	v	North velocity component (m/s)
w	w	upward velocity component (m/s)
x_1		Cartesian component in East direction (m)
y_1		Cartesian component in North direction (m)
z_1		Cartesian component in upward direction (m)
ϕ_1		East longitude at tangent point of Local Coordinate System (LCS) (rad)
L_1		L at tangent point of LCS (rad)
a	a	Earth radius (m)
u_1	u1	velocity component in x1 direction (m/s)
v_1	v1	velocity component in y1 direction (m/s)
w_1	w1	velocity component in z1 direction (m/s)
$\tilde{x}_1$	xtil	Cartesian coordinate in second system (m)
$\tilde{y}_1$	ytil	Cartesian coordinate in second system (m)
$\tilde{z}_1$	ztil	Cartesian coordinate in second system (m)
$\hat{x}_1$	xhat	Cartesian coordinate in third system (m)
$\hat{y}_1$	yhat	Cartesian coordinate in third system (m)
$\hat{z}_1$	zhat	Cartesian coordinate in third system (m)

(Note that $(\tilde{x}_2, \tilde{y}_2, \tilde{z}_2)$ and $(\hat{x}_2, \hat{y}_2, \hat{z}_2)$ are similarly defined in another LCS at another point of tangency.)

J_{jk}	J(j,k)	Jacobian matrix (var)
"g"	g	suffix indicating geographic coordinates
a	asemi	semimajor ellipse axis (m)
b	bsemi	semiminor ellipse axis (m)
e	e	eccentricity (ndim)
(x_0, y_0)	(x0,y0)	LCS location of ellipse center (m)
(x_{f1}, y_{f1})	(xf1,yf1)	LCS location of ellipse focus (m)
(x_{f2}, y_{f2})	(xf1,yf1)	LCS location of other focus (m)
ϕ_a	phia	trend (direction) of line of apsides (rad)
θ	theta	angular polar coordinate (rad)
j	j	index for defended asset
k	k	threat index
$W_j^{(a)}$	Wa	actual value per unit area (m^{-2})
$W_j^{(p)}$	Wp	perceived value per unit area (m^{-2})

Chapters 3 and 4

n	n	number of threats (ndim)
n_a	na	number of cruise-missile tracks (ndim)
n_t	nt	number of ballistic missile tracks (ndim)
m	m	number of defended assets (ndim)
m_p	mp	number of defended points (ndim)
m_a	ma	number of defended areas (ndim)
n_d	nd	number of data points in trajectory (ndim)
f_m	fm	maneuver factor (ndim)
$\vec{r}_0$	r0vec	initial threat position (m)
$\vec{\dot{r}}_0$	r0dotvec	initial threat velocity (m/s)
$\vec{r}_s$	rsvec	asset position (m)
V_t	Vt	threat speed (m/s)
b_m	bm	minimum allowed turn radius (m)
a_m	am	maximum allowed lateral acceleration (m/s^2)
ϕ	phi	heading error (rad)
ϕ_m	phim	maximum allowed heading error (rad)
M_k	M(k)	threat "Menace" (ndim)

A, B	A,B	undetermined constants
$\vec{r}_c$	rcvec	center of curvature (m)
E, F	E,F	undetermined constants
$\vec{r}_t$	rtvec	transition point (m)
$\hat{A}$	Ahat	undetermined constant
$\hat{B}$	Bhat	undetermined constant
$\hat{C}$	Chat	undetermined constant
θ_t	thetat	arc length traversed (rad)
θ	theta	arc length (rad)
b	b	radius of curvature (m)
θ_s	thetas	another arc length (rad)
$\vec{r}_i$	rivec	splash point or impact point (m)
a, b	a,b	legs of a right triangle (m)
s	s	length of a CV segment (m)

Chapter 6

F_D	FD	drag coefficient (ndim)
F_L	FL	lift coefficient (ndim)
κ	kappa	a physical parameter of air (km/m)
C_{D0}	Cdo	drag coefficient at no lift (ndim)
K	K	an aerodynamic parameter for a threat (ndim)
ρ	rho	air density (kg/m^3)
S	S	threat cross section area (m^2)
m	m	threat mass (kg)
$\ddot{\vec{r}}_0$	rddotvec	initial threat acceleration (m/s^2)
$\vec{F}_D$		drag force (kg m/s^2)
$\vec{F}_L$		lift force (kg m/s^2)
$\vec{T}_h$		thrust force (kg m/s^2)
$\vec{g}$		acceleration of gravity (m/s^2)
$\vec{k}$		upward unit vector (ndim)
$\vec{u}$		unit vector in direction of lift (ndim)
a	a	acceleration magnitude (m/s^2)
$\vec{a}$		acceleration (m/s^2)
L_o	Lo	drag loss (kg m^2/s^2)

Chapter 7

t	t	time (s)
Ω	omega	Earth rotation rate (1/s)
θ_c	thetac	arc length traversed (rad)
T	T	flight time (s)
X_0	X0	flight range in Keplerian trajectory (m)
X_a	Xa	flight range in air (m)
T_0	T0	flight time in Keplerian trajectory (s)
T_a	Ta	flight time in air (s)
V_0	V0	initial TBM speed (m/s)
R_e		radial coordinate of defended area (m)
λ	lambda	parameter in Keplerian calculation (ndim)
μ	mu	parameter in Keplerian calculation (m^3s^{-2})
h	hatm	altitude where air density is 1/e surface value (m)
σ	sigma	parameter in Keplerian calculation (ndim)
T_F	TF	Keplerian flight time (s)
γ	gamq	flight path angle (rad)
γ_0	gamq0	initial flight path angle (rad)
δ		Gray's drag parameter (1/m)
ζ	zeta	square of threat speed (m^2/s^2)
α	alpha	an angle in spherical triangle (rad)
	Xfall	horizontal range of fall through air (m)
	Tfall	flight time of fall through air (s)
	espi	parameter in Runge Kutta integration
	h1	parameter in Runge Kutta integration
	hmin	parameter in Runge Kutta integration

Chapter 8

J	J	Jacobian (matrix)
$C0$	C0	threat-state error covariance matrix
Ci	Ci	TBM footprint covariance matrix (m^2)
$\overline{\delta}$	deltab	expected drag parameter value (1/m)
σ_δ	sigmad	standard error in drag parameter (1/m)
T_{F1}	TF1	flight time with different drag (s)
θ_1		arc length with different drag (rad)

C_s	Cs	footprint covariance from state errors (m^2)
C_d	Cd	footprint covariance from drag error (m^2)

Chapter 9

P_{kj}	P(k,j)	Objective Probability (ndim)
T_{kj}	T(k,j)	ETA arrival time (s)
L_{kj}	L(k,j)	ETA drag loss (kg m^2 s^{-2})
E_{kj}	E(k,j)	Maximum Expected Value Loss (ndim)
$E_{kj}^{(p)}$	Ep(k,j)	Maximum Possible Value Loss (ndim)
$\tilde{P}_{kj}$		Objective Probability for defended point (ndim)
i	iunit	ordered index for defended asset

Conflicts

a	Earth radius, semimajor axis, acceleration, leg of triangle
b	radius of curvature, semiminor axis, leg of triangle
ϕ	heading error, E longitude

DISTRIBUTION

	Copies
DOD ACTIVITIES (CONUS)	
ATTN CODE A76 (TECHNICAL LIBRARY) COMMANDING OFFICER CSSDD NSWC 6703 W HIGHWAY 98 PANAMA CITY FL 32407-7001	1
DEFENSE TECH INFORMATION CTR 8725 JOHN J KINGMAN RD SUITE 0944 FORT BELVOIR VA 22060-6218	2
ATTN MR GARY TOTH COMMAND AND CONTROL PROGRAM OFFICER MATHEMATICAL COMPUTER AND INFORMATIONAL SCIENCES DIVISION CODE ONR311 OFFICE OF NAVAL RESEARCH BALLSTON CENTER TOWER ONE ROOM 607-14 800 NORTH QUINCY STREET ARLINGTON VA 22217-5000	1
NON-DOD ACTIVITIES (CONUS)	
ATTN DOCUMENT CENTER THE CNA CORPORATION 4825 MARK CENTER DRIVE ALEXANDRIA VA 22311-1850	1
ATTN DR GREG COXSON 137-128 LOCKHEED MARTIN NE & SS 199 BORTON LANDING ROAD MOORESTOWN NJ 08057	1
ATTN DR RON HELMICK TECHNOLOGY SERVICE CORPORATION 962 WAYNE AVENUE SUITE 800 SILVER SPRING MD 20910	1
ATTN DALE BLAIR PHD SENIOR RESEARCH ENGINEER SENSORS AND ELECTROMAGNETIC APPLICATIONS LABORATORY GEORGIA TECH RESEARCH INSTITUTE GEORGIA INSTITUTE OF TECHNOLOGY 7220 RICHARDSON ROAD SMYRNA GA 30080	1
ATTN DR OLIVER E DRUMMOND 10705 CRANKS ROAD CULVER CITY CA 90230	1
ATTN MR JOSEPH PRIMERANO PLANNING CONSULTANTS INC P O BOX 1676 DAHLGREN VA 22448	1
ATTN DR YAAKOV BAR-SHALOM DISTINGUISHED PROFESSOR INFORMATION COMMUNICATION AND DECISION SYSTEMS GROUP ELECTRICAL AND COMPUTER ENGINEERING DEPARTMENT UNIVERSITY OF CONNECTICUT U-260 GLENBROOK ROAD #209 STORRS CT 06269	1
INTERNAL	
B32 MR JOHN E GRAY	5
B32 MS SARA LEITE	1
B32 DR H DENNIS MCCABE	1
B32 MS SUNSHINE SMITH-CARROLL	1
B35 DR WILLIAM FARR	1
B35 DR CHARLES FENNEMORE	1
B35 MR ROBERT HARRISON	1
B35 MR MICHAEL MASTERS	1
B35 MR ROBERT TAFT	1
B60 TECHNICAL LIBRARY	3
G23 MR JOHN BIBEL	1
G23 MR ERNIE OHLMEYER	1

DISTRIBUTION (Continued)

		Copies
G23	MR CRAIG PHILLIPS	1
N	DR KEN BAILLE	1
N05	MR GREG MILLER	1
N05	MS DAWN MURPHY	1
N05	MR REUBEN PITTS	1
N14	DR DEMETRIOS SERAKOS	1
N23	MR DONALD D BOYER	1
N92	DR GEORGE FOSTER	1
N92	DR GORDON GROVES	5
N92	MR CHRIS KUHLMAN	1
N92	MR HARRY LAMBERTSON	1
T14	DR WILLIAM LUCAS	1